PROPAGATION OF REFRACTION ERRORS IN TRIGONOMETRIC HEIGHT TRAVERSING AND GEODETIC LEVELLING

G. A. KHARAGHANI

November 1987

TECHNICAL REPORT
NO. 132

PREFACE

In order to make our extensive series of technical reports more readily available, we have scanned the old master copies and produced electronic versions in Portable Document Format. The quality of the images varies depending on the quality of the originals. The images have not been converted to searchable text.

PROPAGATION OF REFRACTION ERRORS IN TRIGONOMETRIC HEIGHT TRAVERSING AND GEODETIC LEVELLING

Gholam A. Kharaghani

Department of Surveying Engineering
University of New Brunswick
P.O. Box 4400
Fredericton, N.B.
Canada
E3B 5A3

November 1987

PREFACE

This report is an unaltered printing of the author's M.Sc. thesis of the same title, which was submitted to this Department in August 1987.

The thesis supervisor was Professor Adam Chrzanowski.

Any comments communicated to the author or to Dr. Chrzanowski will be greatly appreciated.

ABSTRACT

The use of trigonometric height traversing as an alternative to geodetic levelling has recently been given considerable attention. A replacement for geodetic levelling is sought to reduce the cost and to reduce the uncertainty due to the refraction and other systematic errors.

As in geodetic levelling, the atmospheric refraction can be the main source of error in the trigonometric method. This thesis investigates the propagation of refraction errors in trigonometric height traversing. Three new models for the temperature profile up to 4 m above the ground are proposed and compared with the widely accepted Kukkamäki's temperature model. The results have shown that the new models give better precision of fit and are easier to utilize.

A computer simulation of the influence of refraction in trigonometric height traversing suggests that the accumulation of the refraction effect becomes randomized to a large extent over long traverses. It is concluded that the accumulation of the refraction effect in short-range trigonometric height traversing is within the limits of Canadian specifications for the first order levelling.

TABLE OF CONTENTS

LIST OF TABLES

LIST OF FIGURES

ACKNOWLEDGEMENTS

I wish to express my deepest gratitude and sincere thanks to my supervisor, Dr. Adam Chrzanowski. His interest in the topic and constructive suggestions were invaluable. His guidence, immeasurable support and continuous encouragement throughout the course of this work were highly appreciated.

In addition, I would like to thank Dr. Yong-Qi Chen from Wuhan Technical University of Surveying and Mapping for his many hours spent in discussion and reading the original manuscript and for his constructive criticism while he was on leave at the Department of Surveying Engineering, University of New Brunswick. I also wish to thank Dr. Wolfgang Faig for his critical review of this thesis and for his guidance and sound advice.

I would like to express my sincere thanks to Mr. James Secord who spent many long hours to discuss, to read and to render my difficult script into a readable form.

I am indebted to Dr. A. Jarzymowski a visiting scholar from Poland for his help in making the meteorological measurements possible and his assisstance during long days of field work.

My thanks are extended also to many of my colleaques for their generous assistance with the field work. Among them, Messrs J. Kornacki, J. Mantha, C. Faig, K. Donkin, P. Romero, Z. Shi and M. Katekyeza are particularly thanked.

Thanks are also due to the personnel at the Geodetic Survey of Canada for providing the data used in this study.

The work described in this thesis has been financially supported by the Geodetic Survey of Canada, the National Science and Engineering Research Council and by the University of New Brunswick.

Chapter 1

INTRODUCTION

The refractive properties of the atmosphere have placed a limit on the accuracy of conventional geodetic levelling. Geodetic levelling is a slow survey procedure which is confined by its horizontal line of sight. Along inclined terrain, refraction influences the measurements systematically because the horizontal line of sight passes obliquely through different isothermal layers of air. Under certain extreme conditions such as the long easy gradient along railways, an accumulation in the order 20 mm per 100 m of height difference can be expected [Bomford, 1971]. A suggested remedy is to shorten the sight length, because the influence of refraction is proportional to the square of the sight distance [e.g. Angus-Leppan, 1985]. For precise levelling, Bomford [1971] recommends keeping the length of sight under 30 m, even though the slope may allow longer lengths. This restriction makes the survey progress even slower and more expensive.

Because of these reasons, developement has been intiated in the last few years to increase production and reduce the systematic error effects by using the trigonometric height traversing method as an alternative to geodetic levelling. In the trigonometric methods, the differences in elevations are determined from measured vertical angles and distances using the new state-of-art modern electronic theodolites and compact and accurate EDM (Electromagnetic Distance Measuring) instrumentation.

Two types of trigonometric height traversing can be distinguished (see Figure 1.1):

1. Simultaneous reciprocal: the zenith angles are measured in both directions simultaneously.
2. Leap-frog: the instrument is set up midway between two target-reflector stations.

At the University of New Brunswick, the leap-frog method with elevated multiple targets was developed and tested from 1981 to 1985. This variant of the leap-frog trigonometric height traversing is called the "UNB-method".

In the trigonometric methods, vertical angle observations are affected by the long-term temperature gradient variations which cause vertical displacement of the target image. The short-term temperature gradient fluctuations cause the blurring of the image (image dancing). As in geodetic levelling, the atmospheric refraction can be the main source of error in the trigonometric methods, though its systematic effect is expected to be much smaller than in geodetic levelling.

Many authors have investigated both practical and theoretical aspects of refraction error in geodetic levelling [e.g. Kukkamäki 1938, Holdahl 1981, Angus-Leppan 1979b,1980]. These investigations have arrived at formulae for the refraction correction, and practical experiments have shown that the results from various formulae are similar and are close to actual values [Angus-Leppan 1984, Heer and Niemeier [1985], Banger 1982, Heroux et al. 1985]. These formulae are generally based on estimated (modelled) or measured temperature gradients.

In the trigonometric methods, a similar refraction correction can be derived if the lengths of sight are compatiable with the length of sight used in geodetic levelling, i.e. not exceeding 100 m. If the lines of sight are longer, then the correction for refraction becomes a more complicated task. On the other hand, as it will be shown in this thesis, the influence of refraction in trigonometric height traversing becomes randomized to a large extent, if the lines of sight are short, i.e. less than 100 m.

This thesis investigates the propagation of refraction errors in the optical height difference determination methods with more emphasis on the trigonometric height traversing. The objectives can be summarized as follows:

1. To determine an optimal model for the temperature profile up to 4 m above the ground on the basis of several long term test surveys over three typical ground surfaces (gravel, grass and asphalt) and

profiles; to investigate the influence of refraction on these surfaces and to compare the measured refraction effect against the computed refraction correction.

2. *To* develop new models and to compare them against the available models such as *Kukkamäki's* and *Heer's* temperature functions.

3. *To* confirm in practice the designed precision of the *UNB*-method under controlled field conditions, to add to the understanding of the refraction effect and to compare the *UNB*-method against the reciprocal method with regard to the influence of refraction.

4. *To* simulate the refraction effect in the trigonometric methods along a line of geodetic levelling, to assess the dependence of the refraction errors on the profile and to compare the refraction effect in the trigonometric methods versus the refraction effect in geodetic levelling.

An overview of the solutions to the refraction problem in optical height difference determination methods is given in Chapters 2, 3 and 4. Chapter 2 reviews the method already developed for the refraction correction computations based on the evaluation of the temperature gradient, the so called "meteorological method" and three other approaches namely:

1. the dispersion (the two wavelength system),
2. the variance of the angle-of-arrival, and
3. the refraction by reflection.

The development of these methods depends on further advances in technology and they are promising a better performance than the meteorological method [Brunner, 1979a; Angus-Leppan, 1983]. Chapters 3 and 4 review in details the meteorological approach in the optical height difference determination methods. Chapter 4, also summarizes a new approach in solving for the refraction effect in the reciprocal method proposed by the author. Chapter 5 deals with the 1985 test surveys, their analysis, and discussion of results. The outcome of the simulations is given in Chapter 6.

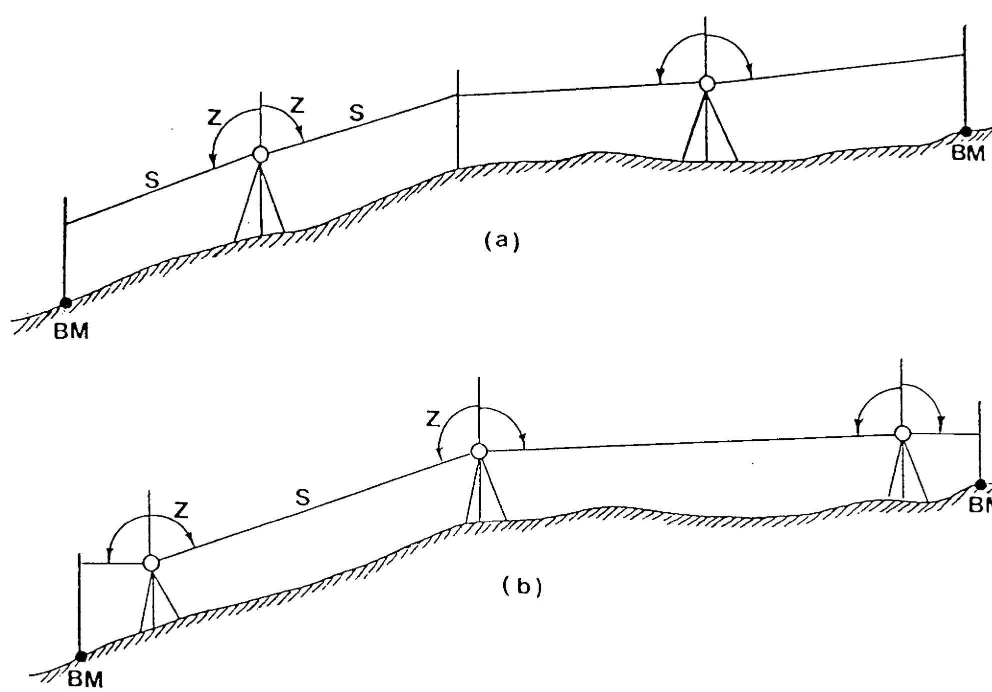

Figure 1.1: Methods of trigonometric height traversing
(a) leap-frog (b) reciprocal

Chapter 2

A REVIEW OF METHODS FOR THE DETERMINATION OF THE REFRACTION CORRECTION

The most significant source of error in trigonometric height traversing, as well as in geodetic levelling, is the effect of atmospheric refraction. Several solutions are suggested by different researchers. The most popular method that has been applied in geodetic levelling is based on temperature gradients which can be obtained either through the direct measurements of air temperature at different heights or by modelling the atmosphere using the theories of atmospheric physics. This approach to the vertical refraction angle computation is referred to, here, as the meteorological method.

Besides the above method, the following three other approaches are discussed in various literature. These methods are [e.g. Brunner, 1979a; Angus-Leppan, 1983]:

1. Determination of the vertical angle of refraction using using the dispersive property of the atmosphere.
2. Determination of the vertical angle of refraction derived from the variance of the angle-of-arrival fluctuations.
3. Determination of the vertical refraction correction using the "reflection method" [Angus-Leppan, 1983].

This chapter summarizes the above methods. The meteorological approach will be discussed with more detail in Chapters 3 and 4.

2.1 Determination of the Vertical Refraction Angle by the Meteorological Approach

2.1.1 Refractive index of air

Determination of errors due to atmospheric refraction using the meteorological method requires knowledge of the refraction properties of the atmosphere. The refractive index n of a medium is defined as the ratio of the velocity of light in a vacuum, c°, to the velocity c of light in the medium: n = c°/c. Variation in the refractive index of air depends on the variation of temperature, pressure and humidity. In 1960 a formula was adopted by the International Association of Geodesy in terms of temperature t [°C], pressure p [mb] and partial water vapour pressure e [mb], which is [Bomford, 1971]:

$$(n - 1) = (n^\circ - 1) . \frac{1}{(1 + \alpha\, t)} . \frac{p}{1013.25} - \frac{4.2\, e}{(1 + \alpha\, t)} \; 10^{-8} \tag{2.1}$$

where $\alpha = 1/273 = 0.00366$ is the thermal expansion of air and n° is the refractive index of light in standard air at a temperature 0 °C with a pressure of 1013.25 mb and with a carbon dioxide content of 0.03% and is given by [e.g. Hotine, 1969]

$$(n^{\circ} - 1)\,10^{6} = 287.604 + 1.6288\,\lambda^{-2} + 0.0136\,\lambda^{-4} \qquad (2.2)$$

in which λ is the wavelength [μm] of monochromatic light in a vacuum. Substituting an average value of $\lambda = 0.56\ \mu$m for white light and $\alpha = 0.00366$ into equation (2.1) yields

$$(n - 1) = 293 \times 10^{-6} \cdot \frac{1}{1 + 0.00366\,t} \cdot \frac{p}{1013.25} - \frac{4.1\,e}{1 + 0.00366\,t} \cdot 10^{-8} \qquad (2.3)$$

The vertical gradient of the refractive index can be expressed by differentiating equation (2.3) with respect to z

$$\frac{dn}{dz} = \frac{78.9}{T} \left[\left(\frac{dp}{dz} - 0.14\,\frac{de}{dz} \right) - \left(\frac{p - 0.14\,e}{T} \right) \frac{dT}{dz} \right] 10^{-6} \qquad (2.4)$$

where, T is the absolute temperature [K]. In the second term, 0.14 e, is negligible and 0.14 (de/dz) in normal condition is less than 2% of (dp/dz) and it can be neglected [Bomford, 1971]. The vertical gradient of pressure is approximated by [e.g. Bomford, 1971]

$$\frac{dp}{dz} = -\,\frac{g}{M} \cdot \frac{p}{T} \qquad (2.5)$$

where g is the gravitational acceleration and *M* is the specific gas constant for dry air. In this equation, g/M has the numerical value of 0.0342 *K*/m . This value is known as the autoconvective lapse rate [Shaw and Smietana, 1982]. Lapse rate is the rate of decrease of temperature with height. The simplified formula for vertical gradient of the refractive index is then given by

$$\frac{dn}{dz} = \frac{-78.9\ p}{T^2} \left(0.0342 + \frac{dT}{dz} \right) 10^{-6} \qquad (2.6)$$

In a homogeneous atmosphere, density is independent of height. Equation (2.6) shows that under such conditions, a lapse rate of -0.0342 *K*/m is necessary to compensate for the decrease in atmospheric pressure with height.

2.1.2 Angle of refraction error

Considering Figure 2.1 the vertical refraction angle ω is the angle between the chord and the tangent to the optical path *AB*. If dn/dz is known at all points along *AB*, the vertical refraction angle can be calculated from the eikonal (optical path length) equation [Brunner and Angus-Leppan 1976]

$$\omega = \frac{\sin Z}{S} \int_0^S dn/dz \ (S - x)\ dx \qquad (2.7)$$

where, S = the chord length *AB*,

Z = the zenith angle, and

x = the distance along the chord.

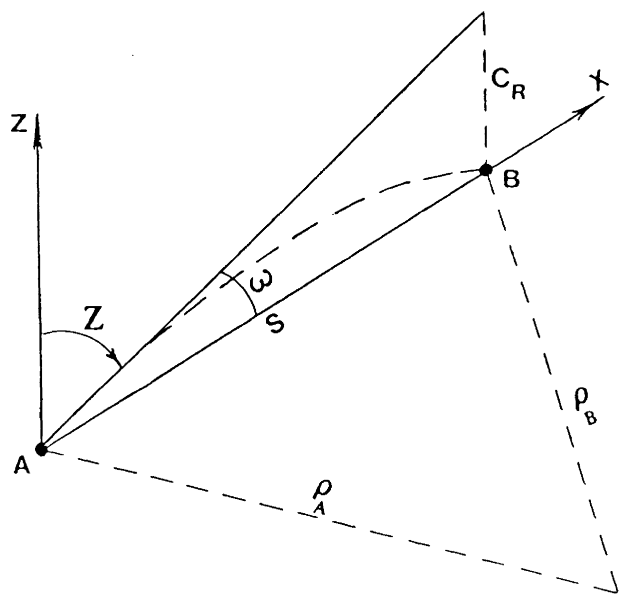

Figure 2.1: Vertical Refraction Angle

Substituting equation (2.6) into (2.7) and assuming $\sin Z = 1$, gives

$$\omega = \frac{10^{-6}}{S} \int_0^S \left[\frac{-78.9\ p}{T^2} \left(0.0342 + \frac{dT}{dz} \right) \right] (S - x)\, dx \tag{2.8}$$

From Figure 2.1, the refraction correction is

$$C_R = - \omega \cdot S \tag{2.9}$$

The correction may be also calculated in terms of the curvature of the light path and the coefficient of refraction. The curvature is given by

$$1/\rho = - (dn/dz) \; . \sin Z \qquad (2.10)$$

The coefficient of refraction is defined as the ratio of the radius of the earth R to the radius of the curvature of the light path

$$k = R / \rho \qquad (2.11)$$

Substituting equation (2.6) and (2.10) in (2.11) and assuming $R = 6371000$ m gives

$$k = \frac{502.7\ p}{T^2} \left(0.0342 + \frac{dT}{dz} \right) \qquad (2.12)$$

Then equation (2.9) can be written as

$$C_R = - \omega \; . \; S = - \frac{1}{R} \int_0^S k \; . \; (S-x)\ dx \qquad (2.13)$$

In the simple case when the coefficient of refraction is constant along the line of sight AB, the refraction angle is given by

$$\omega = \frac{S}{2\ \rho} \qquad (2.14)$$

Substituting ρ from equation (2.11) into (2.14), gives

$$\omega = \frac{S\,k}{2\,R} \tag{2.15}$$

Then, the refraction correction for a circular refraction path (constant k along the line of sight) is

$$C_R = -\frac{S^2}{2\,R} \cdot k \tag{2.16}$$

Which means that the refraction error is a function of the square of the sight length.

Equation (2.8) shows that, in order to compute the refraction angle, one needs to know the temperature gradient, dT/dz, along the line of sight. Thus, dT/dz has to be known as a function of height above the ground. The temperature gradient can be obtained either by observing the temperature of air at different heights above the ground and then fitting these observed values to a temperature function (see section 3.2), or by modelling in terms of sensible heat flux and some other meteorological parameters. Please refer to Chapters 3 and 4 for a detailed discussion of the refraction correction using meteorological method.

2.2 Determination of the Vertical Refraction Angle Using Lasers of Different Wavelengths

The dispersive property of the atmosphere can be used to determine the angle of refraction. In this approach the fact that blue light is bent slightly more than red light when propagating through a dispersive medium is used. A dispersometer measures the angle between the arriving beams of two different wavelengths by considering the time delay or phase difference between two photomultiplier signals related to the red and blue arriving refracted beams. Based on this measurement, the angle between arriving beams, $\Delta\omega$, can be computed. This $\Delta\omega$ has to be multiplied by a known factor V to obtain the angle of refraction ω [Williams and Kahmen, 1984]

$$\omega = V \cdot \Delta\omega \tag{2.17}$$

in which $V = N/\Delta N$, and N is the refractivity at standard values of pressure and temperature. The value of N for dry air at 288.15 K and 1013 mb is given by [Williams and Kahmen, 1984] as

$$N = \left[83.4213 + \frac{24060.3}{130 - w^2} + \frac{159.97}{38.9 - w^2} \right] \cdot 10^{-6} \tag{2.18}$$

where w is the wavenumber [μm^{-1}] of the light in vacuo. For red and blue colours with wavelengths of 633 nm and 442 nm respectively, ΔN is about 0.000004 while N for the mean of the two wavelengths is around 0.000279 which means that the value of V is close to 70. The variance of the refraction angle can be found by applying the propagation law of variances to equation (2.17)

$$\sigma_{\omega}^{2} = V^{2} \cdot \sigma_{\Delta\omega}^{2} \tag{2.19}$$

According to equation (2.19) the precision of $\Delta\omega$ has to be about 70 times higher than the required precision of the angle of refraction ω. This requirement puts a limit on the performance of this method; however, according to Brunner [1979a], an accuracy of 0.5" for the vertical refraction angle can be expected in the near future under favourable observation conditions using the dispersion method.

Using this dispersion method, a number of tests were carried out in the Spring and Autumn of 1978 and January of 1980 by Williams [1981]. The tests were made over a 4 km line using two bench marks with a known height difference. A T3 theodolite was used along with a dispersometer to measure the vertical angle and its corresponding refraction angle. On average, the observed refraction effect deviated from the estimated value by about -1.6" in 1978 and by about +0.9" in 1980.

2.3 Angle of Refraction Derived from the Variance of the Angle-of-Arrival Fluctuations

A method based on studies of light propagation in the atmosphere (turbulent medium) was first proposed by Brunner [1979a]. This method gives the angle of refraction in terms of the variance of the angle-of-arrival fluctuations σ^2 caused by atmospheric turbulence.

The angle-of-arrival fluctuations correspond to the fluctuations of the normal to the wavefront, arriving at the telescope [Lawrence and Strohbehn, 1970]. Brunner [1980] refers to the variance of the angle-of-arrival fluctuations as the variance of the image fluctuations.

σ^2 could be inferred from the spread of the image dancing, estimated by visual observations through the telescope [Brunner, 1979a]. For a precise determination of the mean and the variance of the angle-of-arrival, the image of a suitable light source can be continuously recorded in the telescope using a photo detector connected to a data logger [Brunner, 1980].

Brunner [1979a] has derived a formula for the angle of refraction in terms of the standard deviation of the angle-of-arrival, σ, and some meteorological parameters. Since this formula needs a detailed background, it is not given here. Brunner [1979a, 1979b, 1980, 1982, 1984] provides a complete treatment of the subject.

The major advantage of this method over the other established methods is that the computed angle of refraction is a better representation of the whole optical path, since it is derived from measurements along the actual line of sight [Brunner, 1980].

2.4 Determination of the Vertical Refraction Correction Using the Reflection Method

Figure 2.2 illustrates the principle of the reflection method with an exaggerated scale in the vertical angle α. The target can be a point light source with the same elevation as the cross-hair of the level instrument.

When there is no refraction, the reflected image of target would be seen on the cross-hair. When the line of sight is refracted, the incident angle to the mirror is no longer a normal but makes an angle, α, to the normal. The reflected ray will be also refracted to the same direction and the final image will be seen lower or higher than the cross-hair at point A'. If the coefficient of refraction happens to be constant along the line of sight (circular refraction path) then, point A' and the cross hair will be separated by 4C, where C is the magnitude of refraction affecting the levelling observations. The factor of 4 is not unexpected since the ray has traversed twice the length of the line and as it was shown before, the refraction effect is proportional to the square of the distance for a circular refraction path. However, in general the coefficient of refraction varies along the line of sight and the magnitude of the separation could be smaller or larger than 4C which makes the method inaccurate. This is the major drawback of the method.

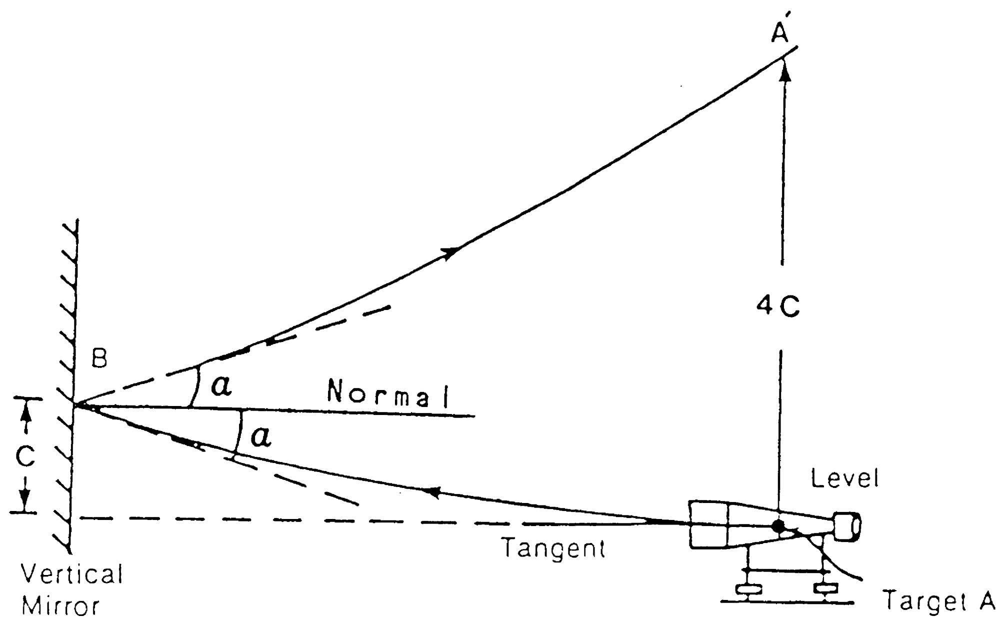

Figure 2.2: Principle of refraction by reflection (after Angus-Leppan [1985])

2.5 Comments on the Discussed Methods

Among the four approaches considered in the above discussion, the meteorological method is the only one which has been developed and applied in practice for refraction corrections in geodetic levelling. The dispersion and the variance of the angle-of-arrival methods are promising and they may show a better performance in the near future since they both rely on further advances in technology.

Because the angle between the two receiving beams is very small in the dispersion method, it must be measured to a very high accuracy. This makes severe demands on the performance of the dispersometer. Although recent technology has made it possible to measure the differential dispersion angle with a good precision, test measurements have shown that atmospheric turbulence imposes considerable limitations and good measurements are only possible under favourable conditions.

The variance of the angle-of-arrival method is in its developement stage and the instrumentation for the very precise measurement of the fluctuations of the image has still to be built. But it has the potential of being a useful approach, since it takes into account the variations of refraction effect due to the refractive index fluctuations along the actual line of sight.

The main disadvantage of the reflection method is that for a non-circular refracted line of sight, it is not possible to estimate the total refraction effect and some residuals remain in the results of measurements.

Further discussion in this thesis is based mainly on the application of the meteorological method.

Chapter 3

REFRACTION CORRECTION IN GEODETIC LEVELLING USING THE METEOROLOGICAL METHOD

Geodetic levelling, though remarkably simple in principle, is an inherently precise measurement approach which has remained practically unchanged since the turn of the century. Over a long distance its results depend on a great number of instrument stations with a very small systematic error in each set-up that accumulates steadily. The most troublesome errors are due to rod calibration and refraction. These are both height gradient correlated systemtic errors which may not be detected in loop closure analysis.

Error in rod calibration can be controlled through a combination of field and laboratory procedures. Refraction error is less easily controlled and is more complex because, in addition to height difference, it is a function of temperature gradients and the square of the sight length [Vaníček et al., 1980].

In this chapter, methods of refraction correction in geodetic levelling derived from meteorological measurements are discussed.

3.1 Refraction Correction Based on Direct Measurement of Temperature Gradient

The first important step in solving the refraction error problem was taken in 1896 by Lallemand when he suggested a logarithmic function for temperature, t [°C], in terms of height, z [m], above the ground [Angus-Leppan, 1984]

$$t = a + b \ln(z + c) \tag{3.1}$$

where a, b and c are constants for any instant.

Lallemand's model was applied in research work by Kukkamäki [1939a, 1961] with respect to the lateral refraction error in horizontal angle observation on a sideward slope. In geodetic levelling, Heer [1983] has shown that Lallemand's model works almost like some of the recently proposed models. Lallemand's theoretical investigations in geodetic refraction were never applied in practice, since up to a few decades ago there were other greater errors involved such as errors in poorly designed rods and instruments.

About forty years after Lallemand, Kukkamäki [1938, 1939b] formulated his temperature model and corresponding refraction correction which was based on the following assumptions:

1. the refraction coefficient of air depends mainly on temperature since the effect of humidity is negligibly small for optical propagation,
2. isothermal surfaces are parallel to the ground, and

3. the terrain slope is uniform in a single set-up of the instrument.

The Kukkamäki temperature model is an exponential function of height

$$t = a + b\,z^{c} \qquad (3.2)$$

Where t [°C] is the temperature at height z [m] above the ground and a, b and c are constants for any instant and vary with time. The constant a does not play any role since the refractive coefficient is a function of the temperature gradient and constants b and c can be easily computed using three temperature sensors at different heights arranged such that

$Z_1 / Z_2 = Z_2 / Z_3$, then, with $t_i = a + b\,Z_i^{c}$

$$\Delta t_1 = t_2 - t_1 = b\,(Z_2^{c} - Z_1^{c})$$

$$\Delta t_2 = t_3 - t_2 = b\,(Z_3^{c} - Z_2^{c})$$

so,

$$\ln\left[\frac{\Delta t_2}{\Delta t_1}\right] = \ln\left[\frac{Z_3^{c} - Z_2^{c}}{Z_2^{c} - Z_1^{c}}\right] = \ln\left[\frac{Z_3^{c} / Z_2^{c} - 1}{1 - Z_1^{c} / Z_2^{c}}\right]$$

Replacing Z_3^c / Z_2^c by Z_2^c / Z_1^c yields

$$c = \ln (\Delta t_2 / \Delta t_1) / \ln (Z_2 / Z_1) \tag{3.3}$$

$$b = \Delta t_1 / (Z_2^c - Z_1^c) \tag{3.4}$$

In a simple case, when only two temperature sensors are used, an average value can be used for c. Holdahl [1981] recommends a value of -1/3 for c which agrees with the theories of turbulent heat transfer in the lower atmosphere [e.g. Priestley, 1959 and Webb, 1964].

3.1.1 Kukkamäki's equation for geodetic levelling refraction correction

In geodetic levelling, the line of sight starts out horizontally at the instrument while making an angle α_1 with the assumed surfaces of constant refractive index that are parallel to the ground. This makes α_1 also the slope of the ground surface. Then, the following relation holds [e.g. Kukkamäki, 1938]

$$n \cos \alpha_1 = \text{constant.} \tag{3.5}$$

Differentiating with respect to the refractive index n and α_1 results in

$$d\alpha_1 = (dn/n) \cot \alpha_1 \tag{3.6}$$

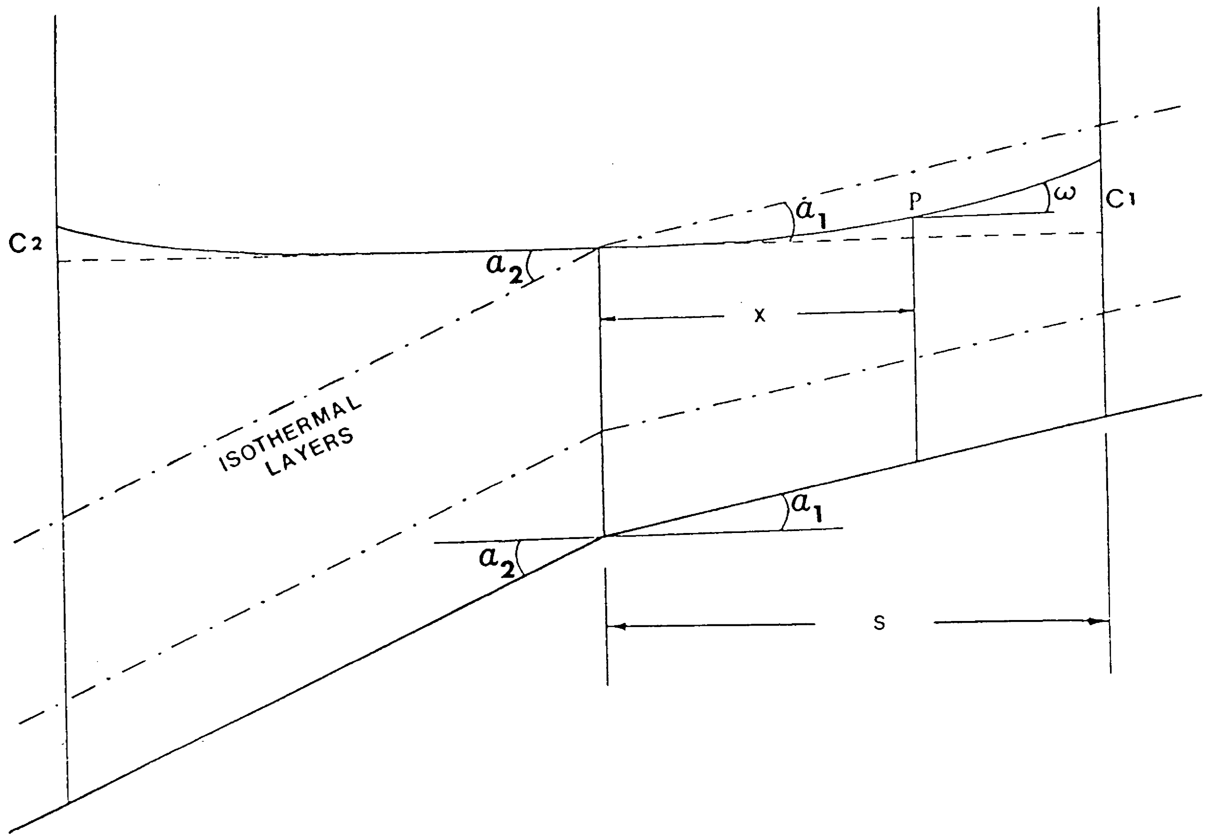

Figure 3.1: Refraction effect in a geodetic levelling set-up

Due to the change in refractive index along the line of sight at a point, *P*, at a distance x, the line of sight inclines at an angle, ω (see *Figure* 3.1). The angle ω is given by integration along the line of sight

$$\omega = \int_{n_o}^{n} \frac{1}{n} \cot \alpha_1 \, . \, dn \tag{3.7}$$

where n_o and n are the refractive indices at the instrument and at the point *P*, respectively. From equation (3.7) we have

$$\omega = - \cot \alpha_1 \ \ln (n/n_o) \tag{3.8}$$

or, with sufficient accuracy [Kukkamäki, 1938]

$$\omega = - \cot \alpha_1 \ (n - n_o)/n_o \tag{3.9}$$

Equation (3.9) shows that ω is a function of the differences of the two refractive indices and of α_1, the angle of the slope of the ground surface.

Differentiation of equation (2.3) with respect to t after neglecting the e term gives

$$dn = - \frac{293 \times 0.00366}{(1 + 0.00366\ t)^2} \cdot \frac{p}{1013.25} \cdot 10^{-6} \cdot dt \tag{3.10}$$

or, with sufficient accuracy [Kukkamäki, 1938]

$$dn = - [\ 0.931 - 0.0064\ (\ t - 20\ )\ ]\ \frac{p}{1013.25} \cdot 10^{-6} \cdot dt \tag{3.11}$$

where, t is the temperature [°C] and p is the pressure [mb].

If $dt = (t - t_o)$ and $dn = (n - n_o)$ are considered to be infinitely small increments and substituting equation (3.4) into equation (3.11) and assuming $dt \simeq \Delta t$, gives

$$n - n_o = d \cdot b \cdot (z^c - Z_i^c) \tag{3.12}$$

in which,

$$d = - 10^{-6} [0.931 - 0.0064 (t -20)] \frac{p}{1013.25}, \tag{3.13}$$

where, z = the rod reading [m], and

Z_i = the instrument height [m].

In Figure 3.1 the vertical refraction effect at a distance x is given by integrating ω along the line of sight

$$Cl = \int_0^x \omega \, dx = - \frac{d \cdot b}{n_o} \cdot \cot \alpha_1 \cdot \int_0^x (z^c - Z_i^c) \, dx \tag{3.14}$$

From Figure 3.1

$$x = (z - Z_i) \cot \alpha_1 \tag{3.15}$$

and from equation (3.15)

$$dx = dz \cdot \cot \alpha_1$$

then

$$Cl = - \frac{b \cdot d}{n_o} \cdot \cot^2 \alpha_1 \cdot \int_{Z_i}^{Z_b} (z^c - Z_i^c) \, dz \tag{3.16}$$

Assuming n_o = 1.000, the refraction correction in the back-sight is found to be [Kukkamäki, 1938]

$$C1 = - \cot^2 \alpha_1 . d . b . \left[\frac{1}{c+1} Z_b^{c+1} - Z_i^c Z_b + \frac{c}{c+1} Z_i^{c+1} \right] \tag{3.17}$$

A similar expression can be obtained for the fore-sight

$$C2 = - \cot^2 \alpha_2 . d . b . \left[\frac{1}{c+1} Z_f^{c+1} - Z_i^c Z_f + \frac{c}{c+1} Z_i^{c+1} \right] \tag{3.18}$$

The total refraction correction for one instrument set-up is given by

$$C_R = C2 - C1$$

$$C_R = \cot^2 \alpha . d . b . \left[\frac{1}{c+1} (Z_b^{c+1} - Z_f^{c+1}) - Z_i^c (Z_b - Z_f) \right] \tag{3.19}$$

where, Z_b and Z_f are backward and forward rod readings [m], C_R is the refraction error [m] and $\alpha = \alpha_1 = \alpha_2$ is assumed.

The temperature profile adopted by Kukkamäki was based on direct temperature measurement at different heights from the surface. His empirical studies utilized the temperatures measured by Best in 1935 at heights of 2.5 cm, 30 cm and 120 cm above the ground [Kukkamäki, 1939b]. There are some other models based on direct temperature measurements, suggested by researchers such as Garfinkel

[1979] and Heer and Niemeier [1985]. Heer and Niemeier [1985] have given a summary of eight models including Kukkamäki's model. In the last few years, a research study was conducted at the University of New Brunswick that lead to the development of new models which are discussed in Chapter 5.

3.2 Refraction Correction Formulated in Terms of Sensible Heat Flux

The second group of models is based on the laws of atmospheric physics. There is extensive literature available in this field and for comprehensive treatment one can refer to Webb [1984].

Webb [1969] was the first who explained at a conference in 1968 that it could be feasible to evaluate an approximate vertical gradient of mean temperature through its relationship with other meteorological parameters. Subsequently a number of papers were written on this subject [e.g. Angus-Leppan, 1971 and Angus-Leppan and Webb, 1971]. The following section is a review of the meteorological parameters.

3.2.1 Review of the meteorological parameters

1. Potential Temperature Θ

Potential temperature is defined as the temperature that a body of dry air would take if brought adiabatically (with no exchange of heat) to a standard pressure of 1000 mb

[Angus-Leppan and Webb, 1971]. Potential temperature can be related to the absolute temperature, T [K], at a pressure, p [mb], using Poisson's equation [e.g. Fraser, 1977]

$$\theta = T\,(\,1000/p\,)^{0.286} \qquad [K] \qquad (3.20)$$

Equation (3.20) shows that for pressure near the standard (1000 mb), the difference between the potential temperature and the absolute temperature is very small. The gradients of absolute and potential temperature are related by

$$d\theta/dz = dT/dz + \Gamma \qquad [K/m] \qquad (3.21)$$

Where $\Gamma = 0.0098$ [K/m] is the adiabatic lapse rate.

2. Friction velocity u*

Friction velocity is a reference velocity which is related to the mean wind speed, U, and is given by

$$u^* = k\,U\,/\,\ln\,(\,Zv\,/\,Zr\,) \qquad [m/s] \qquad (3.22)$$

where k is von Karman's constant with numerical value 0.4, U is measured at height Zv, and Zr is the roughness length. This roughness length, Zr, is the height at which the wind velocity is equal to zero. For grassland, Zr is about 10% of the grass height, and for pine forests, this value is between 6% to 9% of the mean height of the trees [Webb, 1984]. For more details see e.g. Priestly [1959].

3. Sensible heat flux H

Sensible heat flux forms one element of the energy balance equation at the surface of the earth where it combines with other elements, namely: net radiation, Q; heat flux into the ground, G; and evaporation flux, λE. According to the energy balance equation, the sensible heat flux is given by [e.g. Munn, 1966]

$$H = Q - G - \lambda E \qquad [\ W/m^2\ ] \qquad (3.23)$$

in which

$$Q = Sd - Su + Ld - Lu \qquad (3.24)$$

where, Sd = the downward short-wave radiation flux (0.3 to 3 μm) from sun and sky; Sd is not present at night,

Su = the short-wave radiation reflected from the surface,

Ld = the downward long-wave radiation flux (4 to 60 μm) received by the earth from the atmosphere,

Lu = the upward long-wave radiation flux emitted by surface,

G = the heat flux into ground [W/m^2], and

λE = the latent heat flux of evaporation or condensation in [W/m^2], with λ being the latent heat of the vapourization of water and E is the rate of evaporation.

3.2.2 Thermal stability parameter

According to meteorological literature regarding the distribution of the average wind velocity, the temperature gradient parameter which governs the degree of thermal stability is a very significant element [Obukhov, 1946]. There exists one governing nondimensional parameter which is height dependent. At each height it indicates the thermal stability condition. This parameter is the well known Richardson number Ri that has the following appearance [e.g. Priestley, 1959]

$$Ri = (g \cdot d\Theta/dz) / (\Theta \cdot (dU/dz)^2) \qquad (3.25)$$

where g is the acceleration due to gravity [m/sec^2].

Three regimes of thermal stability can be distinguished:

1. Stable stratification occurs when $Ri > 0$ (inversion). This condition appears when the surface is cooled. Under this condition, the thermal buoyancy forces suppress the turbulence and cause the downward transfer of heat.
2. Neutral stratification occurs when $Ri = 0$. It appears a short time after sunrise and a short time before sunset. Under this condition the distribution of temperature with height is adiabatic (no exchange of heat).

3. Unstable stratification occurs when $Ri < 0$ (lapse). It appears typically on a clear day when the ground is heated by incoming solar radiation, the heat is being carried upwards by the current of air and the turbulence will tend to be increased by thermal bouyancy forces.

For conditions near to neutral when the Ri value is small [Webb, 1964]

$$Ri = z / L \tag{3.26}$$

where L is the Obukhov scaling length [m]. Using the above equations the following expression can be found for L

$$L = - \left[\frac{u_*^3 \, C_p \, \rho \, \theta}{k \, g \, H} \right] \tag{3.27}$$

where C_p and ρ are respectively the specific heat at constant pressure and the density of the air ($C_p \cdot \rho = 1200$ [$J/K\ m^3$]), and k is von Karman's constant ($k = 0.4$).

3.2.3 Profile of mean potential temperature gradients

According to equation (3.26), z/L can be regarded as another form of stability parameter. Equation (3.27) shows that L is a function of fluxes and constants which can be momentarily considered as constant throughout the surface layer, then L may be regarded as a characteristic height which determines the thermal structure of the surface layer.

In other words, the whole structure of the behavior expands and contracts in height according to the magnitude of *L* [e.g. Webb, 1964].

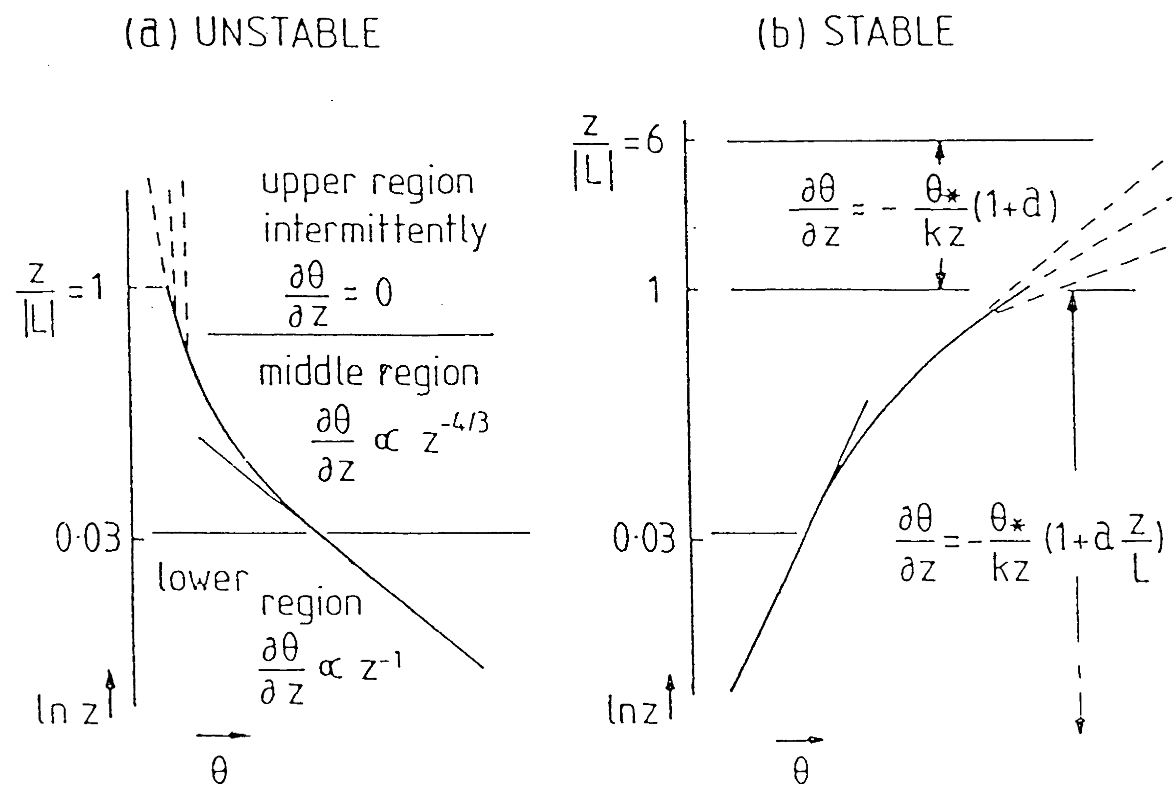

Figure 3.2: Profile of mean potential temperature Θ (a) unstable and (b) stable conditions. Broken lines indicate variablity over time intervals of several minutes in (a) or between 30-min runs in (b), (after Webb [1984]).

In this Figure, $\Theta^* = H / (C_P \rho u^*)$, and $a = 5$.

a. <u>Unstable conditions</u> Within the unstable turbulent regime, the mean potential temperature profile takes a different form in three different height ranges. Figure 3.2a shows the three regions of different physical behavior and the profile of θ in the unstable case. These three height ranges are defined according to L rather than absolute terms.

The lower region extends in height to $z = 0.03\ |L|$. In this region, the gradient of potential temperature is found to be inversely proportional to height

$$\frac{d\theta}{dz} = - \left[\frac{H}{C_p\ \rho\ k\ u*} \right] \cdot z^{-1} \tag{3.28}$$

The middle region extends over a height range of $0.03|L| < z < |L|$. Heat transfer in this region is mostly governed by a kind of composite convection (interaction of wind and thermal buoyancy effects) or free convection (in calm conditions) caused by density differences within the moving air. The potential temperature gradient profile in this region is given by

$$\frac{d\theta}{dz} = - \left[\frac{H}{C_p\ \rho} \right]^{2/3} \cdot \left[\frac{\theta}{g} \right]^{1/3} \cdot z^{-4/3} \tag{3.29}$$

This equation is uniquely dependent on H and z and independent of friction velocity u_* which means the middle region is independent of wind speed.

On a typical clear day when the Obukhov length varies between 25 m and 45 m, the middle region starts at a height 0.75 m to 1.35 m above the ground. This means that in most of geodetic optical measurement the critical part of the sight-line lies within this region.

Equation (3.29) can be simplified by substituting approximate values for g, θ and $C_p \rho$

$$g = 9.81\ [m\ s^{-2}],\ \theta = 290\ [K],\ \text{and}\ C_p \rho = 1200\ [j\ K^{-1}\ m^{-3}]$$

then,

$$\frac{d\theta}{dz} = -\ 0.0274\ H^{2/3} \cdot z^{-4/3} \qquad (3.30)$$

The upper region begins at a height approaching $|L|$ where the gradient of θ is often averaging near zero over a period of several minutes.

b. <u>Stable conditions</u> Figure 3.2b shows the profile of potential temperature in stable conditions. Within the stable regime, the following profile forms are found [Webb, 1969]

$$\frac{d\Theta}{dz} = - \left[\frac{H}{C_p \ \rho \ u_* \ k} \right] . \left[1 + \frac{5 z}{L} \right] . z^{-1} \qquad \text{for } z < L \tag{3.31}$$

and

$$\frac{d\Theta}{dz} = - \left[\frac{6 H}{C_p \ \rho \ u_* \ k} \right] . z^{-1} \qquad \text{for } z > L \tag{3.32}$$

In the lower region ($z < L$) the gradient changes rapidly with height for very small z, i.e. close to the surface, and with increasing height, the gradient dependence on height becomes weaker.

3.2.4 The Angus-Leppan equation for refraction correction

Once the temperature gradient is determined, the refraction correction computation can be simply carried out by using some equation similar to the Kukkamäki formula, equation (3.19).

The refraction effect on a back-sight in the unstable case is given by

$$Cl = 10^{-6} . p / T^{2} . s^{2} . B \qquad [m] \tag{3.33}$$

in which,

$$B = 1 - 3.3\, H^{2/3} \cdot \frac{Z_i^{2/3} + 2\, Z_i^{-1/3} \cdot Z_b - 3\, Z_b^{2/3}}{(Z_i - Z_b)^2}$$

and s is the length of line of sight [m] and the rest of the variables have already been defined above. Replacing the back rod reading by forward reading in this equation will give the refraction effect on fore-sight. This equation was first presented by Angus-Leppan [1979a]. A similar expression was given by him for the stable and neutral cases [Angus-Leppan, 1980]. However, he suggested [Angus-Leppan, 1984] that further investigation is needed, because data for estimating H for stable and neutral conditions is not yet adequate.

3.2.5 Investigation by Holdahl

Holdahl [1979] developed a method for correcting historical levelling observations obtained without Δt measurements. He was able to model the required meteorological parameters for estimation of sensible heat flux, H, by using the historical records of solar radiation, precipitation, cloud cover and ground reflectivity from many locations across the United States. The estimated sensible heat flux can be used to obtain temperature differences between two heights say Z and Z above the ground by integrating equation (3.29) [Holdahl, 1981]

$$\Delta t = t_2 - t_1 = 3 \left[\frac{H^2 T}{(C_p \rho)^2 g} \right] (Z_2^{-1/3} - Z_1^{-1/3}) - \Gamma \Delta Z \qquad (3.34)$$

where $\Gamma = 0.0098$ is the adiabatic lapse rate, $\Delta Z=(Z_2 - Z_1)$, and T is the absolute temperature [K] of air. In equation (3.34) the adiabatic lapse rate has very little influence on the estimated Δt and it can be neglected because ΔZ is at the most 2.5 m. Then, by letting [Holdahl, 1981]

$$b = 3 \left[\frac{H^2 T}{(C_p \rho)^2 g} \right] \qquad \text{and} \qquad c = - \frac{1}{3} ,$$

it can be seen that Δt from equation (3.34) is compatible with the form suggested by Kukkamäki in equation (3.4). Hence, equation (3.19) can be applied for refraction correction computation with Δt obtained by equation (3.34). In addition, Holdahl takes into account the effect of cloud cover by multiplying a sun correction factor to the predicted temperature differences. The sun correction factor is based on sun codes which have traditionally been recorded during the course of levelling by the National Geodetic Survey of the United States. During the transitional stage, when the condition is near neutral, Δt can also be affected by wind and the influence is taken into account by considering another code for wind similar to the one for sun.

3.3 Comments on the Meteorological Methods

The two meteorological methods for determination of the refraction correction based on either measured or modeled temperature gradient were reviewed in this chapter. Due to the large fluctuations in temperature, the direct measurement of temperature gradient has to be carried out over a period of a few minutes in every meteorological station along a route of precise levelling. The mean of these temperature gradients can be used for correcting the levelling done in the corresponding period of temperature gradients measurements. The second approach tends to smooth out the time fluctuations which can be considered as an advantage of this method over the direct approach. However, the results of either may be satisfactory for correcting geodetic levelling measurements. For example, Whalen [1981] compared Kukkamäki's approach against Holdahl's method and reported that a net reduction in refraction error of at least 70% is achieved using either of the methods.

Chapter 4

REFRACTION CORRECTION IN TRIGONOMETRIC HEIGHT TRAVERSING

A numerical integration of equation (2.13) will give the magnitude of refraction correction. This can be carried out using the trapezoidal rule by dividing the line into n sections of length

$$s_1, s_2, s_3 \quad \ldots\ldots \; s_n$$

with corresponding refraction coefficients

$$k_1, k_2, k_3 \quad \ldots\ldots \; k_n$$

then the integration part of equation (2.13) is

$$I = \int_0^S k\,(S - x)\,dx$$

$$= \frac{s_1}{2}\left[k_1 S + k_2 (S - x_1) \right]$$

$$+ \frac{s_2}{2}\left[k_2 (S - x_1) + k_3 (S - x_2) \right] + \ldots.$$

$$\ldots. + \frac{s_n}{2}\left[k_n (S - x_{n-1}) + k_{n+1} (S - x_n) \right] \qquad (4.1)$$

where

$$x_1 = s_1 , \quad x_2 = s_1 + s_2 , \ldots , x_n = s_1 + s_2 + \ldots + s_n = S$$

In equation (4.1), refraction coefficients along the line of sight can be calculated by using equation (2.12) which is in terms of the vertical gradient of temperature. The temperature gradient at a height z above the ground can be either determined: a) from a temperature function such as Kukkamäki's model, equation (3.2), or b) from equations which are in terms of sensible heat flux and are dicussed for the case of geodetic levelling in Chapter 3. The line of sight in trigonometric height traversing is longer than in geodetic levelling and one cannot assume that the terrain slope is uniform. On the other hand, when the refraction correction is needed, the meteorological measurement cannot be carried out in more than one location in practice. To overcome this problem, one may choose a location characteristic for a set up of trigonometric height traversing and make the meteorological measurements as frequent as possible during the period when the vertical angle observations take place. According to this gathered meteorological information, the temperature model and the profile of the terrain, the coefficient of refraction for the points along the line can be computed.

The following sections discuss the required temperature gradient accuracy and the difficulties involved for correcting refraction in reciprocal and leap-frog trigonometric height traversing.

4.1 Reciprocal Trigonometric Height Traversing

On a moderately uniform terrain, the refraction effect in reciprocal trigonometric height traversing is more or less symmetrical, and in optimal conditions of overcast and mild wind speed, the refraction effect is minimal on such terrain. But terrain changes in slope and in texture of the surface. Usually a combination of asphalt at the centre of the road, gravel at the side and vegetation come into effect. These make the evaluation of the refraction error using equation (2.9) very difficult or impossible, if the meteorological data is gathered only at one point of the line of sight. In addition, as it will be shown below, a very accurate temperature gradient is needed to compute the refraction error.

A simultaneous reciprocal vertical angle observation is considered by many researchers as the only reliable, yet only partial, solution to the refraction problem.

For the sake of error analysis, the formulation of height difference computation in the reciprocal method is reviewed below.

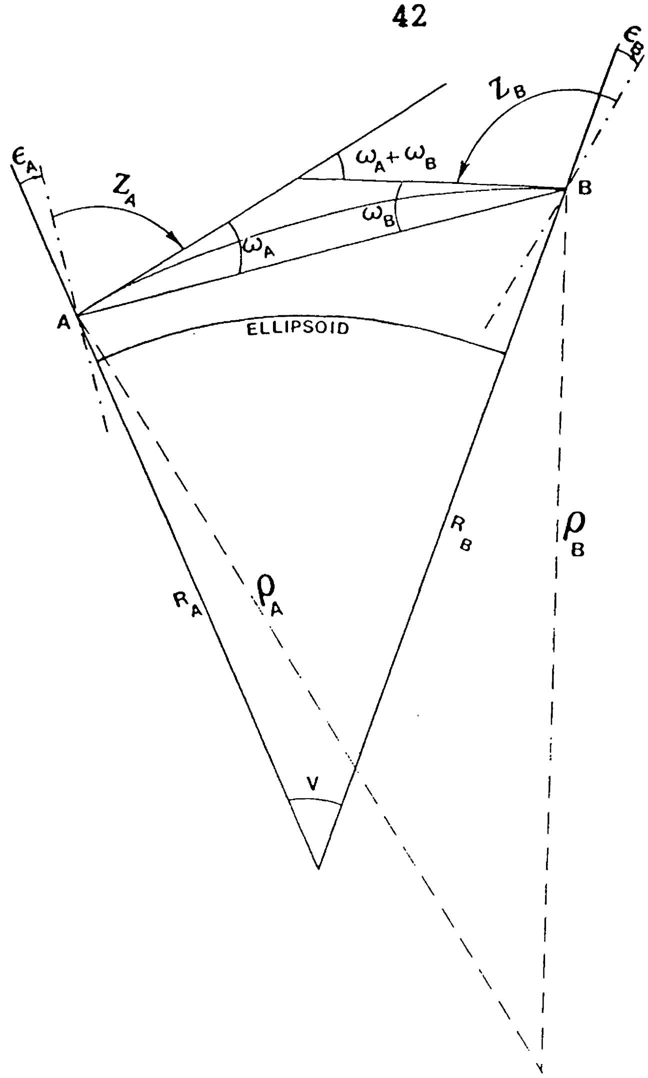

Figure 4.1: Ellipsoidal section for reciprocal trigonometric height traversing

4.1.1 Formulae of reciprocal trigonometric height traversing

Assuming a circular refracted path *AB*, the refraction angle, ω, in term of the angle between *A* and *B* subtended at the centre of the earth, V, and the refraction coefficient at point *A* is given by

$$\omega_A = k_A V / 2 \tag{4.2}$$

and from Figure 4.1 the angle V is

$$V = \frac{S}{R} \cdot \sin Z_A \tag{4.3}$$

then

$$\omega_A = \frac{S}{2R} \cdot k_A \cdot \sin Z_A \tag{4.4}$$

which is the same as equation (2.15). In this equation R is the radius of the earth and k is the coefficient of refraction. Considering Figure 4.1, the ellipsoidal height difference from A to B is given by Brunner [1975a] as

$$\Delta h_{AB} = S \cos Z_A - S \sin Z_A \; (\varepsilon_A - \omega_A - V/2) \tag{4.5}$$

where ε_A = the deflection of the vertical at point A.

Subsitution of ω_A and V from equations (4.3) and (4.4) into (4.5) gives

$$\Delta h_{AB} = S \cos Z_A - \frac{1}{2R} (S \sin Z_A)^2 \; (1 - k_A) - S \sin Z_A \; (\varepsilon_A) \tag{4.6}$$

A similar expression can be written for the height difference from B to A

$$\Delta h_{BA} = S \cos Z_B - \frac{1}{2R} (s \sin Z_B)^2 \; (1 - k_B) - S \sin Z_B \; (-\varepsilon_B) \tag{4.7}$$

Assuming $\sin z_A \simeq \sin z_B$ and combining 4.8 and 4.9 gives

$$\Delta h = \frac{S}{2} (\cos Z_A - \cos Z_B) - \frac{1}{4R} D^2 (k_A - k_B) -$$

$$\frac{S}{2} \sin Z_A (\varepsilon_A + \varepsilon_B) \qquad (4.8)$$

where $D = S \sin Z$ is the horizontal distance. In this equation, the second term is the correction due to refraction. The third term is the effect of the deviation of the vertical which can be neglected for lengths of sight of less than 500 m and in moderately hilly topography without any loss of accuracy [e.g. Rueger and Brunner, 1982].

4.1.2 Achievable accuracy using reciprocal trigonometric height traversing

Ignoring the effect of the deviations of the vertical, the variance of a measured height difference can be found by applying the law of propagation of variance to equation (4.8) [Brunner, 1975a]

$$\sigma^2 = (\cos Z_A)^2 \sigma_S^2 + \frac{1}{2} D^2 \sigma_Z^2 + \frac{1}{16 R^2} D^4 \Delta k^2 \qquad (4.9)$$

where $\Delta k = k_A - k_B$ is treated as a random error and $\cos Z_A$ is assumed to be equal to $-\cos Z_B$ for the purpose of error analysis.

Using equation (4.9) and assuming uncertainties of 1.0" in zenith angle and 5 mm in slope distance and 0.3 in the coefficient of refraction (for simultaneous observation), a precision of 3.1 mm$\sqrt{K}$ (K in km) is expected over an average slope angle of 10° and traverse legs of 300 m. Under the same assumption with traverse leg lengths of 500 m, the estimated precision is 5.0 mm$\sqrt{K}$ (K in km).

Rueger and Brunner [1981] have reported a precision of 4.3 mm$\sqrt{K}$ (K in km) in a practical test of reciprocal non-simultaneous trigonometric height traversing with an average sighting distance of 310 m and an average zenith angle of 88° 30'. This result shows that in non-simultaneous observations the uncertainty in the coefficient of refraction is more than 0.3. The ΔK estimated by Rueger and Brunner [1981] for non-simultaneuos observations is about 0.57.

By using recently developed precision electronic theodolites to measure zenith angles, the standard error can be as small as 0.5" if performing four sets of measurements [Chrzanowski, 1984]. If the uncertainty due to the slope distance measurement is reduced to 3.0 mm with a proper calibration and use of the *EDM*, then the achievable accuracy in the above cases will be 2.4 mm$\sqrt{K}$ and 4.4 mm$\sqrt{K}$ (K in km) for the traverse legs of 300 m and 500 m, respectively.

The National Geographic Institute (*IGN*) in Paris has carried out extensive reciprocal trigonometric height traversing tests from 1982 to 1985. The results are very impressive. *IGN* claims errors of 1 mm$\sqrt{K}$ and 3 mm$\sqrt{K}$ (K in km) with lengths of sight to 400 m and 1500 m, respectively [Kasser, 1985]. The National Geodetic Survey (*NGS*) in the United States has tried reciprocal trigonometric height traversing on a 30 kilometer loop. The standard error of a mean double run of 1 mm$\sqrt{K}$ (K in km) was achieved with lengths of sight of up to 148 m [Whalen, 1985]. Reciprocal trigonometric height traversing was used to determine heights in a network with a total length of the interconnecting lines of over 70 km by the Department of Surveying Engineering at the University of New Brunswick [Chrzanowski, 1985]. The area was moderately flat with a general inclination of less than 5°. According to a feasibility study carried out a year earlier, the overall accuracy was expected to be around 1.5 mm$\sqrt{K}$ (K in km) or better [Chrzanowski, 1984]. An adjustment of the network after rejection of one line, gave the estimated standard deviation of 1.8 mm$\sqrt{K}$ (K in km) which was almost the same as the expected value.

4.1.3 Precision of refraction corrections in reciprocal method

In equation (4.8) the second term is the magnitude of the refraction effect in the reciprocal method. The difference in the refraction coefficients between direct and reverse measurements is needed to compute the refraction correction. Substituting equation (2.12) into (4.9) and considering only the refraction correction term, yields

$$C_R = \frac{D^2}{4\,R}\left[\frac{17.2\,p_A}{T_A^2} + \frac{502.7\,p_A}{T_A^2}\cdot\frac{dT_A}{dz} - \frac{17.2\,p_B}{T_B^2} - \frac{502.7\,p_B}{T_B^2}\cdot\frac{dT_B}{dz}\right] \tag{4.10}$$

where $D = S \sin Z$ is the horizontal distance. Assuming $p = p_A = p_B$ and $T = T_A = T_B$ simplifies equation (4.10) to

$$R_R = \frac{D^2}{4\,R}\cdot\frac{502.7\,p}{T^2}\left[\frac{dT_A}{dz} - \frac{dT_B}{dz}\right] \tag{4.11}$$

Applying the error propagation law of variance to equation (4.11) yields

$$\sigma_C = \left(\frac{D^2}{4\,R}\cdot\frac{502.7\,p}{T^2}\right)\left[\sigma^2_{dA} + \sigma^2_{dB}\right]^{1/2} \tag{4.12}$$

where dA and dB stand for $\frac{dT_A}{dz}$ and $\frac{dT_B}{dz}$ respectivily and σ_C is the standard deviation of a refraction correction. Assuming $\sigma = \sigma_{dA} = \sigma_{dB}$, $p = 1013$ mb and T=300 K, equation (4.12) will be simplified to

$$\sigma_C = \frac{2\,D^2}{R}\,\sigma \tag{4.13}$$

where σ is the standard deviation of the measured or modeled temperature gradient. Figure 4.2 shows the standard deviation of the refraction correction versus sighting distance D.

According to equation (4.12), for sighting distances greater than 100 m, a very accurate temperature gradient along the line of sight is required to compute the refraction correction. Measuring the temperature gradient along the line of sight is neither practical nor economical. On the other hand, as it will be shown later, when the lines of sight are shorter than 100 m, the effect of refraction becomes randomized to a large extent and the refraction correction is not required (see Chapter 6). Although limiting the line of sight seems to be a more reliable solution than carring out the refraction correction, it is not economical.

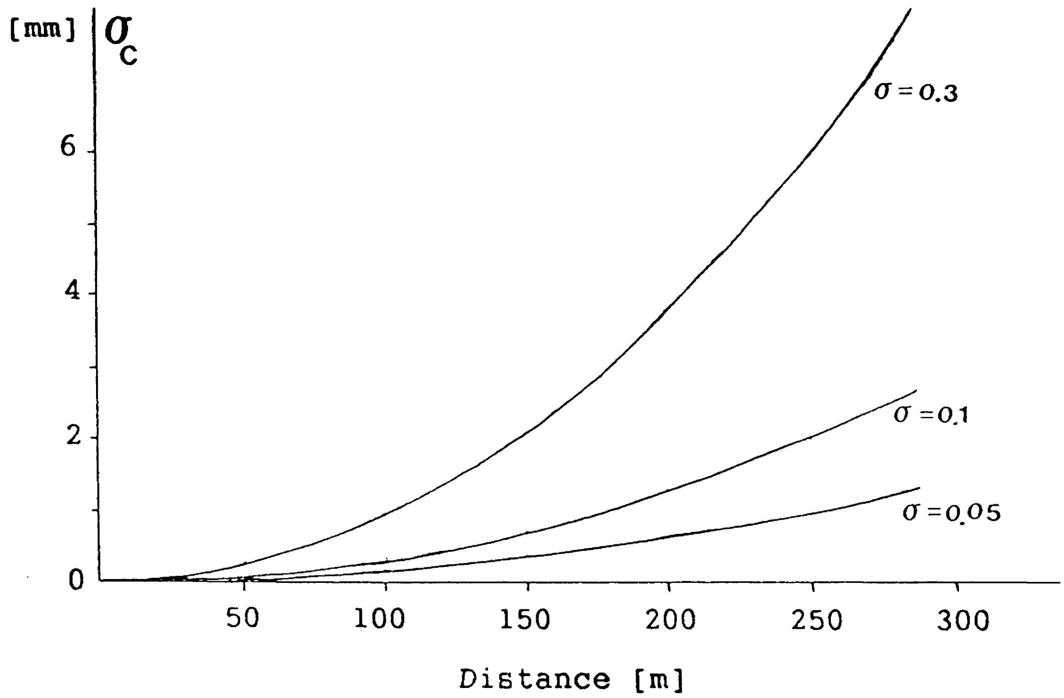

Figure 4.2: Standard deviation of refraction correction in reciprocal height traversing as a function of distance. Curves show standard deviation of refraction correction for temperature gradient precision of 0.05 °C/m, 0.1 °C/m and 0.3 °C/m, assuming *P*=1013. mb and *T*=300 *K*.

Three other methods for the determination of the refraction angle were discussed in Chapter 2. The author believes that these methods can be used indirectly to compute the refraction effect in the reciprocal method. The following section is a summary of this new proposed method.

4.1.4 Proposed method for the calculation of refraction correction

Considering equation (4.5) a similar expression can be written for the ellipsoidal height difference from *B* to *A*

$$\Delta h_{BA} = S \cos Z_B - S \sin Z_B \, (-\varepsilon_B - \omega_B - V/2) \qquad (4.14)$$

Theoretically the sum of two direct and reverse height differences must be zero [Brunner, 1975a]

$$\Delta h_{BA} + \Delta h_{AB} = 0$$

or

$$S\ (\cos Z_A + \cos Z_B) - D\ [\ \varepsilon_A - \varepsilon_B + \omega_A + \omega_B - V\ ] = 0$$

then,

$$\omega_A + \omega_B = \frac{S}{D}\ (\cos Z_A + \cos Z_B) + V - (\ \varepsilon_A - \varepsilon_B\ ) \tag{4.15}$$

where, $D = S \sin Z_A = S \sin Z_B$

The effect of the deviation of the vertical for short distances (less than 500 m) can be neglected without any loss of accuracy, because the total of two refraction angles are affected by

$$\Delta\varepsilon = \varepsilon_A - \varepsilon_B$$

The angle V can be estimated with sufficient accuracy by using equation (4.3). Then the total of the refraction angles can be written as

$$\omega_A + \omega_B = \frac{S}{D}\ (\cos Z_A + \cos Z_B) + \frac{S}{R}\ \sin Z_A \tag{4.16}$$

According to this equation the total of refraction angles can be computed in terms of either measured or approximately known quantities.

In reciprocal levelling, as it can be seen from equation (4.11), the main concern is the difference of the two refraction angles

$$\Delta\omega = \omega_A - \omega_B$$

which affect the result of measurements. Therefore, in order to make corrections to reciprocal observations, one has to compute individual refraction angles or divide the total of refraction angles by considering different weights for each refraction angle. A weight can be estimated using either the dispersion or the reflection or the angle-of-arrival method discussed in Chapter 2. Here only the angle-of-arrival approach is considered which can be more appropriate for unstable conditions and does not need any special instrumentation. The angle-of-arrival method was proposed by Brunner [1979a] for estimation of angle of refraction. As it was mentioned in Chapter 2, Brunner [1979b, 1980 and 1982] gives a detailed discription of the variance of angle-of-arrival measurements and its application for refraction angle computation by using some meteorological observations. In a reciprocal mode of observation, the amplitude of image dancing can be measured from both sides and these two measured amplitudes can be used as the weights to split the total refraction angle into two separate refraction angles. Kukkamäki [1950] has measured the amplitude of image fluctuations (spread of the image dancing) from 10 second long visual observations through the telescope of a level instrument. A more accurate method of measuring the image fluctuation using a photo detector is described by Brunner [1980]. However, for further investigation on the proposed total of refraction angles method, only the visual measurement may be sufficient, because information beyond the frequency sensitivity of the human eye (15 Hz) is not necessary [Brunner, 1979b].

This method is recommended for observations during clear days under unstable conditions.

4.2 Refraction in Leap-Frog Trigonometric Height Traversing

An alternative approach to the reciprocal method could be leap-frog trigonometric height traversing. This method over a terrain that is uniform both in slope and the material with which the surface is covered can be affected by refraction symmetrically for the back- and the fore-sight. But in practice when levelling along a highway the slope of the route is not uniform and the back-sight may pass over a ground covered by material (e.g. grass) different from the fore-sight (e.g. asphalt). These are the situations that can magnify the differential refraction effect in the leap-frog method. The greatest weakness of the leap-frog method is the necessity of finding the mid-point (theodolite station) before the actual measurement takes place and it has to be located to better than 10 m. In mountainous terrain a careful reconnaissance to find the mid-point is a difficult and time consuming task.

4.2.1 Leap-Frog Trigonometric Height Traversing Formulae

Two expressions similar to equation (4.5) can be written for the back- and the fore-sight in leap-frog arrangement:

$$\Delta h_{MA} = S_A \cos Z_A - S_A \sin Z_A \,(-\varepsilon - \omega_A - V_A/2) \qquad (4.17)$$

$$\Delta h_{MB} = S_B \cos Z_B - S_B \sin Z_B \,(\varepsilon - \omega_B - V_B/2) \qquad (4.18)$$

A combination of these two equation gives

$$\Delta h = \Delta h_{MB} - \Delta h_{MA} = (S_B \cos Z_B - S_A \cos Z_A) - \varepsilon\,(D_B + D_A) -$$

$$(D_B\,\omega_B - D_A\,\omega_A) - 1/2\,(D_B V_B - D_A V_A) \qquad (4.19)$$

where $D_A = S_A \sin Z_A$ and $D_B = S_B \sin Z_B$ are horizontal distances. The contents within the first bracket represents the height difference, and the second term is the effect of the deflection of the vertical. Since the lengths of sight in the leap-frog method are usually short (less than 300 m), the effect of the deflection of the vertical can be neglected. The third term is due to refraction and the last term is the effect of earth curvature which can be ignored as long as the theodolite station is close enough to the mid point (less than 10 m) or it can be computed without any difficulty.

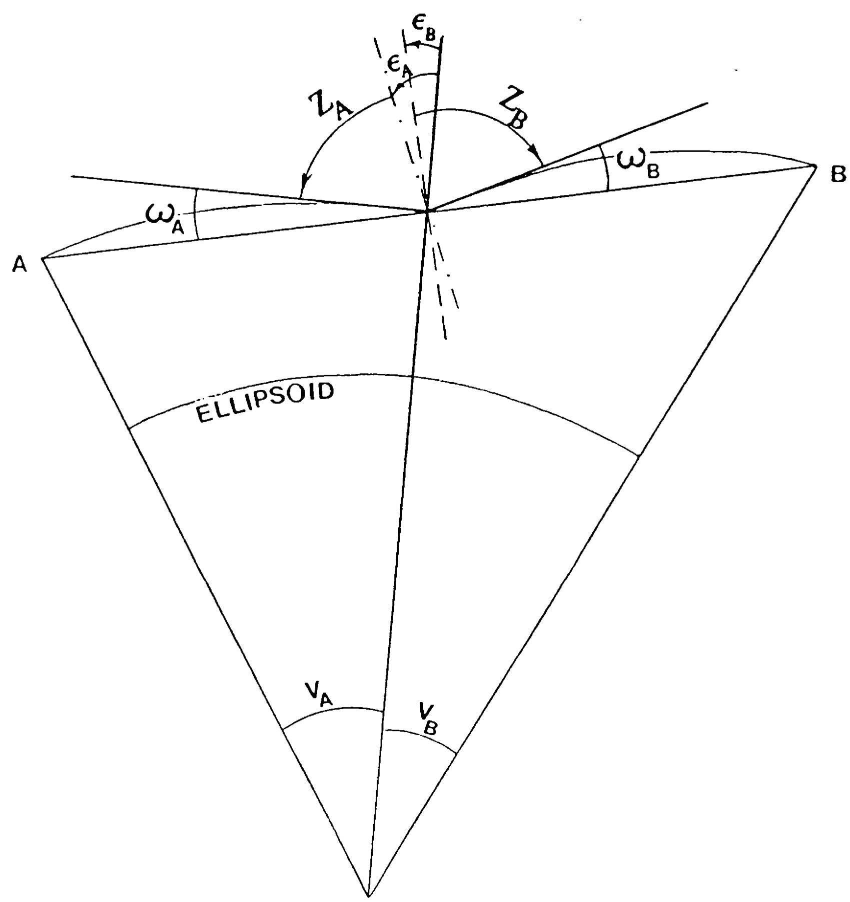

Figure 4.3: Ellipsoidal section for leap-Frog trigonometric height traversing

Substituting equation (4.4) into (4.19), omitting the third and the last terms and assuming $D = D_A = D_B$ yields

$$\Delta h = S_B \cos Z_B - S_A \cos Z_A - \frac{D^2}{2R} (k_B - k_A) \qquad (4.20)$$

4.2.2 <u>Achievable Accuracy Using Leap-Frog Trigonometric Height Traversing</u>

By applying the law of propagation of variances to equation (4.20) the variance of a measured height difference using the leap-frog method can be obtained as

$$\sigma^2 = (2 \cos^2 Z) \sigma_s^2 + 2 D^2 \sigma_Z^2 + \frac{D^4}{4 R^2} \Delta k^2 \qquad (4.21)$$

in which $\Delta k = k_B - k_A$.

Equation (4.20) is valid when the lengths of the back- and fore-sights are equal. If they are not equal then two other terms proportional to their differences should be added to the equation (see Rueger and Brunner [1982] for details). According to equation (4.21), with standard deviations of 5 mm for slope distances, 1" for zenith angles and with a coefficient of refraction difference from back- to fore-sight of 0.5, the accuracies of 3.8 mm$\sqrt{K}$ and 4.6 mm$\sqrt{K}$ (K in km) were found for average sight lengths of 200 m and 250 m respectively over a terrain with average slope of 10°. Using electronic theodolites and properly calibrated *EDM* with accuracies of 0.5" for the angle and 3 mm for the distance observation under the above mentioned conditions, the standard errors of 2.9 mm$\sqrt{K}$ and 3.8 mm$\sqrt{K}$ (K in km) for sight lengths of 200 m and 250 m were found by using equation (4.21).

The National Geodetic Survey in United States tested leap-frog trigonometric height traversing on a 30-kilometre loop. A standard error of a mean double run of 0.66 mm$\sqrt{K}$ (K in km) was achieved with lengths of sight up to 85 m [Whalen, 1985]. The *UNB* leap-frog method was used to determine heights in the network mentioned in Section 4.1.2 with a total of 70 km of interconnecting lines. The least-squares adjustement of the network gave the estimated standard deviation of 1 mm$\sqrt{K}$ (K in km) [Chrzanowski. 1985].

4.2.3 Precision of refraction correction in leap-frog method

The last term of equation (4.20) is the refraction correction to leap-frog trigonometric height traversing. By substituting equation (2.12) into (4.20) for the refraction correction we get

$$C_R = \frac{D^2}{2R} \cdot \frac{502.7\,p}{T^2} \left(\frac{dT_A}{dz} - \frac{dT_B}{dz} \right) \tag{4.22}$$

and the standard deviation of refraction correction with the same assumptions as in equation (4.13) is

$$\sigma_C = \frac{4D^2}{R} \sigma \tag{4.23}$$

where σ is the precision of the measured or modelled temperature. Graphical representation of equation (4.23) for different temperature precisions and sighting distances is similar to Figure 4.2 (see Figure 4.4) with the standard error of refraction corrections being doubled (over a twice longer traverse leg). Equation (4.23) shows that the sight lengths in the leap-frog method should be half the sight lengths in the reciprocal method or a higher precision for the temperature gradient is needed in order to obtain the same refraction correction in both methods.

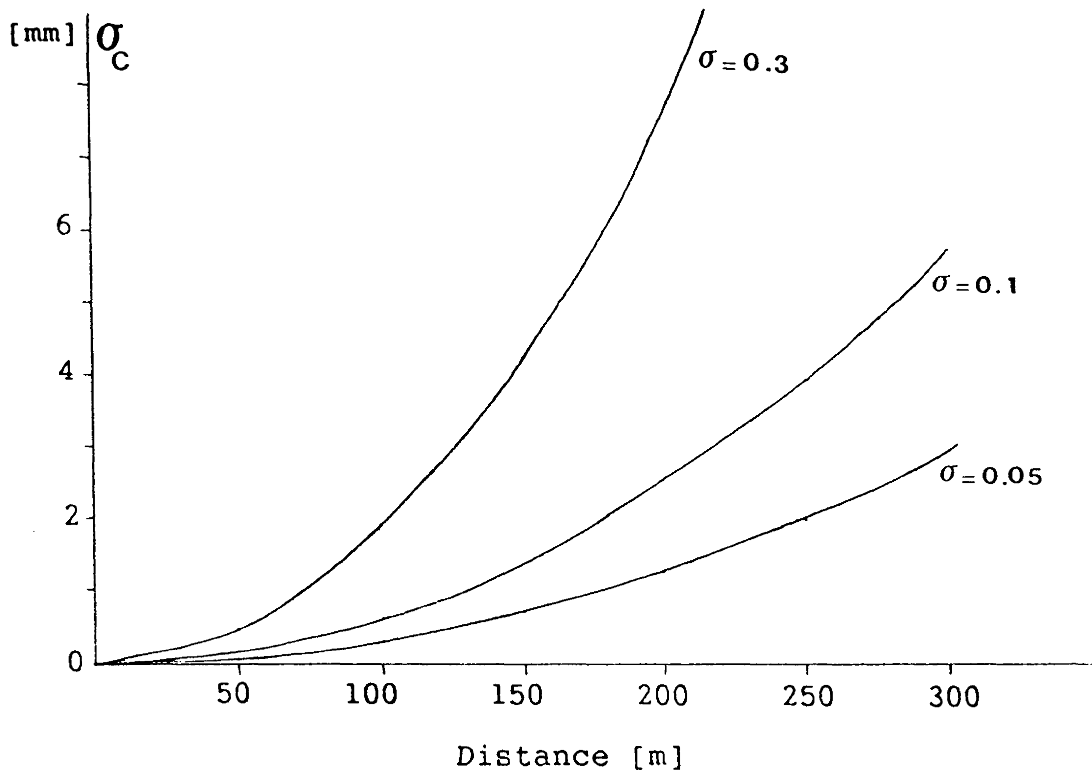

Figure 4.4: Standard deviation of refraction correction in leap-frog height traversing as a function of distance. Curves show standard deviation of refraction correction for temperature gradient precision of 0.05 °C/m, 0.1 °C/m and 0.3 °C/m, assuming P=1013. mb and T=300 K.

Chapter 5

TEST SURVEYS AT UNB

5.1 Background of Trigonometric Height Traversing at UNB

In 1981, the Department of Surveying Engineering at the University of New Brunswick (UNB) initiated a research programme to investigate the feasibility of implementing trigonometric height traversing for precise levelling. A modified leap-frog approach with elevated multiple targets was chosen. The multiple elevated targets were used to randomize the refraction error by changing the clearance of the line of sight, to reduce the effect of pointing errors, and to have a quick check in the field by comparing the results from different targets. This method of leap-frog trigonometric height traversing using multiple elevated targets was named the "UNB-method". The first practical tests of the method were carried out at a site chosen inside the UNB campus, which used to be called the UNB-test line, but is renamed here, to Head-Hall test line, because other test lines have been established on the campus. The results of preliminary tests carried out in the summers of 1981 and 1982 were described as encouraging by Chrzanowski [1983].

In the summer of 1983 the test surveys were extended over a six kilometre route outside Fredericton (Mactaquac test area) and into some loop surveys in the city of Fredericton. A complete description of the projects, including a statistical analysis and dicussion of results is given by Greening [1985].

In the summer of 1984, attempts were made to develop a computerized and motorized system of trigonometric height traversing. The results and descriptions of the system are given by Chrzanowski [1984] and Kornacki [1986].

The computerized system of levelling was further improved in 1985. In the summer of that year, a test network of over 70 kilometres of lines was measured twice: once using the leap-frog UNB-method and the second time using reciprocal height traversing. A total of over 140 kilometres of height traversing was completed [Chrzanowski, 1985].

Besides the test network, a number of individual test surveys were carried out in order to have a better understanding of the atmospheric refraction effect in trigonometric height traversing. The test surveys involved the long term observation of changes of the refraction angle over different types of surface coverage.

The study concentrated mainly on:

1. determination of an optimal model of the temperature profile up to 4 m above the ground;

2. comparison of the available models such as Kukkamäki's temperature function against three new models which were suggested by the author;

3. confirming in practice the designed precision of the UNB-method under controlled field conditions and to add to the knowledge of the refraction effect; and

4. variation of refraction error under unstable, neutral and stable conditions.

The results of the 1985 test surveys have been analyzed by the author and are discussed in this chapter.

5.2 Description of the Test Areas and Scope of the Tests

5.2.1 South-Gym test lines

The South-Gym area is located at the top of the hill at the south side of the UNB campus. As can be seen from Figure 5.1 three bench marks BM1, BM2 and BM3 have equal distances of about 200 m from the central instrument station, IS, forming three lines each of which lies almost entirely over either gravel or grass or asphalt. This combination of different ground surfaces was selected to investigate situations when one sight passes over a surface ground texture which is different from the other. All three legs are open to direct sunlight and their maximum inclination is about 2°.

The height differences between bench marks were precisely measured five times before and after the test surveys. These geodetically determined mean height differences are assumed to be errorless for a quantitative assessment of results. According to this assumption, the discrepancies between results of tigonometric height traversing and geodetic levelling can be considered as true errors.

The stability of the bench marks was also verified by several reference points established near *BM*2 and *BM*3. The outcomes of the geodetic levelling surveys showed that, at the one sigma level, all bench marks were stable to within ±0.2 mm during the period that the surveys were carried out [Chrzanowski, 1985]. The *UNB*-method test was conducted four times in the South-Gym area, on:

20 June, 4 hours between 10:20 and 14:30
19/20 July, 13 hours between 11:10 and 00:30
23/24 July, 38 hours between 09:30 and 23:40
29 July, 6 hours between 11:40 and 17:30.

In most of the tests surveys performed in the summer of 1985, gradient of temperature, speed and direction of wind, barometric pressure and the temperature of the ground surface were measured. Out of the above measurements, only temperature gradients of air were utilized to compute the refraction error, and speed and direction of wind were useful in interpreting some of the results.

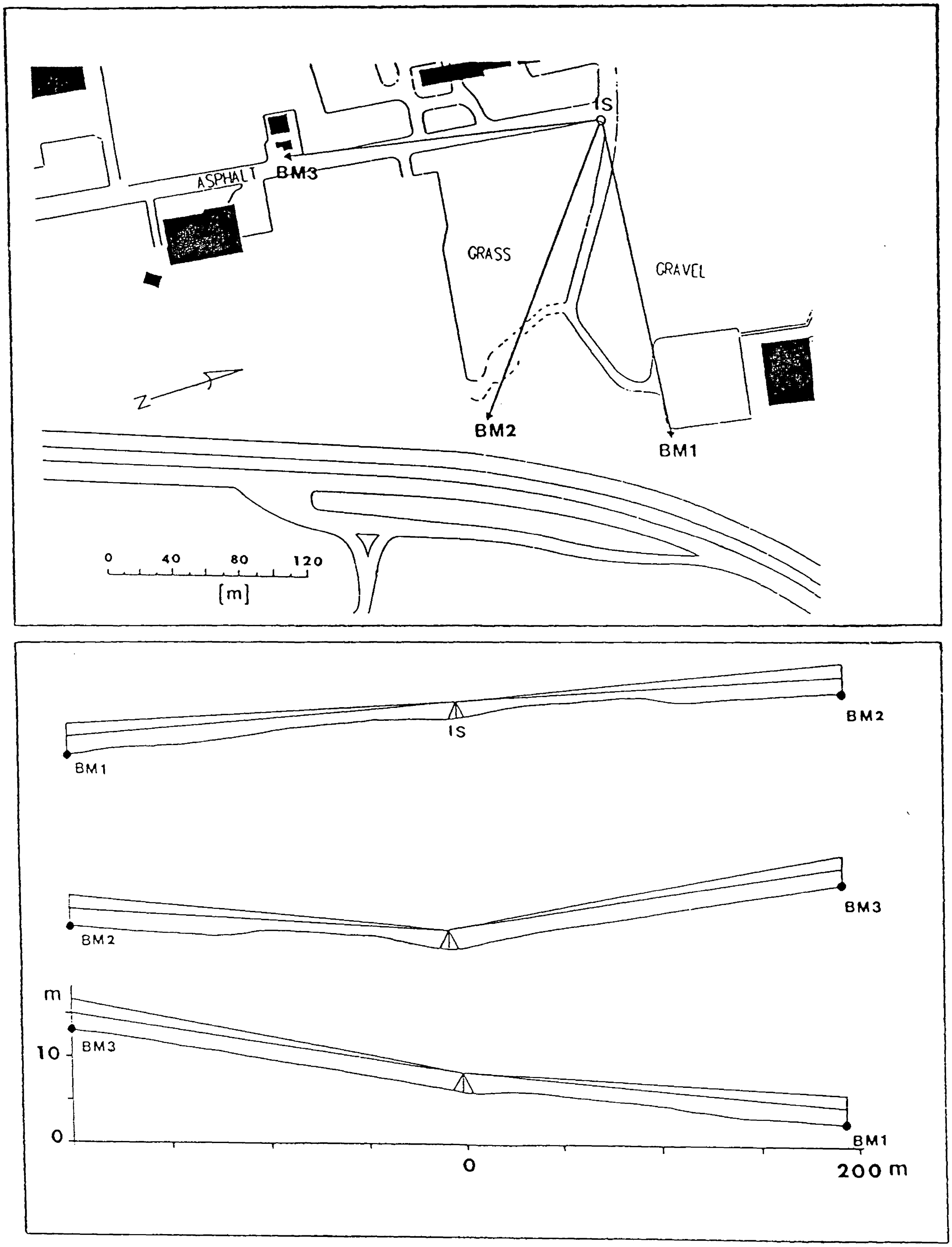

Figure 5.1: Plan and profiles of South-Gym test lines

5.2.2 Head-Hall test line

The Head-Hall test line of a total length of 600 m consists of 3 bench marks located near Head Hall and 3 bench marks near the main building of St. Thomas University. The line passes over asphalt or concrete with the average slope of about 5° (see Figure 5.2). It is mostly open to direct sun-light and is partialy bounded by buildings which can diminish the wind speed. Out of the six bench marks only BM2 and BM4 were used in the summer of 1985. These two bench marks were especially selected so that the lines of sight would experience high refraction effects while the lengths of sights remain lower than 230 m. The minimum clearance along one sight is 0.7 m at about 35 m distance from the instrument station, while the other sight is well above 3 m for the effective part of the line i.e. the half closer to the instrument.

The UNB trigonometric method was used to conduct 8 hours of tests between 12:15 and 20:15, on 06 August 1985. The same meteorological observations that were mentioned for the South-Gym area were carried out for this test survey as well (see section 5.5.6).

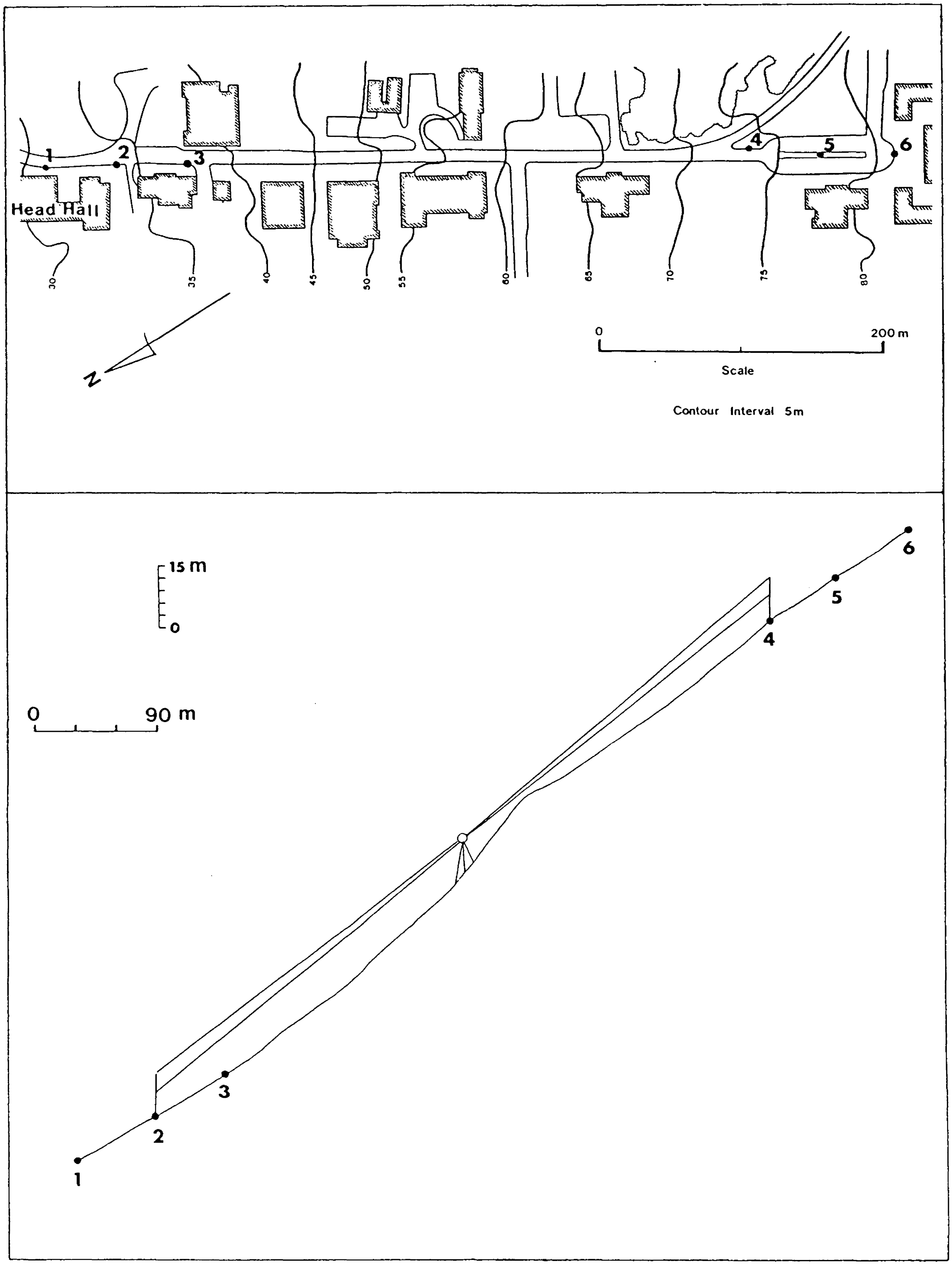

Figure 5.2: Plan and profile of Head-Hall test line

5.3 Description of the Field Equipment

5.3.1 Temperature gradient

A 4-metre wooden rod was constructed so that six temperature sensors could be mounted at the heights 0.3 m, 0.6 m, 1.2 m, 2 m, 3 m and 4 m. The sensors were of thermilinear (combination of thermistor composite and resistor set [Yellow Spring Instrument, 1985]) type in stainless steel housing, produced by Yellow Spring Instrument Co. Inc. This arrangement of sensors was chosen to facilitate temperature profiling up to 4 m height with denser temperature points in the first two metres height above the ground. The sensors were shaded from direct and indirect (reflected from the ground) radiation by the sun.

The accuracy of the sensors according to the manufacturer is better than 0.13 °C; the resolution of a temperature indicator is 0.1 °C with linearity of 2 parts per thousand or better. The sensors were calibrated by the manufacturer and guaranteed for a much longer period than the test surveys' duration. At UNB the sensors were compared against a precision (0.01 °C resolution) quartz temperature sensor (see also Chrzanowski [1985]). The differences and the absolute temperature determination were within the indicator's resolution of 0.1 °C.

5.3.2 Trigonometric height traversing

In all refraction test surveys, the vertical angle observations were made using a Kern E2 electronic theodolite to two targets located at heights 2.1 m and 3.5 m on 3.5 m long aluminum rods. Distances were measured with a Kern DK502 EDM to Kern prisms placed at 2 m height on the rods. A Wild T2000 electronic theodolite was also used together with the Kern E2 in the test on 29 July. Both theodolites were located within a few metres of each other so that the two systems could be compared under strongly correlated conditions (see section 5.5.4). For more details about the instrumentation see Chrzanowski [1985].

5.4 Investigation of Temperature Models as Function of Height

5.4.1 Choice of models

It was mentioned earlier (see Chapter 3) that the first temperature function in terms of height was adopted by Lallemand in 1896 [Angus-Leppan, 1984]

$$t = a + b \,.\, \log(z + c) \tag{5.1}$$

Kukkamäki [1979] reports that during his investigation, he found other models proposed by different researchers. For example, two of such models are

$$t = a + b\, z^2 \tag{5.2}$$

and

$$t = a + b\, z + c\, z^2 \tag{5.3}$$

In 1937 Kukkamäki suggested his temperature model, as

$$t = a + b\, z^{c} \tag{5.4}$$

and his refraction correction formula which was reviewed in section 3.1.1. Three other models have been tested by Heer [1983] and Heer and Niemeier [1985], two polynomials of order 3 and 4, and one exponential function of height, z

$$t = a + b\, z + c\, z^{2} + d\, z^{3} \tag{5.5}$$

$$t = a + b\, z + c\, z^{2} + d\, z^{3} + e\, z^{4} \tag{5.6}$$

$$t = a + b\ .\ \exp(c\ z) \tag{5.7}$$

Equation (5.7) is Heer's temperature model [Heer and Niemeier, 1985]. According to investigations of Heer and Niemeier [1985], the polynomials of greater than second degree failed to work properly.

In the UNB investigations, the author, besides testing some of the above equations, added the following three models

$$t = a + b\, z^{-1/3} + c\, z^{-4/3} \tag{5.8}$$

$$t = a + b\, z^{-1/3} + c\, z^{2} \tag{5.9}$$

$$t = a\, z + b\, z^{c}, \qquad \text{for } z > 0 \tag{5.10}$$

The author has found that models 5.4 and 5.7, when subjected to the least squares estimation of the exponent c, sometimes fail to converge. That is why equations (5.8), (5.9) and (5.10) were suggested. Equations (5.8) and (5.9) are expansions of Kukkamäki's model (5.4) when c = -1/3

$$t = a + b\, z^{-1/3} \tag{5.11}$$

From all the above models seven were investigated by fitting them to observed data and statistically testing the significance of their coefficients. The seven selected models are given by equations (5.3), (5.4), (5.7), (5.8), (5.9), (5.10) and (5.11).

It should be mentioned in here that extrapolation using the above equations is not recommended, especialy for the part closer to the ground which in this case is for under 0.3 m elevation.

5.4.2 Temperature gradient measurement

The most complete field observations were conducted on 23/24 July 1985. The main concentration in this section will be on the collected information on these two days.

The absolute temperature was measured at heights 0.3 m, 0.6 m, 1.2 m, 2 m, 3 m and 4 m. After about 22 hours of observations the sensor at 4 m malfunctioned and the remaining 16 hours of observations were conducted using only five sensors. During this period, the sensor at 0.6 m was transferred to 4.0 m for about 5 hours and then it was returned to its original height.

In section 5.2 the South-Gym test lines were described. Gradients of temperature were determined above all three types of ground surfaces: gravel, grass and asphalt. Starting in the grass field, the measurements of temperature commenced at least 10 minutes after setting up the sensors to make sure that the system was sensing the temperature of the new environment. Then, ten sets of readings of all sensors were completed within 10 to 12 minutes and immediately the system was transferred to the next spot on asphalt and after ten minutes, the new sets of readings were started, and so on, coming back to the intial spot on the grass after about 60 to 70 minutes. In average, all three measurements took 63.3 minutes which means that one complete round of observation was made almost every hour. Thus, the angle of refraction for every line could be determined once every hour. For every one-hour interval, one set of average temperature values is computed out of ten or more individual observations. Tables 5.1, 5.2 and 5.3 show the time averaged measured temperatures.

TABLE 5.1

The Time Averaged Temperatures on Gravel Line

NO	ZONE TIME (ADT)	TEMPERATURES [°C] AT HEIGHT [m] 0.3	0.6	1.2	2.0	3.0	4.0	REMARKS wind m/s	c.c. %	hu. %
1	10:00	20.17	19.65	19.54	19.25	19.04	18.97	4	0	41
2	11:00	21.22	21.06	20.89	20.83	20.76	20.68	4	0	28
3	12:00	20.58	20.27	20.19	20.10	19.87	19.63	4	50	32
4	13:00	20.94	20.49	20.06	19.74	19.71	19.63	6	50	24
5	14:00	21.65	21.15	20.94	20.60	20.40	20.11	6	50	20
6	15:00	23.19	22.64	22.27	21.82	21.44	21.07	1	50	12
7	16:00	22.15	21.82	21.51	21.26	21.17	21.02	6	50	22
8	17:00	22.40	21.91	21.69	21.34	20.95	21.01	6	100	21
9	18:00	20.96	20.49	20.29	20.14	20.07	19.99	4	75	28
10	19:00	21.09	20.73	20.54	20.39	20.20	20.09	4	75	30
11	20:00	20.35	20.01	19.92	19.71	19.71	19.69	<1	0	49
12	21:00	18.46	18.42	18.47	18.50	18.58	18.51	<1	0	57
13	22:00	15.95	16.23	16.41	16.48	16.58	16.63	<1	0	62
14	23:00	16.83	16.73	16.66	16.63	16.66	16.67	<1	0	62
15	24:00	16.08	15.99	15.92	15.86	15.93	15.90	<1	0	64
16	01:00	14.38	14.36	14.33	14.37	14.49	14.59	<1	0	66
17	02:00	15.26	15.26	15.26	15.23	15.28	15.27	<1	0	66
18	03:00	13.79	13.73	13.64	13.58	13.62	13.58	<1	0	68
19	04:00									
20	05:00	12.73	12.61	12.63	12.60	12.67	12.63	<1	0	69
21	06:00									
22	07:00	13.36	13.18	12.99	12.88	12.85		<1	0	68
23	08:00	16.11	15.89	15.60	15.50	15.48		<1	0	58
24	09:00	18.63	17.98	17.85	17.65	17.47		<1	0	48
25	10:00	21.10	20.74	20.79	20.53	20.32		<1	0	26
26	11:00	23.71		23.18	22.61	22.54	22.53	<1	0	18
27	12:00	24.66		23.70	23.19	22.92	22.77	<1	0	10
28	13:00	25.75		24.82	24.33	23.99	23.84	<1	0	8
29	14:00									
30	15:00	26.55		25.53	25.04	24.66	24.42	<1	0	8
31	16:00	27.66		26.45	26.04	25.85	25.78	<1	30	8
32	17:00	25.95	25.32	25.12	24.94	24.92		<1	90	22
33	18:00	24.95	24.63	24.57	24.46	24.39		1	85	34
34	19:00	24.52	24.23	24.15	24.05	24.09		2	80	32
35	20:00	22.58	22.44	22.38	22.33	22.42		1	80	46
36	21:00	20.46	20.36	20.43	20.53	20.66		<1	80	53
37	22:00	18.88	18.80	18.77	18.81	18.98		1	80	56
38	23:00	18.25	18.22	18.24	18.33	18.39		1	80	58

c.c. : relative cloud cover
hu. : relative humidity

TABLE 5.2

The Time Averaged Temperatures on Grass Line

NO	*ZONE TIME (ADT)*	*TEMPERATURES [°C] AT HEIGHT [m]* 0.3	0.6	1.2	2.0	3.0	4.0	*REMARKS* wind m/s	c.c. %	hu. %
1	10:00	19.36	19.07	18.86	18.80	18.72	18.75	2	0	43
2	11:00	21.75	21.48	21.14	20.62	20.39	20.22	4	0	36
3	12:00	21.76	21.45	21.27	20.89	20.80	20.44	4	50	20
4	13:00	20.48	20.36	20.27	20.15	20.03	19.93	6	50	20
5	14:00	21.31	21.24	21.08	20.85	20.45	20.22	6	50	24
6	15:00	22.89	22.41	22.09	21.59	21.25	20.98	4	50	20
7	16:00	21.47	21.24	21.13	21.04	20.90	20.73	4	50	14
8	17:00	21.04	20.90	20.75	20.64	20.66	20.38	6	50	26
9	18:00	22.44	21.74	21.66	21.44	21.15	21.21	6	0	20
10	19:00	20.11	20.07	20.10	20.02	19.98	19.97	4	75	41
11	20:00	19.66	19.84	19.97	20.06	20.14	20.11	<1	0	38
12	21:00	19.46	19.09	19.30	19.30	19.42	19.40	<1	0	51
13	22:00	16.01	17.04	17.44	17.67	17.80	17.80	<1	0	60
14	23:00	14.73	15.64	16.00	16.21	16.38	16.40	<1	0	62
15	24:00	14.63	15.20	15.45	15.65	15.65	15.68	<1	0	62
16	01:00	14.49	15.21	15.59	15.77	15.91	15.93	<1	0	62
17	02:00	14.43	14.74	14.91	15.02	15.16	15.16	<1	0	66
18	03:00	12.76	13.66	14.06	14.26	14.40	14.40	<1	0	66
19	04:00	12.88	13.66	13.96	14.20	14.34	14.32	<1	0	69
20	05:00	11.58	12.07	12.27	12.48	12.69	12.65	<1	0	69
21	06:00	11.95	12.28	12.37	12.41	12.48	12.46	<1	0	70
22	07:00	11.53	11.83	11.97	12.02	12.08	12.07	<1	0	70
23	08:00	14.24	14.12	13.99	13.85	13.75		<1	0	68
24	09:00	17.50	17.35	17.14	16.89	16.70		<1	0	54
25	10:00	20.17	19.88	19.63	19.34	19.16		<1	0	38
26	11:00	22.78	22.53	22.40	21.99	21.83		<1	0	22
27	12:00	24.62		24.05	23.53	23.39	22.87	<1	0	12
28	13:00	24.63		23.84	23.41	23.10	22.87	<1	0	9
29	14:00	27.20		26.45	25.94	25.47	25.19	<1	0	7
30	15:00	27.52		26.22	25.82	25.55	25.37	2	20	10
31	16:00	26.84		26.05	25.78	25.60	25.45	1	40	12
32	17:00	25.84	25.39	25.38	25.20	25.16		1	70	22
33	18:00	24.93	24.78	24.88	24.97	24.71		1	20	30
34	19:00	23.08	23.28	23.45	23.54	23.67		2	0	35
35	20:00	20.65	21.17	21.28	21.39	21.58		<1	20	48
36	21:00	18.83	19.31	19.66	19.95	20.16		<1	20	54
37	22:00	17.92	18.17	18.40	18.54	18.69		1	20	58
38	23:00	17.32	17.58	17.87	18.05	18.16		2	20	59

c.c. : relative cloud cover
hu. : relative humidity

TABLE 5.3

The *Time Averaged Temperatures on Asphalt Line*

NO	*ZONE TIME* (ADT)	*TEMPERATURES* [°C] *AT HEIGHT* [m] 0.3	0.6	1.2	2.0	3.0	4.0	*REMARKS* wind m/s	cld. %	hum %
1	10:00	19.74	19.51	19.19	18.87	18.82	18.71	2	0	42
2	11:00	21.34	21.20	20.93	20.70	20.53	20.37	4	0	30
3	12:00	20.26	19.97	19.71	19.59	19.46	19.31	4	50	26
4	13:00	20.34	20.06	19.82	19.58	19.46	19.31	6	50	27
5	14:00	21.03	20.65	20.33	20.12	20.02	19.92	6	50	22
6	15:00	20.92	20.56	20.53	20.32	20.20	20.12	5	50	20
7	16:00	23.19	22.70	22.55	22.25	22.11	21.93	6	50	14
8	17:00	21.75	21.38	21.17	20.69	20.42	20.28	6	50	20
9	18:00	21.30	20.92	20.72	20.48	20.35	20.37	4	35	32
10	19:00	21.24	20.77	20.56	20.34	20.21	20.21	4	35	41
11	20:00	20.98	20.63	20.48	20.27	20.19	20.09	<1	0	45
12	21:00	19.20	19.01	18.93	18.88	18.92	18.93	<1	0	57
13	22:00	16.82	17.28	17.55	17.66	17.76	17.73	<1	0	60
14	23:00	16.74	16.69	16.66	16.67	16.77	16.80	<1	0	60
15	24:00	15.37	15.27	15.24	15.25	15.27	15.22	<1	0	62
16	01:00	15.04	15.31	15.50	15.56	15.68	15.69	<1	0	65
17	02:00									
18	03:00	15.16	15.19	15.17	15.15	15.22	15.23	<1	0	65
19	04:00	13.35	13.36	13.44	13.44	13.52	13.51	<1	0	68
20	05:00	11.77	11.89	11.96	12.03	12.08	12.04	<1	0	70
21	06:00	12.77	12.52	12.39	12.33	12.34	12.29	<1	0	69
22	07:00									
23	08:00	14.86	14.77	14.47	14.31	14.21		<1	0	69
24	09:00									
25	10:00	17.86	17.58	17.36	17.08	16.92		<1	0	52
26	11:00	20.54	20.30	20.27	19.95	19.84		<1	0	30
27	12:00	22.79	22.42	22.19	21.82	21.51		<1	0	16
28	13:00	24.19		23.35	23.08	22.85	22.67	1	0	11
29	14:00	26.11		25.47	25.02	24.93	24.78	<1	0	7
30	15:00	26.69		25.92	25.44	25.14	24.89	<1	0	7
31	16:00	27.03		26.10	25.79	25.45	25.20	1	0	8
32	17:00	26.49	26.11	26.08	25.89	25.81		<1	80	16
33	18:00	25.80	25.41	25.41	25.20	25.15		1	70	22
34	19:00	24.65	24.40	24.35	24.30	24.25		2	20	32
35	20:00	23.41	23.21	23.20	23.14	23.23		2	0	41
36	21:00	21.01	21.04	21.25	21.28	21.35		<1	30	51
37	22:00	19.16	19.27	19.31	19.48	19.62		<1	30	55
38	23:00	18.36	18.35	18.39	18.41	18.53		1	30	58

c.c. : relative cloud cover
hu. : relative humidity

5.4.3 Determination of the coefficient of temperature models

The observed temperatures were averaged for every one-hour interval. During 38 hours of continuous height difference determination and temperature observations, 35 intervals were completed for gravel and asphalt, and 38 intervals for the grass field. Table 5.4 lists the tested temperature models and the average standard deviations. These values are calculated by averaging the a posteriori variance factors assuming the weight matrix as identity (a priori standard error of 1 °C) and a unit value for the a priori variance factor for all one-hour intervals in all cases. The number of curve fittings is equal to the number of intervals, except in the case of models #1 and #7 in which the number of intervals were reduced, because sometimes the solution vector failed to converge, as mentioned earlier. According to table 5.4 a constant $c = -1/3$ makes the Kukkamäki model less flexible with larger standard deviation in comparison to other models with the exception of the second order polynomial (model #6).

Tables 5.5 and 5.6 show a detailed computation of these curve fittings of models #1 and #4 for measured temperature over asphalt. The coefficients of refraction computed for different height above the ground show very little change from one model to another.

Figure 5.3 shows the contours of coefficients of refraction with respect to time and height above the ground.

TABLE 5.4

Mean standard deviations

NO	MODEL	Mean Standard Error [°C] South-Gym Area Gravel	Grass	Asphalt
1	$t = a + b\,z^{c}$	0.060	0.043	0.046
2	$t = a + b\,z^{-1/3}$	0.068	0.090	0.061
3	$t = a + b\,z^{-1/3} + c\,z^{-3/4}$	0.058	0.054	0.047
4	$t = a + b\,z^{-1/3} + c\,z^{2}$	0.057	0.068	0.048
5	$t = a\,z + b\,z^{c}$ for $z > 0$	0.055	0.066	0.047
6	$t = a + b\,z + c\,z^{2}$	0.088	0.115	0.076
7	$t = a + b\exp^{(c\,z)}$	0.066	0.063	0.053

Model #4 is used for computation of the coefficients of refraction. The stable, neutral and unstable conditions can be detected from these figures. The solid line contours show the zero refraction coefficient which is associated with the neutral condition time. The time of the neutral condition seems to change with respect to height. This is particularly true for the case over gravel, Figure 5.3 a. There is a slight change from using one model to another, but, model #5 gives the closet results to these figures.

Tables 5.7 and 5.8 show the test of the significance of the coefficients at the 95% confidence level (1-α level) as well as the probability of being insignificant (α level) of the coefficients. These tables show the testing of the null hypothesis that $c = 0$ versus the alternative $c \neq 0$ where c is the estimated coefficient. The t statistic is given by e.g. Draper and Smith [1981] as

$$t = c / Sc$$

where Sc is the standard deviation of c. Figure 5.4 shows the results of the tests on all models presented in Table 5.4 (except model #2, because in this model only two coefficients are involved). The best fit according to this figure is to Heer's model. The main problem with Heer's model, as it was mentioned earlier, is that in least squares estimation of the exponent coefficient c, it sometimes does not converge to a solution. Figure 5.4 shows that Kukkamäki's model is not the best fit to the observed temperatures, and models #3, #4, #5 and #6 are almost the same. Considering both Table 5.4 and Figure 5.4, one can choose either of the models #3 or #4 or #5, for their ease and precision of fit.

TABLE 5.5

Curve fitting and coefficient of refraction computations
(*Kukkamäki's model, #1 in Table 5.4, over asphalt*).

#	TIME	RESIDUALS					VARNCE	A	B	C	POINT COEFFICIENT OF REFR. K0.50	K1.5	K2.5	K3.5	K4.5	ITE#
¬ 1	10.00	0.02	-0.05	-0.02	0.09	-0.02	0.0042	11.90	7.35	-0.06	-5.0	-1.4	-0.7	-0.5	-0.3	13
¬ 2	11.00	0.02	-0.03	0.00	0.02	-0.01	0.0006	22.04	-1.04	0.34	-3.1	-1.4	-1.0	-0.7	-0.6	6
¬ 3	12.00	-0.01	0.01	0.02	-0.03	-0.03	0.0012	16.55	3.24	-0.11	-4.3	-1.1	-0.6	-0.3	-0.2	5
¬ 4	13.00	-0.00	0.01	-0.02	0.02	-0.02	0.0005	33.55	*****	0.03	-4.3	-1.4	-0.8	-0.5	-0.3	13
¬ 5	14.00	0.00	-0.01	-0.00	0.02	-0.01	0.0002	19.03	1.37	-0.31	-6.1	-1.3	-0.6	-0.3	-0.2	3
¬ 6	15.00	-0.03	0.10	-0.08	-0.01	0.01	0.0058	18.40	2.11	-0.14	-3.6	-0.9	-0.4	-0.2	-0.1	5
¬ 7	16.00	-0.04	0.10	-0.07	0.00	-0.03	0.0064	18.46	4.10	-0.11	-5.6	-1.5	-0.8	-0.5	-0.3	8
¬ 8	17.00	-0.01	0.05	-0.11	0.06	0.04	0.0068	23.30	-2.13	0.26	-5.3	-2.2	-1.5	-1.1	-0.9	8
¬ 9	18.00	-0.00	0.02	-0.05	0.03	0.05	0.0026	19.74	0.99	-0.37	-5.5	-1.1	-0.4	-0.2	-0.1	3
¬10	19.00	-0.01	0.04	-0.05	0.01	0.04	0.0020	19.82	0.75	-0.52	-6.4	-1.0	-0.4	-0.1	-0.0	4
¬11	20.00	-0.01	0.05	-0.05	0.01	-0.01	0.0017	19.21	1.29	-0.26	-4.5	-1.0	-0.4	-0.2	-0.1	4
¬12	21.00	0.00	-0.01	0.00	0.04	-0.01	0.0007	18.90	0.04	-1.64	-2.3	0.1	0.2	0.2	0.2	13
¬13	22.00	-0.00	0.01	-0.00	0.00	-0.03	0.0007	17.88	-0.38	-0.84	7.2	1.1	0.6	0.4	0.3	9
¬14	24.00	0.00	-0.00	0.01	-0.00	-0.03	0.0004	15.24	0.01	-2.35	-0.9	0.2	0.2	0.2	0.2	18
¬15	1.00	0.00	-0.01	-0.01	0.03	-0.02	0.0006	15.94	-0.49	-0.50	4.4	1.0	0.6	0.4	0.4	8
¬16	3.00	-0.00	-0.02	0.01	0.05	-0.02	0.0011	19.77	-4.59	-0.00	0.5	0.3	0.3	0.2	0.2	17
¬17	4.00	-0.02	0.02	-0.01	0.03	-0.03	0.0007	23.78	*****	-0.01	1.1	0.5	0.4	0.3	0.3	16
¬18	5.00	-0.00	0.00	0.01	-0.01	-0.03	0.0006	12.17	-0.22	-0.52	2.2	0.6	0.4	0.3	0.3	21
¬19	6.00	0.00	-0.00	0.00	0.01	-0.02	0.0003	12.27	0.15	-1.00	-3.6	-0.2	0.1	0.1	0.2	11
*20	8.00	0.03	-0.06	0.03	0.02		0.0034	16.10	-1.54	0.20	-3.1	-1.1	-0.7	-0.5	-0.3	6
*21	10.00	-0.01	0.02	-0.03	0.02		0.0012	20.19	-2.79	0.15	-4.3	-1.5	-0.9	-0.6	-0.5	7
*22	11.00	-0.02	0.07	-0.09	0.05		0.0082	20.95	-0.71	0.41	-2.4	-1.2	-0.8	-0.6	-0.5	10
*23	12.00	-0.03	0.07	-0.05	-0.00		0.0041	23.73	-1.49	0.36	-4.7	-2.2	-1.5	-1.2	-1.0	7
@24	13.00	-0.00		0.01	-0.01	-0.01	0.0002	8.39	15.08	-0.04	-6.8	-2.0	-1.1	-0.7	-0.5	23
@25	14.00	0.01		-0.08	0.10	-0.02	0.0089	*****	39.73	-0.01	-5.9	-1.8	-1.0	-0.6	-0.5	35
@26	15.00	0.01		-0.04	0.05	0.00	0.0023	28.56	-2.56	0.26	-6.2	-2.7	-1.8	-1.3	-1.1	8
@27	16.00	-0.00		0.03	-0.03	-0.01	0.0011	31.74	-5.48	0.13	-7.0	-2.6	-1.6	-1.1	-0.9	9
@28	17.00	0.00		0.03	-0.07	0.02	0.0034	-9.92	36.11	-0.01	-2.7	-0.8	-0.4	-0.2	-0.1	35
*29	18.00	-0.02	0.08	-0.10	0.02		0.0089	25.04	0.31	-0.73	-4.1	-0.4	-0.1	0.0	0.1	9
*30	19.00	-0.00	0.02	-0.03	-0.01		0.0009	24.25	0.09	-1.21	-2.8	-0.1	0.1	0.2	0.2	11
*31	21.00	-0.02	0.05	-0.05	0.01		0.0028	19.60	1.58	0.10	1.9	0.9	0.6	0.5	0.4	12
*32	22.00	0.02	-0.04	0.03	-0.01		0.0013	19.10	0.20	0.85	1.3	1.2	1.1	1.1	1.0	9
*33	23.00	-0.03	0.02	0.03	0.04		0.0034	32.98	*****	-0.00	1.0	0.5	0.4	0.3	0.3	29

AVERAGE STANDARD DEVIATION : 0.046

* FIVE TEMPERATURE SENSORS, SENSORS ARE AT HEIGHTS 0.3, 0.6, 1.2, 2.0 AND 3.0 METRES.

@ FIVE TEMPERATURE SENSORS, SENSORS ARE AT HEIGHTS 0.3, 1.2, 2.0, 3.0 AND 4.0 METRES.

¬ SIX TEMPERATURE SENSORS, SENSORS ARE AT HEIGHTS 0.3, 0.6, 1.2, 2.0, 3.0 AND 4.0 METRES.

TABLE 5.6

Curve fitting and coefficient of refraction computations (model, #4 in Table 5.4, over asphalt).

#	TIME	RESIDUALS					VARNCE	A	B	C	POINT COEFFICIENT OF REFR. K0.50	K1.5	K2.5	K3.5	K4.5	ITE#
¬ 1	10.00	0.05	-0.08	-0.04	0.09	-0.01	0.0062	18.08	1.14	-0.01	-5.6	-1.2	-0.7	-0.5	-0.5	2
¬ 2	11.00	0.04	-0.07	-0.02	0.04	0.02	0.0031	20.20	0.79	-0.02	-3.8	-1.1	-0.9	-1.0	-1.2	2
¬ 3	12.00	-0.01	-0.00	0.03	-0.01	-0.02	0.0004	18.88	0.92	-0.01	-4.4	-1.0	-0.6	-0.5	-0.5	2
¬ 4	13.00	0.01	-0.01	-0.03	0.04	-0.00	0.0008	18.89	0.98	-0.01	-4.8	-1.2	-0.7	-0.7	-0.7	2
¬ 5	14.00	0.00	-0.01	-0.00	0.02	-0.01	0.0002	19.12	1.28	-0.00	-6.2	-1.3	-0.6	-0.3	-0.2	2
¬ 6	15.00	-0.03	0.09	-0.07	0.01	0.01	0.0050	19.76	0.76	-0.01	-3.6	-0.8	-0.5	-0.4	-0.4	2
¬ 7	16.00	-0.03	0.09	-0.07	0.03	-0.01	0.0047	21.38	1.19	-0.01	-5.7	-1.4	-0.8	-0.7	-0.7	2
¬ 8	17.00	0.03	-0.00	-0.14	0.08	0.08	0.0121	19.87	1.28	-0.03	-6.3	-1.8	-1.4	-1.4	-1.6	2
¬ 9	18.00	0.00	0.02	-0.06	0.02	0.05	0.0024	19.56	1.17	0.00	-5.6	-1.1	-0.4	-0.1	0.1	2
¬10	19.00	-0.02	0.05	-0.05	-0.00	0.03	0.0021	19.28	1.30	0.01	-6.2	-1.2	-0.4	-0.0	0.2	2
¬11	20.00	-0.02	0.04	-0.04	0.02	-0.01	0.0015	19.56	0.94	-0.00	-4.5	-0.9	-0.5	-0.3	-0.2	2
¬12	21.00	-0.01	0.03	-0.00	0.00	-0.03	0.0006	18.44	0.50	0.01	-2.2	-0.2	0.3	0.5	0.7	2
¬13	22.00	0.02	-0.04	-0.01	0.04	-0.01	0.0012	18.79	-1.31	-0.02	6.7	1.5	0.5	0.1	-0.3	2
¬14	23.00	-0.00	0.00	0.01	0.01	-0.04	0.0006	16.51	0.15	0.01	-0.5	0.3	0.5	0.7	0.9	2
¬15	24.00	-0.02	0.03	0.02	-0.01	-0.04	0.0011	15.09	0.17	0.00	-0.7	0.0	0.2	0.2	0.3	2
¬16	1.00	0.01	-0.02	-0.01	0.04	-0.02	0.0007	16.24	-0.79	-0.00	4.3	1.1	0.6	0.4	0.3	2
¬17	3.00	0.01	-0.02	-0.00	0.03	-0.02	0.0006	15.14	0.02	0.00	0.1	0.3	0.3	0.4	0.5	2
¬18	4.00	-0.01	0.03	-0.01	0.02	-0.03	0.0008	13.57	-0.15	0.00	1.0	0.5	0.4	0.4	0.4	2
¬19	5.00	-0.00	-0.00	0.02	-0.00	-0.03	0.0005	12.36	-0.39	-0.00	2.3	0.6	0.3	0.2	0.1	2
¬20	6.00	-0.02	0.03	0.01	-0.00	-0.04	0.0012	11.78	0.65	0.01	-3.1	-0.4	0.1	0.3	0.5	2
*21	8.00	0.04	-0.09	0.03	0.04		0.0058	13.87	0.69	-0.02	-3.5	-0.9	-0.7	-0.8	-1.0	2
*22	10.00	0.01	-0.00	-0.03	0.05		0.0017	16.50	0.92	-0.03	-4.6	-1.3	-1.1	-1.2	-1.4	2
*23	11.00	-0.01	0.05	-0.09	0.07		0.0081	19.69	0.56	-0.03	-2.8	-1.0	-1.0	-1.2	-1.5	2
*24	12.00	-0.01	0.03	-0.05	0.04		0.0024	21.24	1.04	-0.05	-5.2	-1.9	-1.9	-2.3	-2.7	2
⊖25	13.00		0.00	-0.01	0.00	0.01	0.0001	21.94	1.51	-0.01	-7.2	-1.7	-1.1	-0.9	-0.9	2
⊖26	14.00		0.02	-0.11	0.11	0.00	0.0123	24.09	1.36	-0.01	-6.4	-1.5	-0.9	-0.8	-0.8	2
⊖27	15.00		0.02	-0.10	0.07	0.05	0.0093	24.43	1.53	-0.03	-7.3	-2.1	-1.6	-1.7	-1.9	2
⊖28	16.00		0.00	-0.01	-0.01	0.03	0.0006	24.59	1.64	-0.03	-7.8	-2.1	-1.5	-1.5	-1.6	2
⊖29	17.00		-0.00	0.03	-0.05	0.03	0.0022	25.60	0.59	-0.01	-2.7	-0.6	-0.4	-0.4	-0.5	2
*30	18.00	-0.04	0.11	-0.08	0.02		0.0102	24.58	0.79	0.00	-3.6	-0.6	-0.2	0.0	0.1	2
*31	19.00	-0.03	0.06	-0.02	-0.03		0.0025	23.81	0.55	0.01	-2.4	-0.3	0.1	0.3	0.5	2
*32	20.00	-0.02	0.04	-0.04	0.01		0.0019	22.67	0.48	0.02	-2.0	0.1	0.6	1.0	1.4	2
*33	21.00	-0.03	0.06	-0.04	0.00		0.0034	21.56	-0.39	0.01	2.1	0.8	0.6	0.6	0.7	2
*34	22.00	0.01	-0.02	0.03	-0.02		0.0011	19.54	-0.25	0.03	1.6	1.0	1.2	1.5	1.8	2
*35	23.00	-0.00	0.01	-0.02	0.01		0.0003	18.32	0.02	0.02	0.2	0.6	0.8	1.1	1.3	2

AVERAGE STANDARD DEVIATION : 0.048

* FIVE TEMPERATURE SENSORS, SENSORS ARE AT HEIGHTS 0.3, 0.6, 1.2, 2.0 AND 3.0 METRES.

⊖ FIVE TEMPERATURE SENSORS, SENSORS ARE AT HEIGHTS 0.3, 1.2, 2.0, 3.0 AND 4.0 METRES.

¬ SIX TEMPERATURE SENSORS, SENSORS ARE AT HEIGHTS 0.3, 0.6, 1.2, 2.0, 3.0 AND 4.0 METRES.

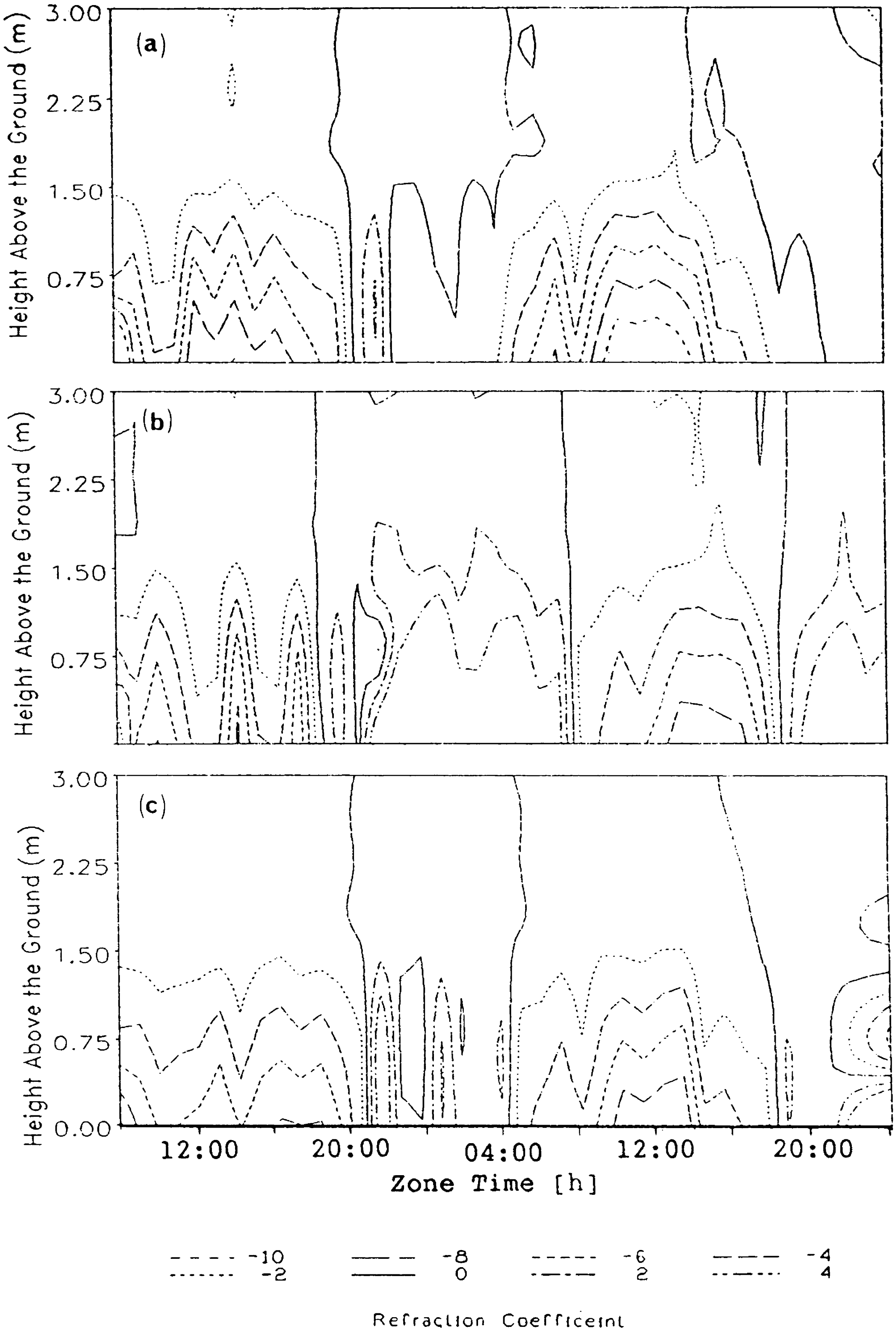

Figure 5.3: Refraction Coefficient Contours
a. gravel, b. grass and c. asphalt
(model, #4 in Table 5.4 is used).

TABLE 5.7

Curve fitting with test of the significance of coefficient
(*Kukkamäki*'s model, #1 in *Table* 5.4).

#	TIME	VARNC FACTR	A	B	C	T-VALUE FOR A	T-VALUE FOR B	T-VALUE FOR C	TABLE VALUE	95% TEST	PRO. OF BEING INSIG. A	PRO. OF BEING INSIG. B	PRO. OF BEING INSIG. C	I#
¬ 1	10.00	0.0086	17.14	2.38	-0.19	5.7	0.8	-0.8	3.2	F	0.0108	0.4940	0.5054	3
¬ 2	11.00	0.0004	19.74	1.20	-0.17	22.3	1.3	-1.3	3.2	F	0.0002	0.2716	0.2720	4
¬ 3	12.00	0.0093	20.76	-0.49	0.57	50.9	-1.1	1.4	3.2	F	0.0000	0.3444	0.2545	10
¬ 4	13.00	0.0043	18.92	1.22	-0.42	39.7	2.4	-2.6	3.2	F	0.0000	0.0967	0.0820	3
¬ 5	14.00	0.0076	25.54	-4.55	0.12	3.4	-0.6	0.6	3.2	F	0.0433	0.5923	0.5846	8
¬ 6	15.00	0.0048	25.08	-2.70	0.28	22.2	-2.3	2.5	3.2	F	0.0002	0.1027	0.0876	7
¬ 7	16.00	0.0008	18.40	3.18	-0.14	9.8	1.7	-1.7	3.2	F	0.0023	0.1922	0.1931	7
¬ 8	17.00	0.0137	3.07	18.62	-0.03	61.9	10.0	-10.5	3.2	P	0.0000	0.0021	0.0018	11
¬ 9	18.00	0.0010	19.82	0.49	-0.68	215.7	4.6	-5.5	3.2	P	0.0000	0.0196	0.0119	5
¬10	19.00	0.0022	16.69	3.91	-0.09	2.7	0.6	-0.6	3.2	F	0.0768	0.5800	0.5827	5
¬11	20.00	0.0028	19.54	0.35	-0.69	129.5	2.0	-2.4	3.2	F	0.0000	0.1435	0.0967	16
¬12	22.00	0.0004	16.90	-0.54	-0.47	136.1	-4.0	-4.3	3.2	P	0.0000	0.0283	0.0226	10
¬13	23.00	0.0005	16.65	0.03	-1.43	787.4	1.2	-2.2	3.2	F	0.0000	0.3182	0.1104	20
¬14	24.00	0.0012	15.88	0.05	-1.15	386.9	0.9	-1.5	3.2	F	0.0000	0.4249	0.2424	13
¬15	1.00	0.0010	14.35	0.01	2.73	711.3	0.7	2.7	3.2	F	0.0000	0.5313	0.0709	7
¬16	3.00	0.0008	13.50	0.16	-0.52	96.9	1.0	-1.1	3.2	F	0.0000	0.3846	0.3369	5
*17	7.00	0.0006	12.38	0.66	-0.33	33.1	1.7	-1.8	3.2	F	0.0009	0.2296	0.2057	2
*18	8.00	0.0024	15.09	0.60	-0.46	37.3	1.4	-1.6	3.2	F	0.0007	0.2994	0.2590	3
*19	9.00	0.0124	17.33	0.49	-0.79	53.3	1.3	-1.8	3.2	F	0.0004	0.3198	0.2215	4
*20	10.00	0.0183	21.59	-0.84	0.35	12.0	-0.4	0.5	3.2	F	0.0069	0.6979	0.6889	11
@21	11.00	0.0302	6.68	16.44	-0.03	0.1	0.2	-0.2	3.2	F	0.9540	0.8875	0.8878	25
@22	12.00	0.0044	*****	58.93	-0.01	-1.0	1.7	-1.7	3.2	F	0.4103	0.2257	0.2313	30
@23	13.00	0.0043	32.86	-7.96	0.09	3.4	-0.8	0.8	3.2	F	0.0753	0.4945	0.4903	13
@24	15.00	0.0010	31.16	-5.51	0.15	16.9	-3.0	3.0	3.2	F	0.0035	0.0982	0.0945	10
@25	16.00	0.0031	24.60	1.94	-0.38	42.1	3.1	-3.3	3.2	F	0.0006	0.0907	0.0795	4
*26	17.00	0.0020	24.84	0.29	-1.13	334.9	3.2	-5.2	3.2	P	0.0000	0.0857	0.0352	5
*27	18.00	0.0023	24.32	0.23	-0.83	182.9	1.5	-2.1	3.2	F	0.0000	0.2784	0.1761	12
*28	19.00	0.0012	24.05	0.09	-1.33	532.1	1.7	-3.1	3.2	F	0.0000	0.2262	0.0878	9
*29	20.00	0.0023	22.37	0.02	-1.85	524.8	0.5	-1.1	3.2	F	0.0000	0.6793	0.3734	21

THE MEAN STANDARD DEVIATION IS : 0.060

* FIVE TEMPERATURE SENSORS, SENSORS ARE AT HEIGHTS 0.3, 0.6, 1.2, 2.0 AND 3.0 METRES.
@ FIVE TEMPERATURE SENSORS, SENSORS ARE AT HEIGHTS 0.3, 1.2, 2.0, 3.0 AND 4.0 METRES.
¬ SIX TEMPERATURE SENSORS, SENSORS ARE AT HEIGHTS 0.3, 0.6, 1.2, 2.0, 3.0 AND 4.0 METRES.

TABLE 5.8

Curve fitting with the significance of coefficient test (model #3 in Table 5.4).

#	TIME	VARNC FACTR	A	B	C	T-VALUE FOR A	T-VALUE FOR B	T-VALUE FOR C	TABLE VALUE	95% TEST		PRO. OF BEING INSIG. A	PRO. OF BEING INSIG. B	PRO. OF BEING INSIG. C	I#
¬ 1	10.00	0.0008	18.48	0.37	0.07	191.9	2.8	2.9	3.2	F		0.0000	0.0679	0.0642	3
¬ 2	11.00	0.0046	18.22	3.22	-0.26	80.9	10.4	-4.7	3.2		P	0.0000	0.0019	0.0179	3
¬ 3	12.00	0.0143	19.09	2.37	-0.18	48.1	4.3	-1.9	3.2	F		0.0000	0.0226	0.1596	3
¬ 4	13.00	0.0016	19.30	1.08	-0.09	146.7	5.9	-2.7	3.2	F		0.0000	0.0096	0.0714	3
¬ 5	14.00	0.0147	18.49	2.97	-0.33	45.8	5.3	-3.4	3.2		P	0.0000	0.0128	0.0436	3
¬ 6	15.00	0.0114	18.89	3.49	-0.25	53.1	7.1	-2.9	3.2	F		0.0000	0.0057	0.0647	3
¬ 7	16.00	0.0054	20.12	1.10	-0.06	82.7	3.3	-1.1	3.2	F		0.0000	0.0467	0.3704	3
¬ 8	17.00	0.0084	19.85	1.02	-0.07	65.2	2.4	-0.9	3.2	F		0.0000	0.0935	0.4236	3
¬ 9	18.00	0.0165	20.63	0.89	0.09	48.3	1.5	0.9	3.2	F		0.0000	0.2281	0.4407	3
¬10	19.00	0.0010	19.76	0.35	-0.04	190.6	2.4	-1.4	3.2	F		0.0000	0.0917	0.2528	3
¬11	20.00	0.0007	20.45	-0.50	-0.01	235.4	-4.2	-0.5	3.2	F		0.0000	0.0253	0.6537	3
¬12	21.00	0.0061	20.18	-1.20	0.21	77.5	-3.4	3.4	3.2		P	0.0000	0.0439	0.0434	3
¬13	22.00	0.0012	18.20	-0.53	-0.28	155.5	-3.3	-9.8	3.2		P	0.0000	0.0456	0.0023	3
¬14	23.00	0.0016	16.91	-0.75	-0.21	126.5	-4.1	-6.5	3.2		P	0.0000	0.0263	0.0075	2
¬15	24.00	0.0014	15.97	-0.40	-0.15	128.6	-2.3	-5.0	3.2	F		0.0000	0.1028	0.0156	3
¬16	1.00	0.0003	16.49	-0.82	-0.16	266.2	-9.6	-10.3	3.2		P	0.0000	0.0024	0.0020	3
¬17	2.00	0.0009	15.65	-0.75	-0.02	154.7	-5.4	-0.8	3.2	F		0.0000	0.0126	0.5040	3
¬18	3.00	0.0007	14.86	-0.64	-0.23	153.6	-5.1	-10.4	3.2		P	0.0000	0.0147	0.0019	2
¬19	4.00	0.0024	14.84	-0.73	-0.17	90.2	-3.2	-4.3	3.2		P	0.0000	0.0480	0.0230	3
¬20	5.00	0.0043	13.36	-1.07	-0.04	61.1	-3.5	-0.7	3.2	F		0.0000	0.0383	0.5514	3
¬21	6.00	0.0006	12.51	-0.05	-0.10	147.8	-0.4	-4.7	3.2	F		0.0000	0.6843	0.0186	3
¬22	7.00	0.0002	12.21	-0.19	-0.08	279.5	-3.2	-7.5	3.2	F		0.0000	0.0510	0.0049	3
*23	8.00	0.0003	13.07	1.02	-0.07	161.1	9.6	-4.1	3.2		P	0.0000	0.0107	0.0556	3
*24	9.00	0.0014	15.43	1.91	-0.16	94.9	9.0	-4.5	3.2		P	0.0001	0.0122	0.0451	2
*25	10.00	0.0018	17.88	1.90	-0.11	95.0	7.7	-2.8	3.2	F		0.0001	0.0163	0.1074	3
*26	11.00	0.0110	20.40	2.14	-0.17	44.4	3.6	-1.7	3.2	F		0.0005	0.0707	0.2319	3
⊖27	12.00	0.0216	20.29	4.37	-0.44	31.2	4.7	-2.8	3.2	F		0.0010	0.0422	0.1047	3
⊖28	13.00	0.0001	20.59	3.71	-0.30	521.7	65.9	-31.8	3.2		P	0.0000	0.0002	0.0010	3
⊖29	14.00	0.0007	22.07	5.08	-0.50	190.4	30.8	-17.9	3.2		P	0.0000	0.0011	0.0031	3
⊖30	15.00	0.0000	23.58	2.86	-0.07	*****	150.4	-20.9	3.2		P	0.0000	0.0000	0.0023	2
⊖31	16.00	0.0002	24.16	2.08	-0.09	432.8	26.1	-6.5	3.2		P	0.0000	0.0015	0.0230	3
*32	17.00	0.0071	25.03	0.19	0.10	67.7	0.4	1.3	3.2	F		0.0002	0.7368	0.3189	3
*33	18.00	0.0208	24.81	0.02	0.01	39.2	0.0	0.1	3.2	F		0.0007	0.9815	0.9288	2
*34	19.00	0.0006	24.24	-0.87	0.03	219.6	-6.0	1.1	3.2	F		0.0000	0.0267	0.3783	3
*35	20.00	0.0079	21.88	-0.50	-0.09	56.0	-1.0	-1.1	3.2	F		0.0003	0.4298	0.3761	2
*36	21.00	0.0012	21.46	-1.92	0.05	143.3	-9.8	1.5	3.2	F		0.0000	0.0102	0.2671	3
*37	22.00	0.0004	19.49	-1.20	0.04	222.2	-10.4	2.3	3.2	F		0.0000	0.0091	0.1479	3
*38	23.00	0.0002	19.09	-1.35	0.05	350.7	-18.9	4.1	3.2		P	0.0000	0.0028	0.0544	3

THE MEAN STANDARD DEVIATION IS : 0.054

---

* FIVE TEMPERATURE SENSORS, SENSORS ARE AT HEIGHTS 0.3, 0.6, 1.2, 2.0 AND 3.0 METRES.
⊖ FIVE TEMPERATURE SENSORS, SENSORS ARE AT HEIGHTS 0.3, 1.2, 2.0, 3.0 AND 4.0 METRES.
¬ SIX TEMPERATURE SENSORS, SENSORS ARE AT HEIGHTS 0.3, 0.6, 1.2, 2.0, 3.0 AND 4.0 METRES.

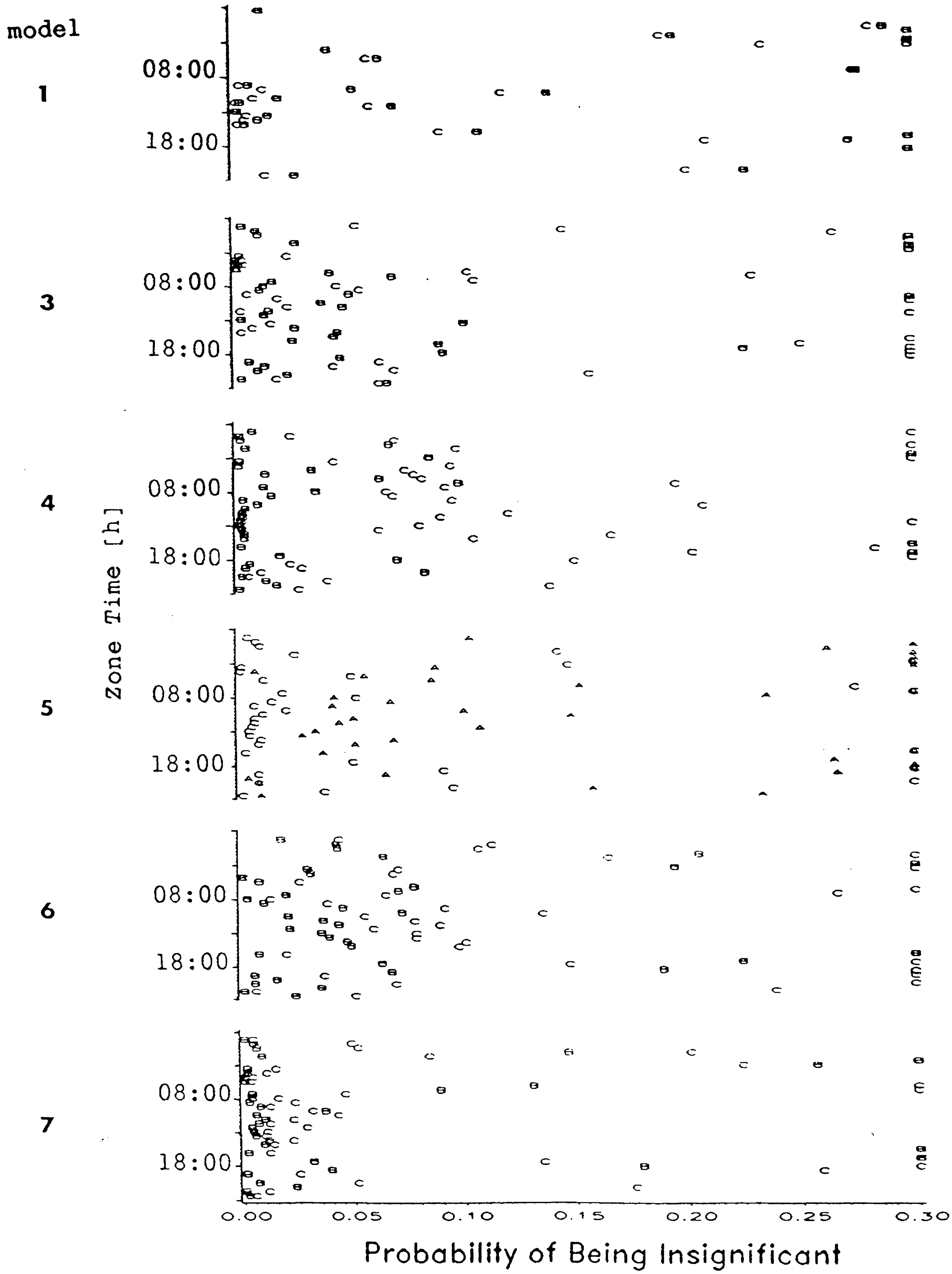

Figure 5.4: Test of the significance of coefficient for models in Table 5.4

5.4.4 Comparison and field verification of the results

The seven models in Table 5.4 were used to compute the refraction correction (see section 4.2.3) to measured height differences using the *UNB* trigonometric method on July 23 and 24, 1985, between each pair of the three bench marks at the South-Gym area. Tables 5.9, 5.10 and 5.11 show the results of the computed refraction effect versus the measured values (discrepancies between geodetic levelling and the *UNB*-method).

For model #1, in order to have the full range of results (all 35 intervals for comparison), software was developed to compute the correction based on either the least squares estimation of the coefficients or the computation of exponent c using equation (3.3) (using the observed temperatures at heights 0.3 m, 0.6 m and 1.2 m); or the assumption of a fixed value −1/3 for exponent c. The other two coefficients, a and b were estimated by least squares. For model #7, whenever the solution did not converge, then c = −1.5 was assummed and the other two coefficients were estimated through least squares. Figures 5.5, 5.6 and 5.7 show the spline fitted of these results. From these plots and the corresponding tables, it can be seen that models #4 and #5 produce very close results in spite of their different appearence. Models #1 and #3 also give very similar results. Model #6 gives some large discrepancies with the measured refraction effect. The same can be seen for model #7. Model #2 also results in values for refraction effect similar to other models.

Table 5.12 shows the correlation coefficient matrices for the three cases. The high values of the correlation coefficient among the results of the seven models are as expected (except for model #7, asphalt-gravel line). The highest correlation exist between models #4 and #5. In the first two matrices, the correlation coefficients between the measured refraction effect and the individual computed values using the seven models are generally significant. In the third case (Table 5.12 c) correlation does not exist as can also be seen from the corresponding Figure 5.7 . The reason for that will be discussed later. At the 1% level of significance the null hypothesis that $r = 0$ (r is the correlation coefficient factor) can be rejected against the alternative hypothesis that $r \neq 0$ if the correlation coefficient is equal to or larger than 0.44. The value 0.44 is the smallest correlation coefficient that can pass the test. The t statistic with (n-2) degrees of freedom is given by e.g. Hamilton [1964] as

$$t = \left[\frac{(n-2)\, r^2}{1 - r^2} \right]^{1/2}$$

where n is the number of observations. For $r = 0.44$, using the above equation: $t = 2.82$ which is greater than t value from corresponding table of percentage points:

$$t = 2.82 > t_{33,0.005} = 2.75$$

For $r = 0.43$, $t = 2.74$ which is smaller than the table value. In total, the r values for models #1, #3, #4 and #5 are larger than 0.44 in the two first cases, Table 5.12 a and b, and for models #2, #6 and #7 are smaller than 0.44 in the first case, Table 5.12 a.

The above discussion shows that the new proposed models can safely replace the Kukkamäki model when the number of temperature sensors is equal to or greater than 3. If the number of sensors is 2, then the model #2 is the only choice. To draw a firm conclusion about which model is the best reperesentative of the temperature profile in the lower atmosphere up to 4 m height and to confirm the validity of the new models, more investigations are needed.

TABLE 5.9

Refraction effect [mm] computed using the seven models versus the measured value (*BM1-BM2*).

NO	*ZONE TIME (ADT)*	*MODEL* #1	#2	#3	#4	#5	#6	#7	meas
1	10:00	-2.0	-1.0	-1.7	-1.7	-1.8	-1.9	-2.6	0.0
2	11:00	5.3	3.6	5.6	4.3	4.9	5.9	5.9	-0.7
3	12:00	1.9	1.7	2.5	1.5	1.8	2.2	-0.6	-1.7
4	13:00	-1.8	-2.0	-1.1	-1.2	-1.0	-2.9	-0.5	-1.4
5	14:00	0.3	-0.5	1.4	-0.2	0.3	-1.1	-3.0	-1.5
6	15:00	0.1	0.6	0.7	-0.2	0.0	0.2	5.2	-1.9
7	16:00	-0.6	-0.9	-0.8	-0.7	-0.6	-1.6	-0.4	-2.1
8	17:00	-2.2	-2.0	-2.2	-2.1	-2.2	-3.6	-2.5	-2.2
9	18:00	1.3	1.4	1.2	1.5	1.7	2.2	2.2	-2.4
10	19:00	-2.3	-2.1	-2.1	-2.4	-2.4	-3.5	-3.0	-1.8
11	20:00	-2.7	-3.3	-2.8	-2.9	-2.9	-5.1	-2.7	-3.4
12	21:00	0.5	0.1	-1.3	-0.3	-0.5	0.0	0.1	-2.6
13	22:00	-1.7	-4.0	-1.8	-3.1	-3.1	-6.0	-0.8	-2.0
14	23:00	-3.7	-5.8	-3.7	-4.9	-4.9	-8.8	-2.8	-1.8
15	24:00	-2.4	-3.9	-2.4	-3.1	-3.0	-5.9	-1.8	-1.9
16	01:00	-2.3	-4.3	-2.1	-2.9	-2.8	-6.2	-2.7	-2.0
17	02:00	-2.3	-2.4	-2.2	-2.3	-2.4	-3.7	-2.5	-1.7
18	03:00	-3.9	-6.0	-4.0	-5.2	-5.2	-9.2	-3.0	-1.8
19	04:00								
20	05:00	-3.4	-3.9	-3.1	-3.5	-3.6	-5.9	-4.0	-2.4
21	06:00								
22	07:00	-2.6	-3.4	-2.8	-3.0	-2.9	-4.1	-2.0	-1.2
23	08:00	0.8	-0.3	0.5	1.1	1.2	1.5	1.4	-0.5
24	09:00	2.6	-0.4	2.2	1.6	2.1	1.6	1.4	-0.3
25	10:00	1.5	1.5	2.2	1.0	1.3	1.4	1.2	0.1
26	11:00	1.1	-0.1	0.1	1.4	1.2	-0.3	0.3	-0.5
27	12:00	1.4	0.0	2.3	0.6	1.1	-0.4	0.7	-0.5
28	13:00	2.3	1.1	3.4	1.5	2.0	1.5	6.4	-0.7
29	14:00								
30	15:00	-0.5	1.3	-0.7	0.1	0.0	1.4	4.7	-2.1
31	16:00	0.1	-0.7	0.2	-0.2	0.0	-1.1	0.5	-1.2
32	17:00	-0.2	-0.7	-0.2	0.6	0.7	1.1	-0.1	-1.8
33	18:00	-0.7	-1.2	-0.8	0.0	0.0	-0.1	-0.2	-2.5
34	19:00	-2.7	-3.1	-2.6	-2.4	-2.3	-3.0	-2.4	-2.5
35	20:00	-0.5	-3.4	-1.9	-2.1	-1.9	-3.1	-1.1	-2.5
36	21:00	-2.9	-4.0	-3.0	-2.6	-2.6	-3.9	-4.8	-2.5
37	22:00	-3.2	-2.5	-1.8	-0.9	-1.0	-1.6	-3.1	-1.7
38	23:00	-2.1	-2.6	-2.3	-1.8	-1.8	-2.6	-3.1	-1.7
	Mean	-0.8	-1.5	-0.7	-0.9	-1.0	-1.9	-0.6	-1.7

TABLE 5.10

Refraction effect [mm] computed using the seven models versus the measured value (BM2-BM3).

NO	ZONE TIME (ADT)	MODEL #1	#2	#3	#4	#5	#6	#7	meas
1	9:00	1.6	0.3	1.5	1.0	1.1	0.6	1.5	-1.4
2	10:00	-3.2	-2.9	-3.9	-2.4	-3.0	-4.2	-6.4	-1.4
3	11:00	-3.1	-1.9	-3.1	-2.2	-2.7	-2.8	-1.0	0.2
4	12:00	1.5	0.5	0.4	0.9	0.7	1.1	0.4	-0.5
5	13:00	-3.0	-0.8	-3.5	-2.2	-3.0	-1.8	-0.7	-0.6
6	14:00	-6.1	-4.3	-6.2	-4.8	-5.6	-6.8	-6.8	0.6
7	15:00	0.3	0.5	0.2	0.8	0.5	1.1	0.0	-0.3
8	16:00	2.7	1.4	2.3	2.6	2.6	3.1	-1.1	-1.8
9	17:00	-1.1	-1.7	-1.0	-1.8	-1.9	-3.0	-1.8	-1.2
10	18:00	1.2	1.9	1.2	1.3	1.2	2.4	1.1	0.0
11	19:00	3.4	3.4	3.4	3.5	3.6	5.4	3.4	1.1
12	20:00	0.1	0.7	2.0	0.6	0.8	0.9	0.1	1.7
13	21:00	2.1	3.7	2.1	3.7	3.8	6.3	1.7	1.7
14	22:00	3.5	5.3	2.9	3.9	3.8	7.5	2.7	1.9
15	23:00	2.2	3.7	2.1	3.0	2.9	5.6	1.8	1.9
16	24:00	2.1	3.3	2.1	2.9	3.0	5.2	2.0	1.1
17	01:00								
18	02:00	3.2	5.3	3.2	4.2	4.3	7.9	2.5	2.0
19	03:00	2.6	4.4	2.7	3.6	3.6	6.7	2.6	1.6
20	04:00	2.8	3.0	2.8	3.1	3.3	4.9	3.4	1.0
21	05:00								
22	06:00	1.3	2.7	1.4	2.0	1.8	3.8	0.5	0.4
23	07:00								
24	08:00	0.2	0.0	0.2	0.5	0.2	-0.9	-0.4	-1.0
25	09:00	-1.3	-1.3	-1.6	-0.7	-1.2	-2.4	-1.9	-2.0
26	10:00	-2.1	-1.6	-2.5	-1.4	-1.9	-2.5	0.4	-1.6
27	11:00	-2.3	-2.1	-4.9	-0.1	-1.8	-3.1	0.2	-1.5
28	12:00	-3.2	-2.2	-4.0	-2.2	-2.8	-3.5	-4.0	-0.5
29	13:00	-5.2	-3.1	-6.5	-3.8	-4.7	-5.3	-5.9	-2.0
30	14:00	-0.9	-2.9	-1.1	-1.2	-1.3	-3.9	-6.5	-0.5
31	15:00	0.7	-0.5	0.4	0.8	0.6	-0.1	-3.8	-1.7
32	16:00	0.8	-0.8	0.8	0.4	0.6	0.2	1.9	0.2
33	17:00	0.7	1.1	0.8	0.0	-0.1	-0.5	0.3	0.4
34	18:00	2.6	2.8	2.5	2.6	2.4	2.9	2.3	-0.3
35	19:00	0.4	3.4	1.7	1.5	1.4	2.2	1.3	1.5
36	20:00	3.8	3.7	3.7	3.8	3.9	5.5	4.2	2.3
37	21:00	0.4	1.6	1.3	0.1	0.5	1.0	0.4	2.6
38	22:00	3.0	2.7	2.6	1.5	1.8	2.2	3.2	1.7
	Mean	0.3	0.8	0.2	0.7	0.5	1.0	-0.1	0.3

TABLE 5.11

Refraction effect [mm] computed using the seven models versus the measured value (BM3-BM1).

NO	ZONE TIME (ADT)	MODEL #1	#2	#3	#4	#5	#6	#7	meas
1	9:00	0.0	0.3	-0.2	0.4	0.3	0.5	0.4	1.7
2	10:00	-2.3	-1.0	-2.1	-1.9	-2.1	-2.2	0.1	1.7
3	11:00	0.9	-0.2	0.3	0.6	0.7	0.2	1.2	1.5
4	12:00	-0.1	1.0	0.2	0.0	-0.2	0.9	-0.6	1.0
5	13:00	2.3	0.9	1.7	2.1	2.3	2.1	3.1	2.1
6	14:00	5.6	3.2	5.1	4.9	5.3	6.1	0.9	2.0
7	15:00	-0.1	0.0	0.1	-0.3	-0.3	-0.3	-0.4	2.8
8	16:00	-0.9	0.1	-0.7	-0.7	-0.8	-0.4	2.8	2.9
9	17:00	-0.5	0.0	-0.5	-0.1	-0.2	-0.1	-0.9	2.5
10	18:00	0.8	-0.1	0.5	0.7	0.8	0.3	1.3	2.1
11	19:00	-1.0	-0.4	-0.9	-0.9	-1.0	-1.0	-1.2	1.6
12	20:00	-0.6	-0.9	-0.7	-0.5	-0.4	-1.2	-0.2	1.2
13	21:00	-0.1	0.6	0.0	-0.1	-0.2	0.5	-0.6	-0.2
14	22:00	0.2	0.6	0.8	0.9	0.9	1.1	0.1	-1.2
15	23:00	0.2	0.2	0.2	0.0	0.0	0.2	-0.1	-0.3
16	24:00	0.3	1.2	0.1	0.1	-0.1	1.3	0.9	0.8
17	01:00								
18	02:00	0.2	0.1	0.2	0.3	0.3	0.3	0.1	0.0
19	03:00	1.2	1.0	1.2	1.1	1.1	1.6	0.6	0.0
20	04:00	0.7	0.9	0.4	0.5	0.4	1.2	0.7	0.8
21	05:00								
22	06:00	0.9	0.4	0.9	0.6	0.6	-0.5	0.9	1.0
23	07:00	-1.3	0.1	-1.0	-1.8	-1.7	-1.5	-1.5	0.8
24	08:00								
25	09:00	-2.0	0.5	-1.3	-1.5	-1.6	-0.9	-2.8	1.8
26	10:00	-0.1	0.1	-0.3	0.2	0.0	0.5	0.4	1.6
27	11:00	-1.7	0.0	-0.1	-2.8	-2.0	-0.4	-2.7	2.2
28	12:00	1.6	1.2	1.9	1.3	1.5	2.0	-1.8	2.0
29	13:00	2.4	1.5	2.5	2.1	2.3	2.8	-1.3	0.9
30	14:00	0.9	1.0	0.9	0.8	0.9	1.5	0.9	2.8
31	15:00	-1.5	0.6	-1.4	-1.0	-1.2	0.0	2.3	2.1
32	16:00	-0.8	1.2	-0.9	-1.3	-1.6	-2.1	-2.1	1.0
33	17:00	-0.2	-0.2	-0.2	-0.3	-0.3	-0.2	-0.3	2.0
34	18:00	0.0	0.2	0.0	-0.5	-0.4	-0.6	0.0	1.9
35	19:00	0.1	0.0	0.2	0.2	0.2	0.2	-0.3	0.5
36	20:00	-0.9	0.4	-0.5	-1.3	-1.3	-1.4	0.8	-0.3
37	21:00	2.8	1.0	0.7	0.5	0.5	0.4	2.8	-1.2
38	22:00	-0.9	0.0	-0.1	0.1	0.0	0.2	0.0	0.4
	Mean	0.2	0.4	0.2	0.1	0.1	0.3	0.1	1.2

TABLE 5.12

Correlation Coefficients Matrices

	MODEL #1	#2	#3	#4	#5	#6	#7	measur.
model #1	1							
model #2	0.89	1						
model #3	0.96	0.89	1					
model #4	0.93	0.94	0.92	1				
model #5	0.95	0.94	0.95	1.00	1			
model #6	0.88	0.96	0.87	0.97	0.97	1		
model #7	0.79	0.78	0.77	0.75	0.75	0.74	1	
measured	0.50	0.42	0.56	0.48	0.49	0.41	0.36	1
	a: gravel-grass (*BM*1-*BM*2) line							
model #1	1							
model #2	0.89	1						
model #3	0.97	0.89	1					
model #4	0.96	0.94	0.92	1				
model #5	0.97	0.94	0.95	0.99	1			
model #6	0.91	0.98	0.89	0.97	0.97	1		
model #7	0.81	0.84	0.79	0.82	0.82	0.82	1	
measured	0.52	0.71	0.60	0.56	0.59	0.67	0.58	1
	b: grass-asphalt (*BM*2-*BM*3) line							
model #1	1							
model #2	0.74	1						
model #3	0.94	0.77	1					
model #4	0.93	0.68	0.91	1				
model #5	0.94	0.68	0.95	0.99	1			
model #6	0.86	0.79	0.92	0.90	0.92	1		
model #7	0.38	0.10	0.18	0.38	0.34	0.25	1	
measured	-.10	-.10	-.04	-.05	-.02	.02	-.03	1
	c: asphalt-gravel (*BM*3-*BM*1) line							

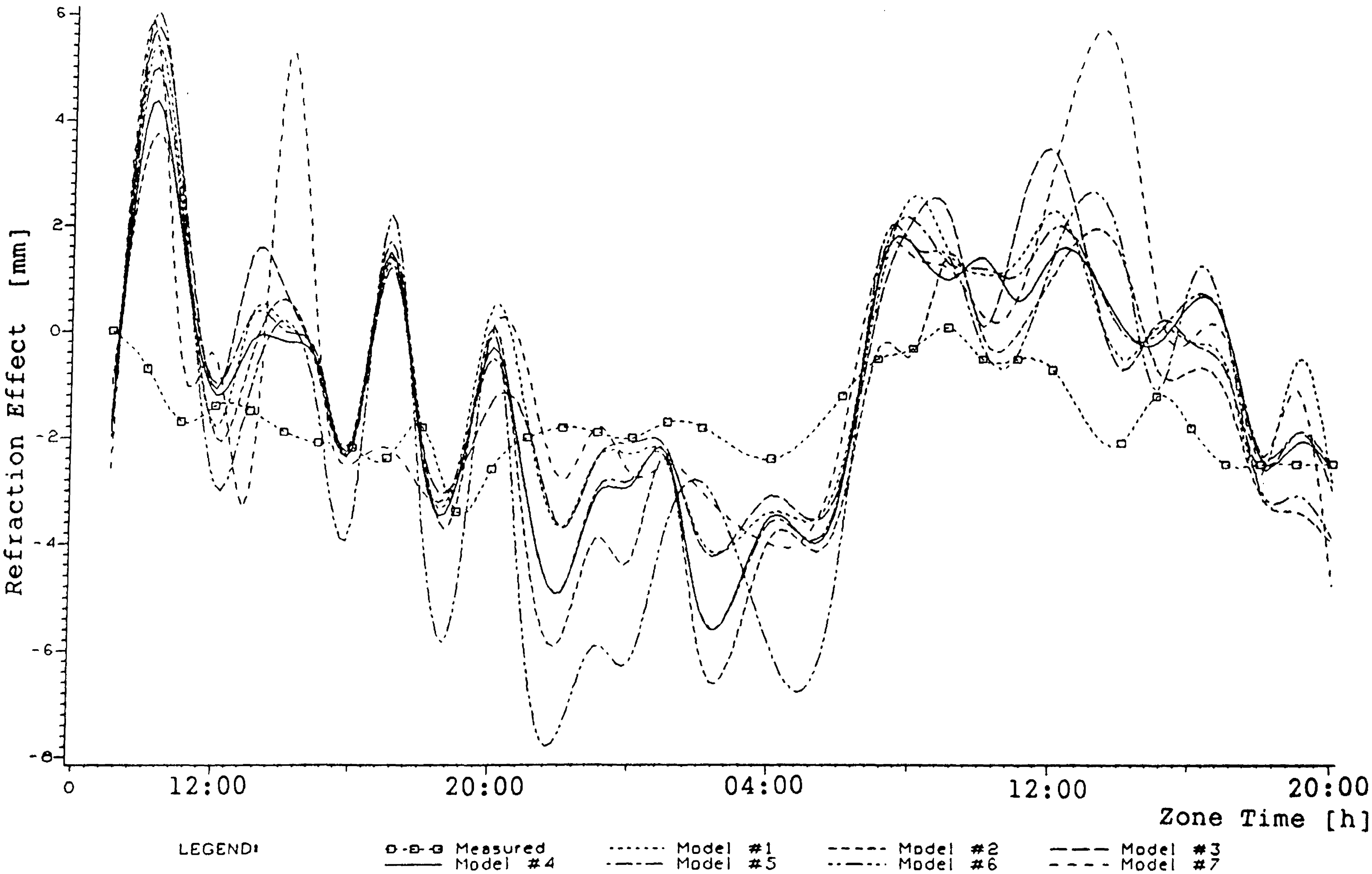

Figure 5.5: Refraction effect computed using the seven models versus the measured value for *BM1-BM2*.

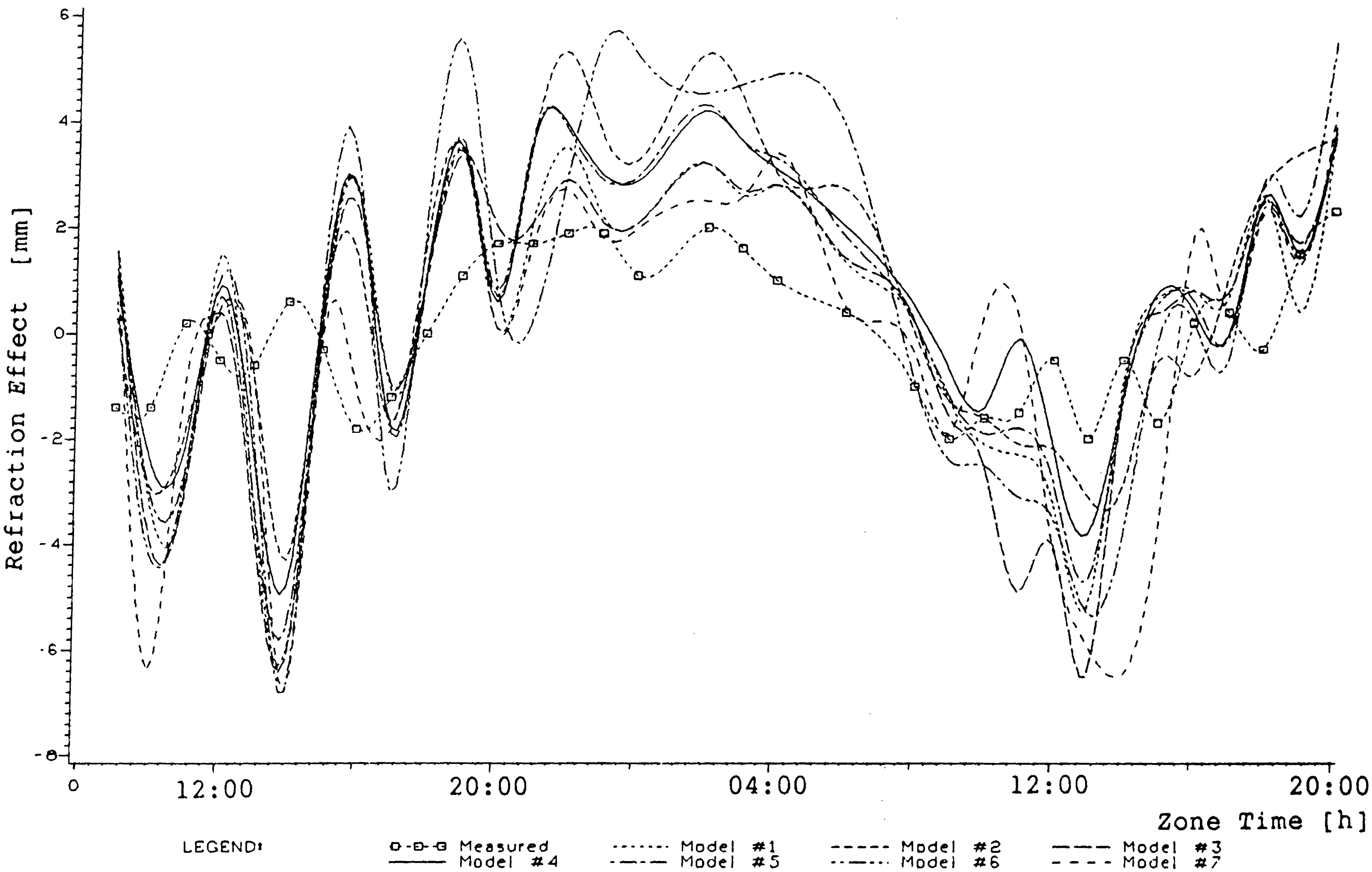

Figure 5.6: Refraction effect computed using the seven models versus the measured value for *BM2-BM3*.

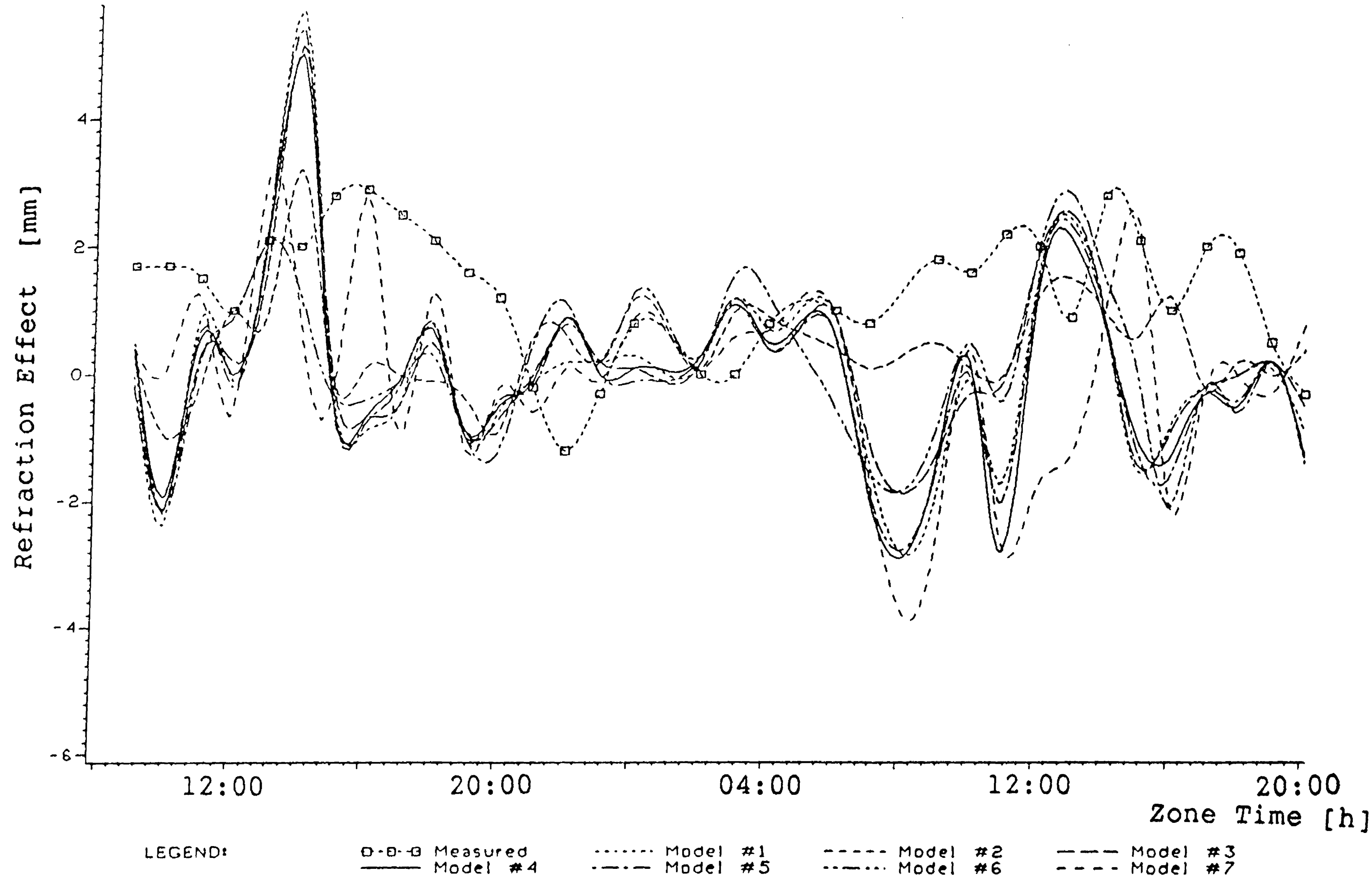

Figure 5.7: Refraction effect computed using the seven models versus the measured value for *BM3-BM1*.

5.5 Computed Versus Measured Refraction Effect

5.5.1 Tests on 20 June 1985

The first test was performed on 20th of June as a preliminary observation preparation for the long term tests. Only the height difference between *BM*1 and *BM*2 was measured repeatedly for four hours from 10:20 to 14:30. Table 5.13 shows the discrepancies between the geodetic height differences and *UNB* method trigonometric height differences.

TABLE 5.13

Preliminary test measurements using *UNB* trigonometric method at South-Gym area from *BM*1 to *BM*2

		Geod. - Trig. [mm]			REMARKS	
NO	*LOCAL TIME*	2.1m tar	3.5m tar	mean of 2 tar	cloud cover %	condition
1	10:25	0.1	-1.9	-0.9	50	Sunny
2	10:45	0.5	-1.2	-0.4	50	Sunny
3	11:02	1.9	-0.4	0.8	50	Sunny, Windy
4	11:16	-0.3	-1.5	-0.9	70	Windy
5	11:32	-1.0	-1.8	-1.4	90	Windy
6	11:54	-3.6	-2.2	-2.9	100	Breeze
7	12:12	-2.1	-1.0	-1.5	100	Windy
8	12:30	-0.1	-1.1	-0.6	75	Sunny periods, windy
9	13:01	-1.6	-2.0	-1.8	50	Sunny periods, windy
10	13:15	0.7	0.2	0.5	50	Sunny periods, windy
11	13:47	-4.1	-3.9	-4.0	75	Windy
12	14:00	-2.2	-2.4	-2.3	75	Windy
13	14:13	-0.6	-1.2	-0.9	75	Windy
Mean		-0.95	-1.57	-1.25		
S. D.		1.72	1.01	1.31		

The day on which the observations were carried out was reported as windy. In a moderatly windy day of summer, the Obukhov length defined in section 3.1.2 is usually longer than 30 m (see e.g. Greening, [1985]). The results of the first three rows show positive values for the lower targets and negative values for the heigher targets. This was first thought to be due to the inversion of the temperature gradient, but later it was found that the magnitude of the refraction effect can change sign with elevating line of sight regardless of the sign of the temperature gradients. On a windy day, region *II* (the middle region of thermal stability, see section 3.1.3 for more detail) extends usually to more than 30 m (one Obukhov length) and according to theories (see e.g. Webb, [1984]), inversion of temperature, on a windy day of summer with light cloud cover, cannot appear below this range. However on calm days, when the horizontal movement of air is less than 2 m/s, one may expect momentarily inversion of temperature gradients within the first three metres of the atmospheric layer. But, this does not necessarily mean that the lower targets will result in a sign of refraction effect different from the results of the higher targets (see also section 5.3.6).

The meteorological observations done on 20 June 1985 were: air temperature and pressure for correcting the measured distances, and a record of cloud cover and wind.

No temperature gradient was measured, therefore the magnitude of refraction effect using the meteorological data could not be obtained for the first test. For all other tests the wind velocity and direction, temperature gradient, atmospheric pressure, humidity, and temperature of the ground surface were measured and cloud cover was recorded. Although all this information was useful for understanding the changes of atmospheric condition and if possible their correlation with the refraction error, only the temperature gradient was used to compute the magnitude of refraction effect.

5.5.2 Tests on 19 July 1985

The second test was carried out on 19 July 1985. It was supposed to continue for 24 hours, but due to unfavourable weather conditions it was interrupted after 13 hours of continuous observations. The height differences between BM1, BM2 and BM3 were measured repeatedly over the whole 13-hour period.

Tables 5.14, 5.15 and 5.16 show the discrepancies between the height differences obtained using precise geodetic levelling and using the UNB-method. These discrepancies can be interpreted as mostly due to the refraction effect by assuming the results of geodetic levelling as being errorless.

***TABLE* 5.14**

Discrepancies between the results obtained using trigonometric height traversing and geodetic levelling for *BM*1 to *BM*2.

		Geod. - *Trig.* [mm]			*REMARKS*	
NO	*LOCAL TIME*	2.1m tar	3.5m tar	mean of 2 tar	cloud cover %	condition
1	11:13	-0.1	-0.9	-0.5	75	
2	12:09	-2.0	0.5	-0.7	100	*Fair*
3	13:24	-1.4	-2.7	-2.0	50	Windy
4	14:54	-2.7	-2.0	-2.3	75	Windy, little rain
5	15:49	-3.6	-1.2	-2.4	100	*Little* wind
6	18:05	-1.7	-1.5	-1.6	100	
7	18:56	-2.4	-0.8	-1.6	100	
8	19:31	-0.8	-1.0	-0.9	100	
9	20:09	-2.6	-0.3	-1.5	100	
10	21:56	-1.7	-2.2	-1.9		After a period of rain
11	22:47	-1.9	-0.7	-1.3		Cloudy
12	23:25	-0.7	-0.7	-0.7		Cloudy
Mean		-1.80	-1.13	-1.45		
S. D.		±0.97	±0.87	±0.64		

Since the profile of surface on the fore-sight of one line is the same as the back-sight of the other, one can expect that over a long period the misclosure of the three height differences would be near zero. *The* mean misclosure for the lower targets is -0.03 mm i.e. as expected. *But* the mean misclosure for the higher targets is -0.85 mm which is considered as too large.

Column 2 of *Table* 5.15 shows that the mean discrepancies for target 3.5 m is a negative number. *This* value was expected

TABLE 5.15

Discrepancies between the results obtained using trigonometric height traversing and geodetic levelling for BM2 to BM3.

		Geod. - Trig. [mm]			REMARKS	
NO	LOCAL TIME	2.1m tar	3.5m tar	mean of 2 tar	cloud cover %	condition
1	11:31	-1.5	-1.8	-1.6	75	shimmers on BM3
2	12:28	-1.6	-2.7	-2.1	25	Shimmers on BM2.
3	14:00	2.2	-0.8	0.7	50	Windy
4	15:16	0.3	-0.5	-0.1	100	Windy, little rain
5	16:04	0.0	-0.1	-0.1	100	Little windy
6	18:29	0.3	-0.1	0.1	100	
7	19:07	0.8	0.4	0.6	100	
8	19:41	2.0	0.7	1.3	100	
9	20:21	2.3	1.7	2.0	100	
10	22:18	1.1	-0.5	0.3	100	After a period of rain
11	22:59	0.7	0.6	0.7	100	Cool
12	23:35	0.6	0.5	0.5	100	Little windy
Mean		0.60	-0.22	0.19		
S. D.		±1.26	±1.18	±1.13		

to be positive. The computed refraction using the profile of the lines and measured temperature gradient in Table 5.17, indicates positive mean values for both targets.

This can be explained by using Figure 5.8 When $RB-RF > 0$ then $\Delta HG-\Delta HT < 0$ and when $RB-RF < 0$ then $\Delta HG-\Delta HT > 0$. The first case had mostly occurred for the lower targets and the second case for the higher targets. The temperature gradient on the grass field close to the ground (0.3 m to 1.2 m) is larger in magnitude than the

TABLE 5.16

Discrepancies between the results obtained using trigonometric height traversing and geodetic levelling for *BM*3 to *BM*1.

		Geod. - Trig. [mm]			*REMARKS*	
NO	*LOCAL TIME*	2.1m tar	3.5m tar	mean of 2 tar	cloud cover %	condition
1	11:49	1.5	1.9	1.7	75	Breeze
2	12:46	2.7	-0.3	1.2	0	Sunny
3	14:17	3.1	1.8	2.4	95	
4	15:36	1.2	0.4	0.8	100	Little rain & wind
5	16:32	1.7	0.9	1.3	100	Little windy
6	18:43	-0.2	0.6	0.2	100	
7	19:19	0.2	-0.1	0.1	100	
8	19:59	0.4	-0.4	0.0	100	
9	22:35	1.1	0.0	0.5	100	After a period of rain
10	23:12	0.8	0.0	0.4	100	
11	00:05	0.4	0.7	0.5	100	
Mean		1.17	0.5	0.83		
S. D.		±1.03	±0.79	±0.75		

temperature gradient over asphalt close to the ground, and it is smaller when going higher above the surface (1.2 m to 4 m). This may explain the different signs of values, but cannot explain the large misclosure of -0.85 mm for the higher targets. However, this rather irregular misclosure was not repeated in the three other cases and was always nearly zero.

TABLE 5.17

Computed refraction using measured temperature gradient

		Computed Refraction [mm]								
	LOCAL	BM1 to BM2			BM2 to BM3			BM3 to BM1		
NO	TIME	2.1m	3.5m	Mean	2.1m	3.5m	Mean	2.1m	3.5m	Mean
1	11:00	2.4	1.6	2.0	-2.8	-1.6	-2.2	-0.2	-0.4	-0.3
2	12:00									
3	13:00	-3.9	-3.6	-3.7	4.9	4.5	4.7	-1.6	-1.3	-1.4
4	14:00									
5	15:00	-1.2	-0.2	-0.7	1.7	1.1	1.4	-0.8	-1.2	-1.0
6	16:00				1.9	1.3	1.6			
7	17:00	0.0	0.3	0.1	0.2	0.2	0.2	-0.5	-0.7	-0.6
8	18:00				0.2	0.2	0.2			
9	19:00	-1.0	-0.7	-0.9				0.7	0.5	0.6
10	20:00	-1.0	-0.4	-0.7	0.1	-0.4	-0.1	0.8	0.6	0.7
Mean				-0.65			0.83			-0.33
S. D.				±1.84			±2.11			±0.85

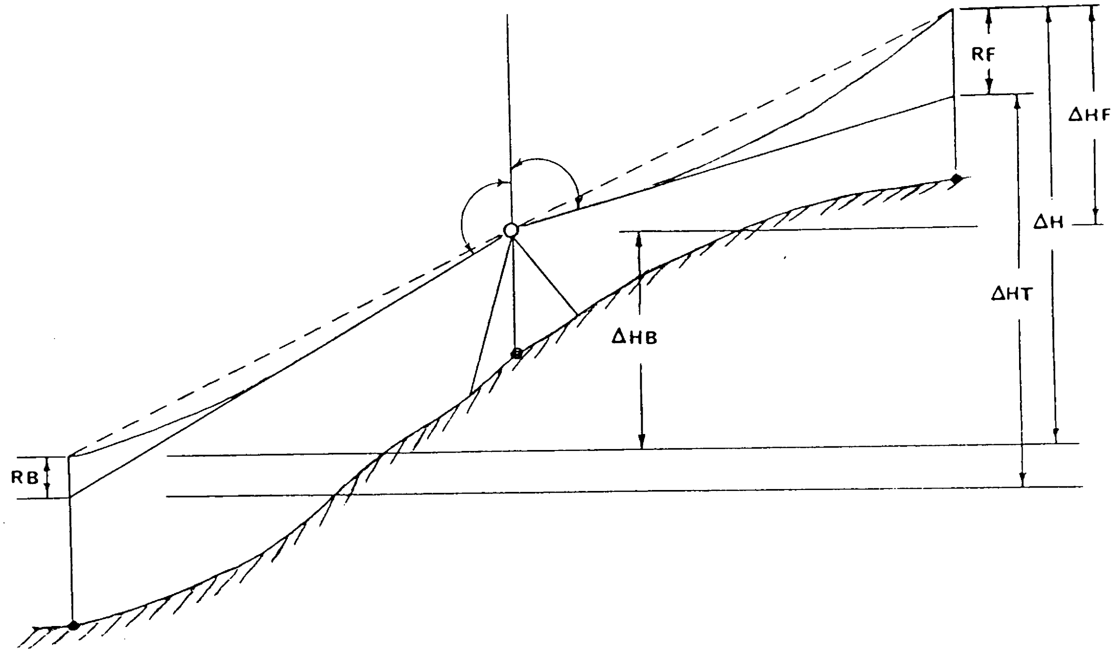

ΔHG : height difference using geodetic levelling
ΔHT : height difference using the leap-frog trigonometric method

$$\begin{aligned}\Delta H &\sim \Delta HG = \Delta HB + \Delta HF \\ \Delta HT &= \Delta HB + RB + \Delta HF - RF \\ &= \Delta HG + (RB - RF)\end{aligned}$$

I) If $(RB - RF) > 0$ THEN : $(\Delta HG - \Delta HT) < 0$

II) If $(RB - RF) < 0$ THEN : $(\Delta HG - \Delta HT) > 0$

Figure 5.8: Back- and fore-sight magnitude of refraction difference

5.5.3 Tests on 23 and 24 July 1985

The third test survey in the South-Gym area started at 9:43 on 23 July 1985 and continued to the next day until 23:50 for a total of 38 hours of continuous observations. The temperature gradient of air was measured during the entire test period. Knowing the profile of the lines and using equations (3.66) and (3.67), the refraction effect for all three lines was computed for one hour intervals. Figure 5.9 shows:

1. The measured refraction effect which is the discrepancy between the height difference determined using geodetic levelling and the results obtained with the *UNB*-method of trigonometric height traversing ($\Delta HG - \Delta HT$).
2. The computed refraction at one hour intervals using the observed temperature gradients.

The error bars in this figure are based on the precision of the observations and they have been increased to take into account other errors (this will be briefly discussed in section 5.3.8.).

The correlation between the two can be seen in Figure 5.9 parts a and b, and the correlation is more pronounced in the latter for *BM*2 to *BM*3. A fitted linear regression line (the solid line) in Figure 5.10 has small deviations from the expected hypothetical regression line (the dashed line: mr = cr). This figure shows the measured refraction effect against the computed refraction effect for the line *BM*2-*BM*3. The relationship between the measured, mr, and computed refraction, cr, is defined by the regression equation (the solid line in Figure 5.10):

$$mr = 0.3 + 1.2\ cr \qquad (5.12)$$

with correlation coefficient, $r = 0.60$. At the 1% level of significance $Ho : r = 0$ is rejected and thus $Ha : r \neq 0$, i.e. correlation exists, can be accepted (for details of the test see section 5.4.4). This is almost the same for the line *BM*1-*BM*2. The lowest correlation exists between the measured and the computed refraction effects for the line *BM*3-*BM*1 (see Table 5.12).

In order to investigate the difference of measured and computed refraction we may consider the lines from the instrument station to the bench marks separately. A good assessment of the refraction computation over each ground surface is also possible by examining them individualy.

The refraction angle can be found by detecting the neutral condition (see section 3.1.2) from temperature measurements. Figure 5.11 depicts the approximate time of neutral condition for different sufaces and elevations, i.e. when the periodic temperature gradient crosses the zero line. Figure 5.12 shows the fluctuations of observed vertical angles to the lower targets. Using these graphs and considering the corresponding time of neutral condition when the refraction effect is expected to be almost zero, the fluctuation around this zero point is mostly because of refraction and can be computed simply by subtracting the angle observed at neutral condition time from all other corresponding measured vertical angles and assuming the difference is the angle of refraction. The angle of

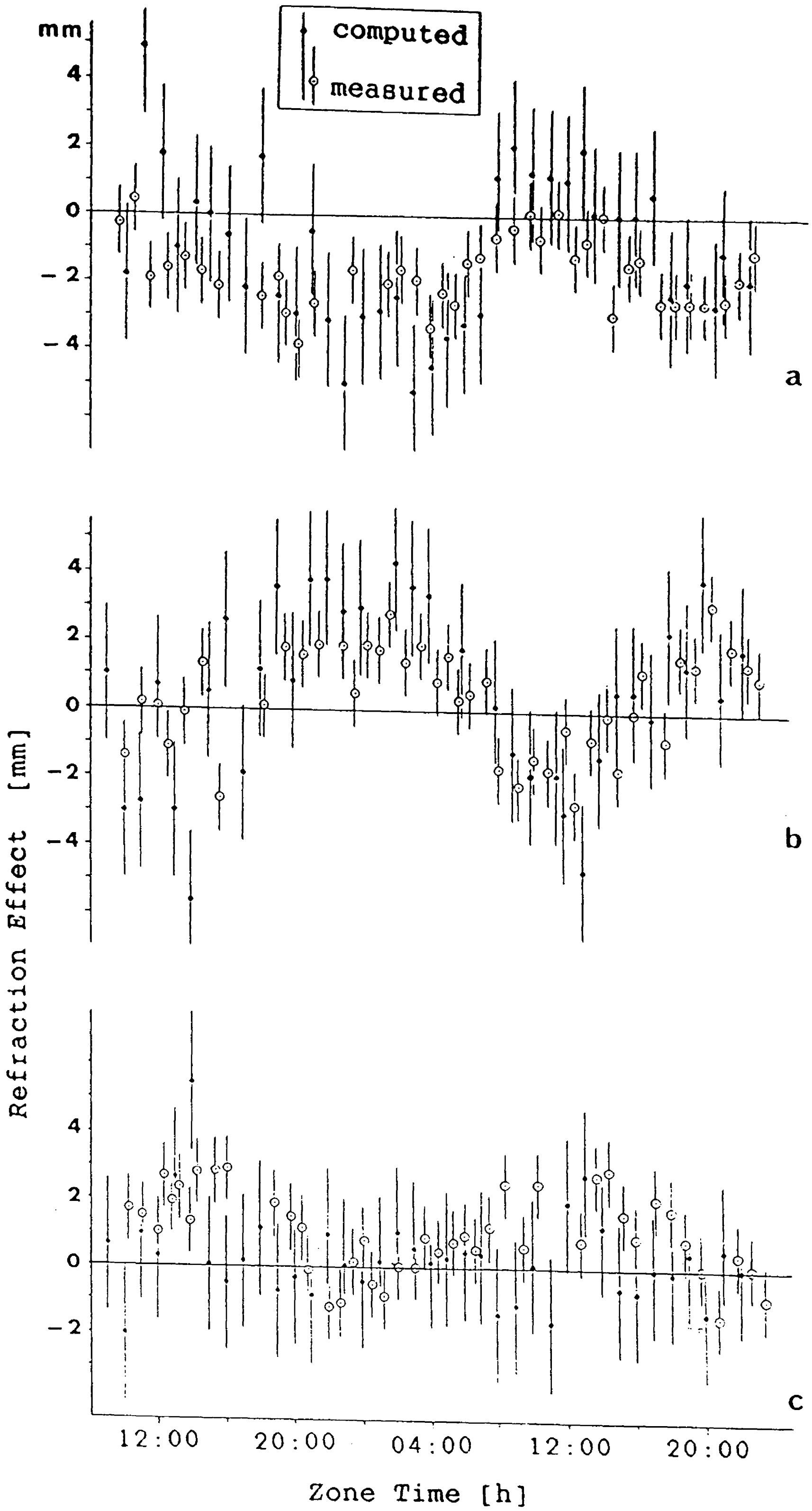

Figure 5.9: Measured refraction effect versus the computed value.
a. *BM1-BM2*, b. *BM2-BM3* and c. *BM3-BM1*.

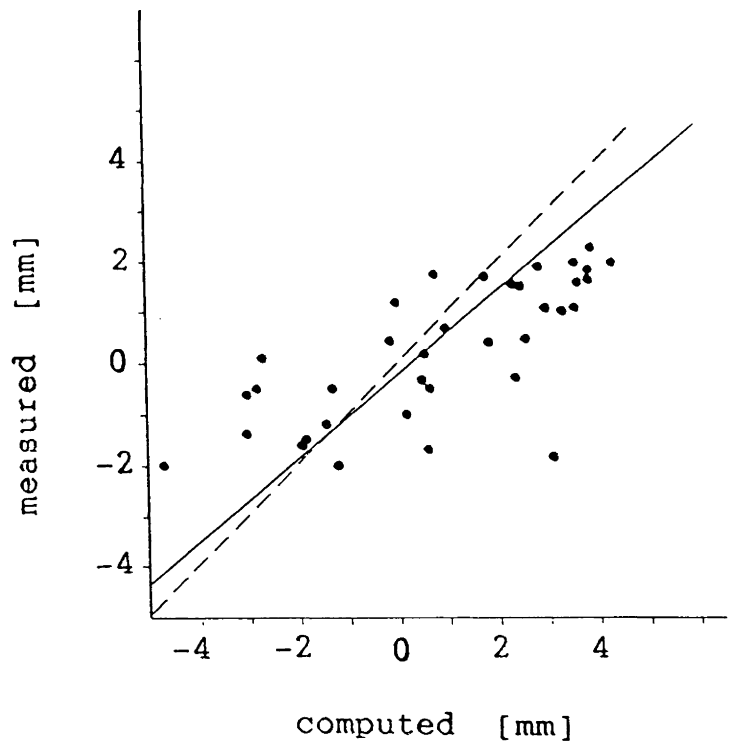

Figure 5.10: The measured refraction effect [mm]. The discrepancies of height difference determined by trigonometric height traversing and geodetic levelling for BM1-BM2 line versus the computed refraction error for the same line. The dashed line is the hypothetical regression line, and the solid line represents the actual linear regression.

refraction found in this way is as precise as the measured vertical angle, i.e. about 0.6" (see section 5.3.8); however, its accuracy can be lower because of the bias introduced due to the uncertaintity for detecting the neutral conditon or the zero refraction angle time.

This angle of refraction is converted to linear refraction and compared with the computed refraction for all three lines in Figure 5.13 . In all three plots the strong correlation between the two computed and measured refraction effects can be seen. These plots are prepared for the mean corresponding values of the two targets.

Figure 5.14 gives the linear correlations which exist between computed and measured refraction effects. Table 5.18 gives the correlation coefficient, linear regression equations relating the computed to the measured refraction effect, and at the 1% level of significance the null hypotheses that there is zero correlation between the measured and the computed refraction effect ($Ho : r = 0$).

In Table 5.18, the regression equations show that the computed refraction effect, cr, is too large compared to the measured refraction effect, mr. Specifically over asphalt, the measured refraction effect is more than four times smaller than the computed one. There are two possible explanations of why the results of asphalt are so different from the other two surfaces:

1. The site chosen to make the temperature gradient measurements was too close to the ground covered by gravel (about 2 m) and was not characteristic of the road on which the line of sight to *BM*3 was extended. The reason for choosing that spot was the lack of proper transportation to move the equipment from one site to another.
2. The wind was blowing almost in the direction of the line of sight to *BM*3. According to Webb [1968] this can

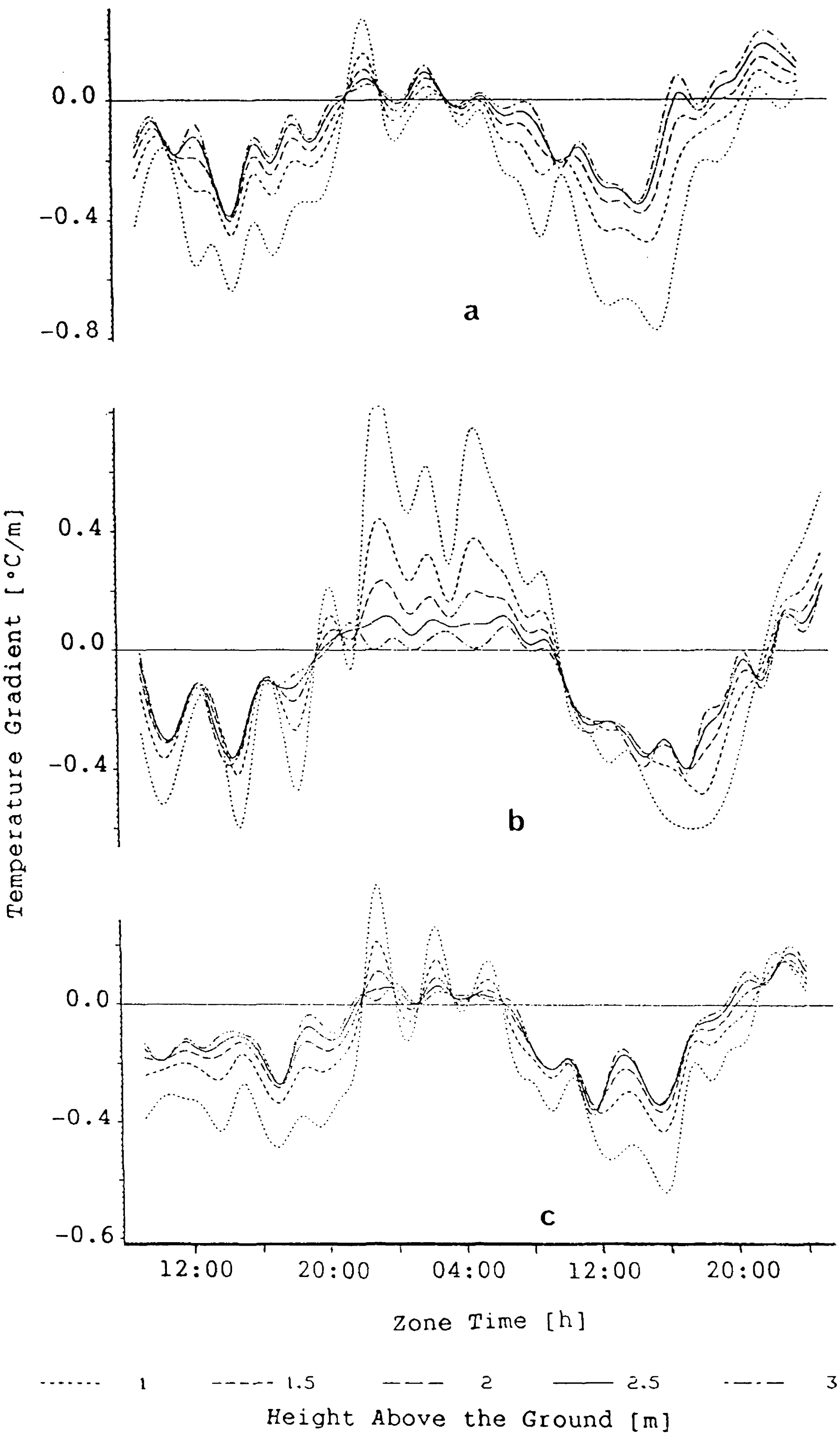

Figure 5.11: Fluctuations of point temperature gradient a. gravel, b. grass and c. asphalt.

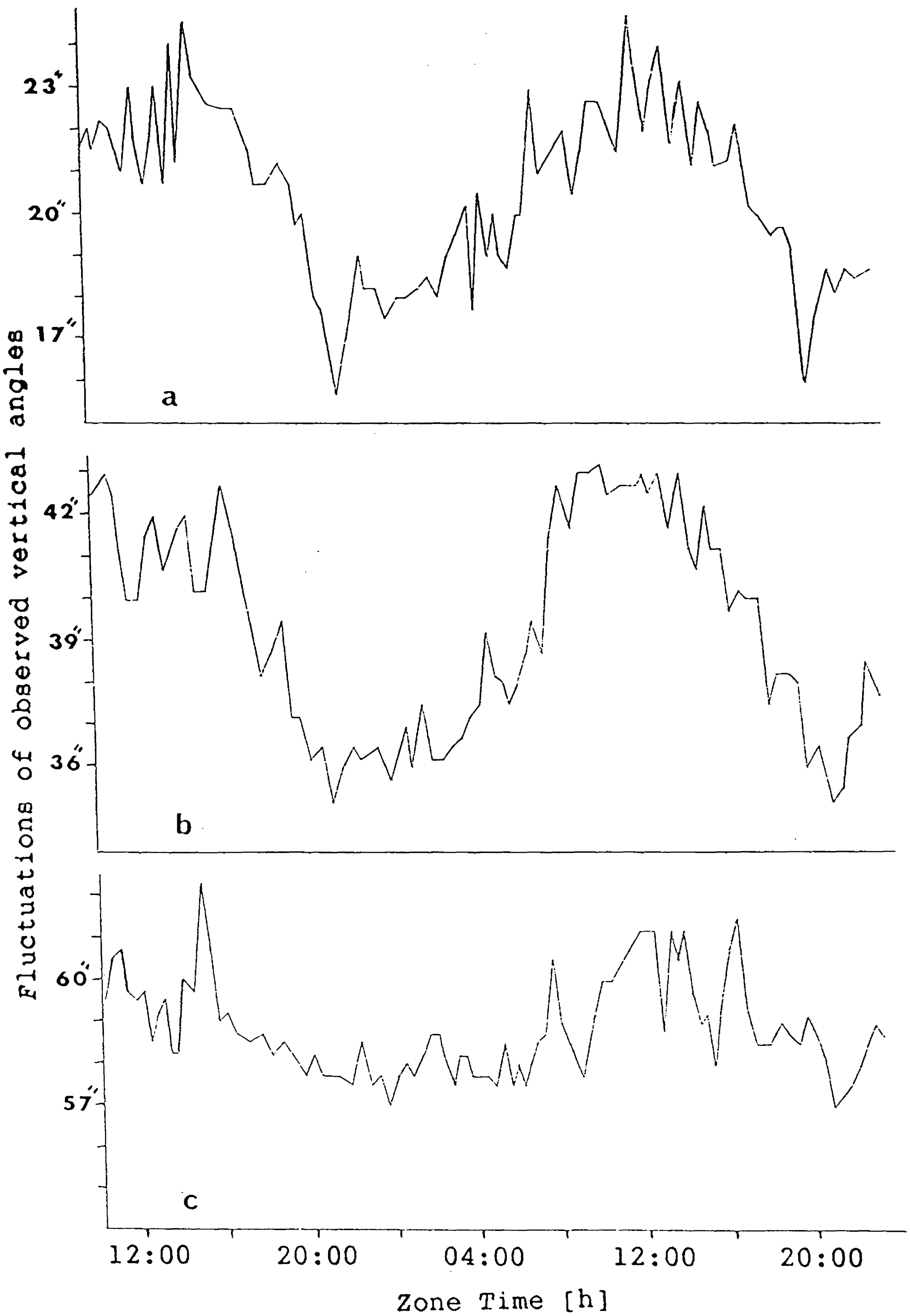

Figure 5.12: Fluctuations of observed vertical angles
a. *BM1* (gravel), b. *BM2* (grass), and c. *BM3* (asphalt).

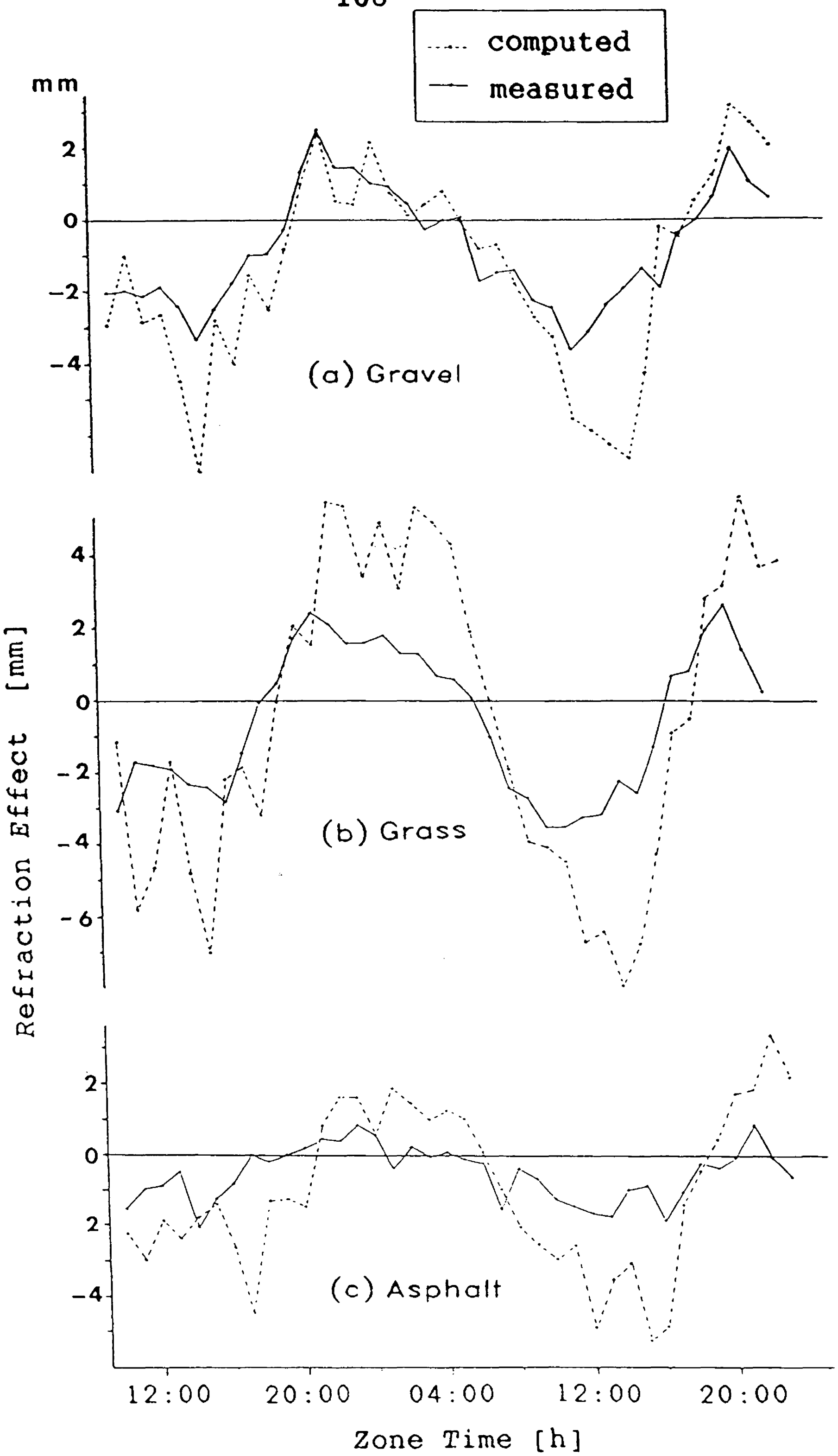

Figure 5.13: Computed refraction effect versus the measured value.
a. *IS-BM1* (gravel), b. *IS-BM2* (grass) and c. *IS-BM3* (asphalt).

result in lower refraction effect than the expected (computed) value. Other than the wind direction, during the day, the traffic on the road could also result in a mixing of the atmosphere and a reducing of the effect of refraction. The lower refraction effect over asphalt can be noticed from the small fluctuations of the vertical angle in comparison to the other two in Figure 5.12

It was previously mentioned that, as can be seen in Figure 5.9 c, the discrepancies between the geodetic levelling and trigonometric height traversing of *BM3-BM1* versus the computed refraction have very weak correlation (Table 5.12). Using the regression equations in Table 5.18 for asphalt and gravel, the computed refraction was corrected according to these two equations, given cr as computed then mr will be the corrected refraction effect. A significant improvement in the correlation coefficient was found between the two after the corrections were made. The correlation coefficient improved to 0.68 .

The significant correlations of the two measured refraction effects (either derived from the angle of refraction or from discrepancies between geodetic and trigonometric methods of height differnce determination) against the computed refraction is mostly due to the detailed knowledge that we have about the surface profiles and to the long term temperature gradient measurements.

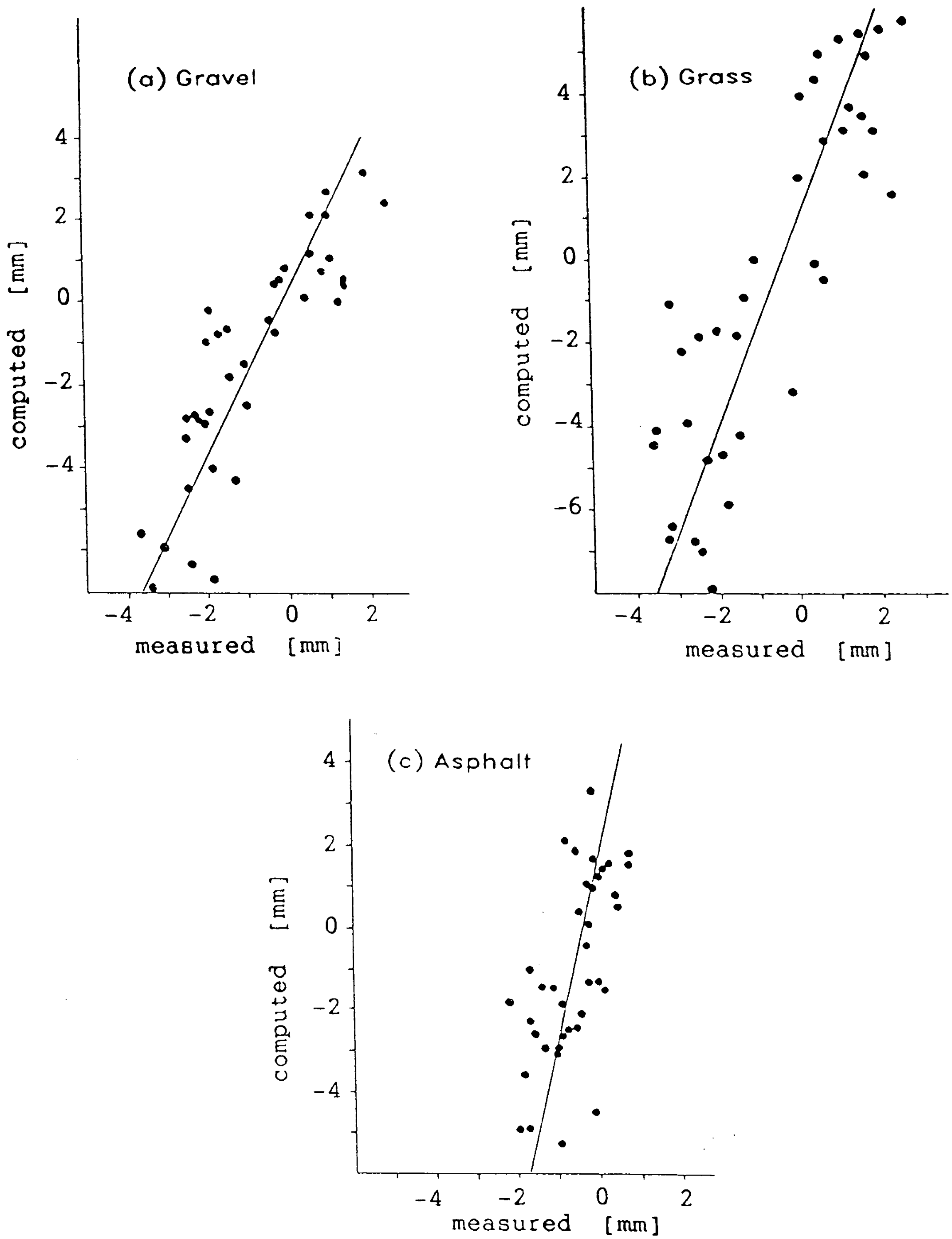

Figure 5.14: Linear correlation between the computed and measured refraction error.
a. *IS-BM1* (gravel), b. *IS-BM2* (grass) and c. *IS-BM3* (asphalt).

TABLE 5.18

t-test on the significance of the correlation coefficients

Surface	from IS to	Corr. Coef.	Regression Equat.	* $t > t_{33,0.005}$	H
gravel	BM1	0.87	mr= -0.13+0.51 cr	10.7 > 2.75	** R
grass	BM2	0.87	mr= -0.36+0.40 cr	10.7 > 2.75	R
asphalt	BM3	0.66	mr= -0.31+0.23 cr	5.3 > 2.75	R

$$* \; t = \left[\frac{(n-2) \; r^2}{1 - r^2} \right]^{1/2},$$ and the table values for t at 0.01 and 0.05 level are: $t_{33,0.005} = 2.75$ and $t_{33,0.025} = 2.0$

** *Ho*: $r = 0$ is rejected and *Ha*: $r \neq 0$ is accepted.

Although the correlations are significantly high, the computed refraction error cannot be trusted in practical work, since it is not accurate enough and may cause too large corrections for lines longer than 100 m in trigonometric height traversing (see section 4.2.3). However, the results proved that simulations of the refraction effect in trigonometric height traversing over a known profile with known temperature gradient along the profile, can be very realistic, and useful information may be extracted from such simulations. For more details see Chapter 6.

5.5.4 Tests on 29 July 1985 and estimation of standard deviation of vertical angle measurements

The last test at the South-Gym area was carried out using two independent theodolites separated by about 2 m on 29 July. The main purpose in making these measurements was to get sufficient data to estimate the actual precision of trigonometric height traversing without the influence of the refraction error. Two electronic theodolites were used, and the observations were taken independently but not simultaneously, for a duration of 5.5 hours starting at 11:45 ending at 17:07. Since the measurements were not synchronized in time, their differences were affected by short-term fluctuation of temperature gradient. Thus, one may expect higher precision than what has resulted from this experiment.

Estimation of the standard deviation of one ΔH is given by Chrzanowski [1985]

$$\sigma = \left[\sum_{i}^{n} d\Delta H_{i}^{2} / 2n \right]^{-1/2} \qquad (5.13)$$

where n is the number of observations (usually simultaneously taken) and $d\Delta H$ is the difference of the two height traversings. An average standard deviation of

0.79 mm was found that corresponds to a standard deviation of 0.58" for a zenith angle measured in four sets with sight lengths of 200 m. The bars plotted in Figure 5.9 were computed considering the above estimated standard deviation as well as the contribution of other sources of errors such as a change of the height of targets due to the expansion or contraction of the rods, non-verticality of the rods, and errors in the distance measurements. These errors are discussed in detail by Chrzanowski [1984] and Greening [1985].

Figure 5.15 shows the following refraction errors:

1. measured using electronic theodolite #1;
2. measured using electronic theodolite #2;
3. computed and corrected according to equations presented in Table 5.18 and temperature gradient measured on 29 July 1985;
4. extracted from measurements carried out in 23 July 1985 and corrected using equations given in Table 5.18; and
5. extracted from measurements carried out in 24 July 1985 and corrected using equations given in Table 5.18 .

Considering the errors involved in both measuring and computing the refraction effect, one can see that the above five groups of values agree closely. This can be an indication that the equations in Table 5.18 are useful (only for these particular lines) and can improve the

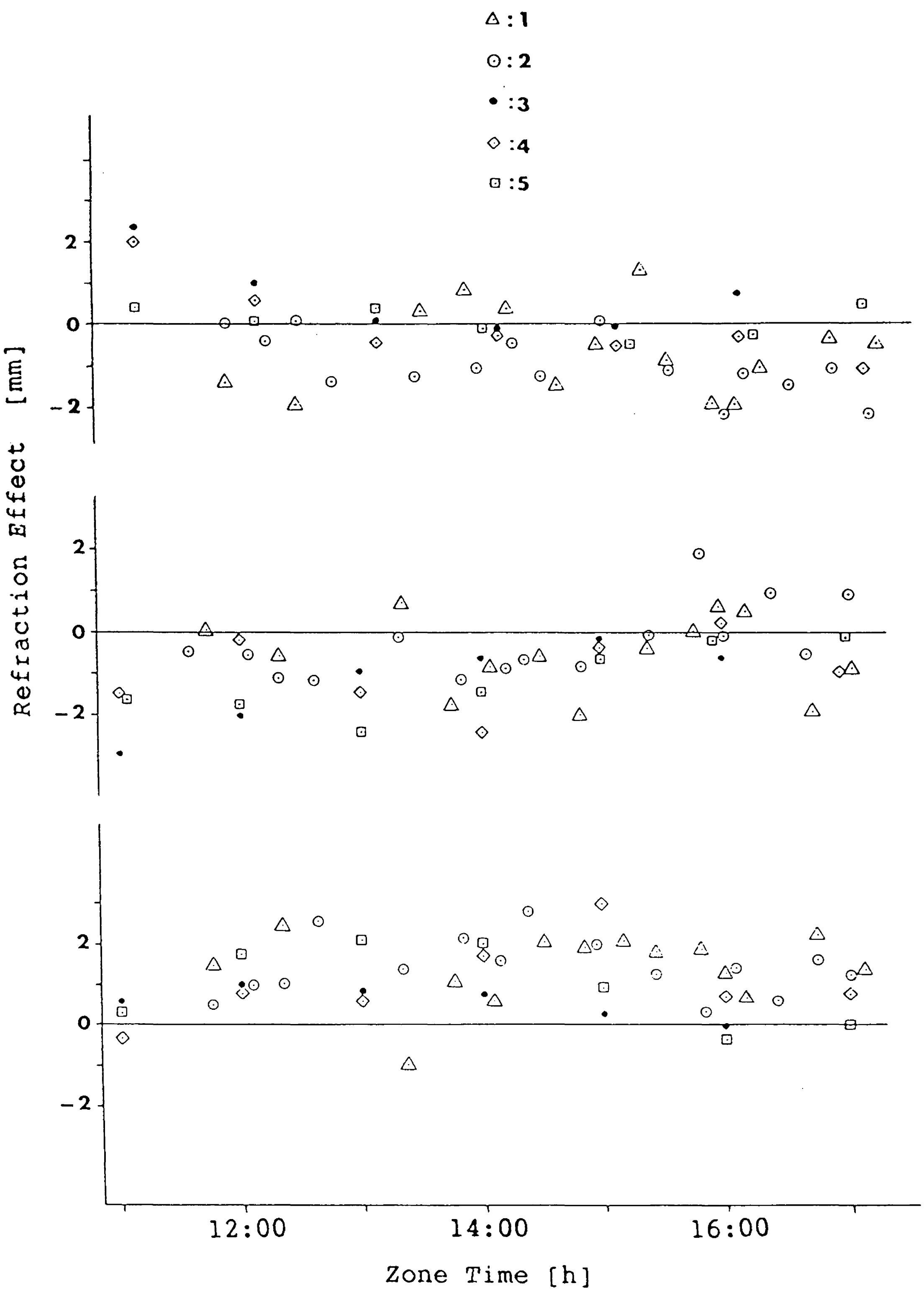

Figure 5.15: Measured refraction error versus the computed value.
a. *BM1-BM2*, b. *BM2-BM3* and c. *BM3-BM1* (a key to this figure is given in section 5.5.4).

computed values. Also, it is realized that the refraction effect from one day to another is almost the same, as long as the measurements are carried out within the same portion of day over the same profile and under similar weather conditions.

5.5.5 Comments on South-Gym test surveys

The refraction effect is successfully estimated by treating the measurements carried out during (or near to) the neutral condition time as free from refraction error. The computed values using this procedure are strongly correlated with the measured refraction effect, with correlation coefficients of 0.78, 0.93 and 0.83 for lines *BM*1-*BM*2, *BM*2-*BM*3 and *BM*3-*BM*1 respectively.

The computed refraction effect for individual lines (i.e. from mid point to the three bench marks) is larger than these estimated (previously called "measured" based on detection of neutral condition) values. The over estimation of the refraction effect can be due to insufficient knowledge of the variablity of the temperature gradient along the line of sight which could not be taken into account. However, in the computation of a full line (i.e. from one bench mark to another) the over estimations mostly cancelled out (see equation (5.12)) , as expected.

The preferable times for observations during clear days are early in the morning, a short time after sunrise, and in the afternoon, a short time before sunset.

Measurements to the higher target (at 3.5 m height) are less affected by refraction, but this does not necessarily always cause randomization of refraction error, although in some of the cases the discrepancies listed in Tables 5.13, 5.14, 5.15 and 5.16 show a sign for lower targets (at 2.1 m height) different from the higher targets.

5.5.6 Tests on 06 August 1985

The final test survey was carried out on the Head-Hall test line. A description of the line is given in section 5.2.2. The change in temperature at different heights from the ground was measured using six temperature sensors. The site for temperature measurements was selected at a spot close to BM4, on asphalt about 0.3 m from the concrete side-walk. 39 setups of measurements were carried out in which, as in the South-Gym observations, each setup consisted of two sets of zenith angle- and distance measurements. Observations started at 12:15 and ended at about 20:00 on 06 August 1985. Figure 5.16 shows:

1. The measured refraction effect which is the discrepancy between the height difference determined using geodetic levelling and results of UNB trigonometric method ($\Delta HG - \Delta HT$).
2. The computed refraction at 15 minute intervals using the observed temperature gradients.

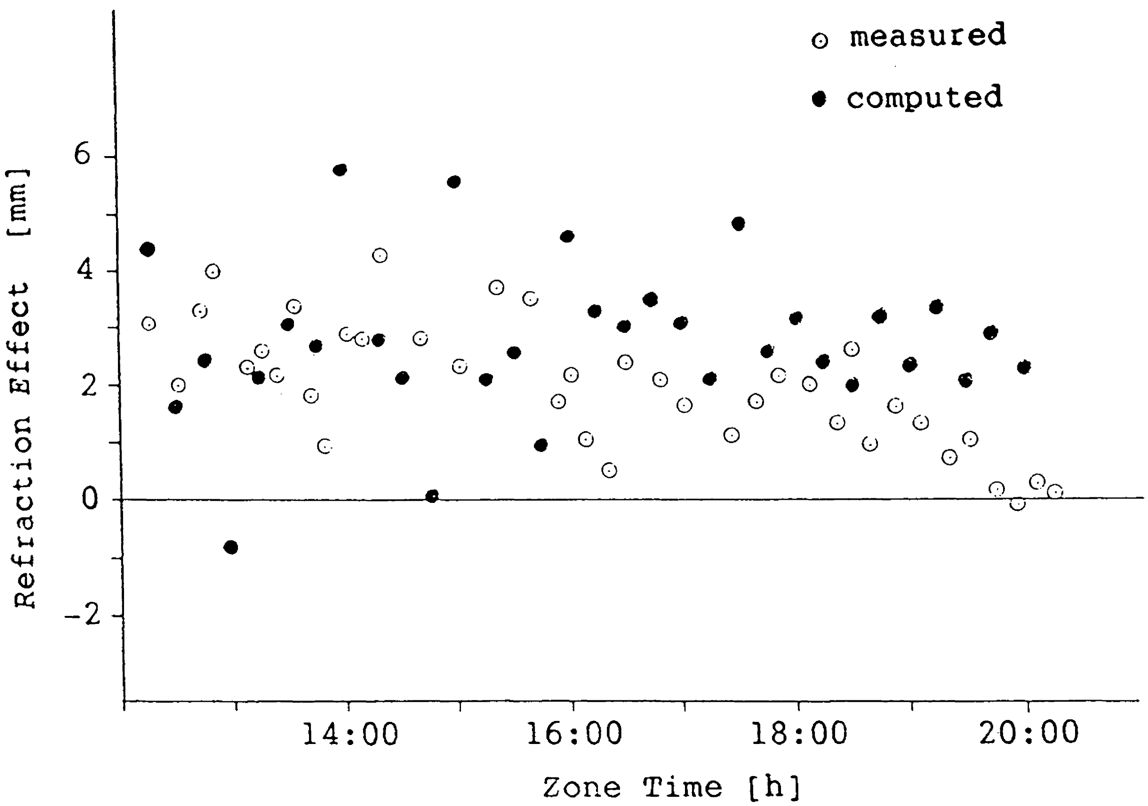

Figure 5.16: The discrepancies of height difference determined by trigonometric height traversing and geodetic levelling, between *BM2* and *BM4* at *Head-Hall* test line.

Applying the computed refraction effect to correct the observed height differences generally improves the results. It should be mentioned that the profile of the baseline was well known and the temperature gradient was determined every five minutes. The average of the measured refraction effect (for the mean of the two targets) came out to be 2.2 mm and the corresponding computed value is 2.7 mm.

Assuming that the last observation at 20:10 is free of refraction error (since it is the closest possible observation to the neutral condition time), the refraction effect on back-sights and fore-sights was obtained separatly. Table 5.19 shows the following values of refraction effect:

1. back-sight,
2. fore-sight,
3. total of the above two (measured, #1),
4. ΔHG - ΔHT (measured, #2), and
5. computed.

The refraction effect on the back-sight is oscillating more or less around the zero value and on fore-sight is always less than zero as expected.

Excellent agreement exists between the two measured values (#1 and #2 in Table 5.19) with a correlation coefficient of 0.93 which substantiates that the measurements carried out during the neutral condition time can be assumed as a reference (free from refraction error) and then the refraction effect can be computed for other measurements. The neutral condition can be detected by measuring temperatures at different elevations above the ground. In this case the profile of the line is not needed. This method of neutral condition detection can be utilized in precise measurements of monitoring the vertical movements of large structures, such as dams.

TABLE 5.19

Computed refraction effect versus the measured value for Head-Hall test line

		1	2	3	4	5		
NO	*LOCAL TIME*	Meas. B.-S. [mm]	Refr. F.-S. [mm]	Meas. #1 [mm]	Refr. #2 [mm]	Comp. Refr. [mm]	Temp. [°C]	Remarks
	12:00							
1	:15	0.13	-2.84	2.97	3.1	4.40	29.3	calm and clear all day
2	:30	-0.61	-2.06	1.45	2.4	1.60	30.7	
3	:45	0.25	-3.0	3.25	3.6	2.45	30.9	
4	13:00	0.42	-2.49	2.91	3.2	-0.75	31.2	
5	:15	0.23	-3.20	3.43	2.6	2.25	29.8	
6	:30	0.26	-2.8	3.06	3.2	3.20	31.0	
7	:45	1.09	-1.2	2.29	1.1	2.70	31.6	
8	14:00	0.06	-2.65	2.71	2.9	5.85	31.4	
9	:15	-0.25	-4.45	4.20	3.9	2.85	32.8	
10	:30	-0.05	-2.58	2.53	3.5	2.20	32.3	
11	:45	-0.23	-2.60	2.37	2.6	0.15	31.1	
12	15:00	-0.59	-2.55	1.96	2.3	5.55	30.4	
13	:15	0.51	-3.0	3.51	3.2	2.05	32.4	
14	:30	0.03	-3.5	3.53	3.7	2.60	31.5	
15	:45	-0.08	-2.5	2.42	2.7	0.85	31.8	
16	16:00	0.22	-1.87	2.09	2.3	4.65	31.3	
17	:15	0.35	-0.20	0.55	0.7	3.35	31.0	
18	:30	-0.68	-2.89	2.21	2.4	3.0	31.3	
19	:45	-0.69	-2.75	2.06	2.3	3.50	31.0	
20	17:00	-0.66	-2.21	1.55	1.7	3.15	31.1	
21	:15	-0.84	-2.0	1.16	1.4	2.10	30.6	
22	:30	-0.85	-2.0	1.15	1.3	4.75	30.3	
23	:45	-0.41	-2.2	1.79	2.0	2.65	29.8	
24	18:00	-0.28	-2.2	1.92	2.1	3.25	29.7	
25	:15	-0.12	-1.5	1.38	1.7	2.25	29.4	
26	:30	-0.41	-2.5	2.09	2.4	2.0	29.1	
27	:45	-0.17	-1.30	1.13	1.2	3.20	28.9	
28	19:00	-0.28	-1.5	1.22	1.3	2.75	28.3	
29	:15	-0.09	-0.83	0.74	1.0	0.35	27.5	
30	:30	0.24	-0.50	0.74	1.0	2.20	27.0	
31	:45	-0.40	-0.40	0.0	0.2	2.85	26.3	
32	20:00	-0.24	-0.27	0.03	0.2	2.30	25.7	
33	:10	0.	0.					
	Mean			2.01	2.16	2.70		

A key to this table is given in section 5.5.6.

Chapter 6

SIMULATIONS OF REFRACTION ERROR IN TRIGONOMETRIC HEIGHT TRAVERSING

6.1 Simulation Along a Geodetic Levelling Line on Vancouver Island

In 1984 a number of levelling simulations were carried out at *UNB* to assess the dependence of the refraction errors on the profile of the terrain in extreme environmental conditions. The simulations were helpful to understand the cumulative influence of refraction error in trigonometric height traversing. The influence of refraction in geodetic levelling and trigonometric heighting were simulated along an 82 km long simulated profile with an assumed average temperature gradient. The results of these simulations are reported in details by Chrzanowski [1984] and Greening [1985].

A number of new simulations has been done by the author with the same purpose as in previous simulations but using actual levelling data. The new simulations have been conducted along a line of actual geodetic levelling of special order (the allowable discrepancy between independent forward and backward levelling between bench marks is less than $\pm 3 \text{ mm}\sqrt{K}$ [Surveys and Mapping Branch, 1978], where K is the distance between bench marks in kilometres). During the geodetic levelling operations, temperatures were observed at heights 0.5 m and 2.5 m in every set-ups. The distances from the instrument to back- and fore-sight levelling rods were measured using stadia cross hairs. The geodetic levelling was carried out on Vancouver Island by the Geodetic Survey of Canada, Department of Energy, Mines and Resources Canada, Surveys and Mapping Branch. The project started in late May 1984 and was finished in the middle of October 1984. The simulations have been carried out over a ≃224 km line chosen from the above data . The line is divided into two parts for forward and backward levelling traverses:

line			from	to
#1	Forward	108.5 km	Nanoose Bay	Merville
#2	Forward	115.7 km	Merville	Kelsey Bay
#3	Backward	115.5 km	Kelsey Bay	Merville
#4	Backward	109.2 km	Merville	Nanoose Bay

Lines #1 and #4 are extended totally over a flat terrain, parallel to the southern shore-line of the Strait of Georgia. Lines #2 and #3 pass partially over a hilly terrain south of the Menzies, Kitchener and Hkusam mountains with maximum height differences of about 300 m. The profile of the line was generated for 10 m (or less) intervals along the line based on measured stadia distances and height differences of turning points. Assuming the slope of the ground between two adjacent turning points as being constant, every two adjacent turning points were connected by a straight line and then the height of points with maximum 10 m horizontal separation was interpolated along the line. See Figures 6.2 to 6.5 for the profile of the lines.

The actual accumulation of the refraction effect in geodetic levelling has been computed and the simulation of refraction accumulation in trigonometric height traversing was done using the same temperature gradient and the same profile.

6.1.1 Computation of the refraction error in geodetic levelling

The temperature differences measured during levelling were used in Kukkamäki's formulae for refraction correction using equation (3.19). This equation was simpilified by Kukkamäki [1939a] to a form more convenient for computation using a hand calculator

$$Cr = 10^{-5} \cdot G \cdot (s/50)^{2} \cdot \Delta h \cdot \Delta t \qquad (6.1)$$

in which,

$$G = \frac{5.94}{250^{c} - 50^{c}} \left[\frac{1}{c+1} \left(50^{c+1} - 250^{c+1} \right) + 150^{c} \cdot 200 \right] \qquad (6.2)$$

where, Δh = the levelled height difference in scale division 0.5 mm, and

Δt = the measured temperature difference between 2.5 m and 0.5 m above the ground surface.

In equation (6.1), Kukkamäki assumes that the refraction correction varies linearly with the height difference Δh, and the measured temperature difference Δt.

In equation (6.2), c is the exponent in Kukkamäki's model. Based on Hytönen's [1967] investigations, Kukkamäki [1979], suggests that an average value of c = -0.1 with corresponding G = 69.4 can be used in all circumstances without causing any significant loss of accuracy. However, the author assumed a constant value of -1/3 for c as in equation (5.11), obtaining G = 80.5. For c = -1/3, Cr = 0.07 mm and for c = -0.1, Cr = 0.08 mm can be found assuming Δt = -0.25 °C, S = 50 m and Δh = 2 m.

Geodetic refraction was also computed using Remmer's formula which is an adaptation of equation (3.19) given by Kukkamäki [Remmer, 1980]

$$Cr = \frac{S^2}{6} \left(\frac{dn}{dt}\right)\left(d2 \ \Delta h + \frac{d4}{80} \ \Delta h^3 \right) \tag{6.3}$$

where: dn/dt is given by equation (3.11), d2 and d4 are the second and the fourth derivatives of Kukkamäki's temperature function respectively which are

$$d2 = (c-1)\ c\ b\ z^{c-2}$$

and

$$d4 = (c-3)\ (c-2)\ (c-1)\ c\ b\ z^{c-4}$$

S is the sight length and Δh is the height difference for a single set-up. All three equations (6.1), (3.19) and (6.3) were used to compute the refraction effect in geodetic levelling along the above lines and as can be seen in Figure 6.1, the answers came out to be in close agreement. The figure shows the effect of refraction in geodetic levelling along the line #3. The mean of the three is used for comparison with the simulated refraction effect in the trigonometric methods (see e.g. Figurs 6.2 to 6.5).

6.1.2 Refraction error in trigonometric height traversing

The refraction effect in trigonometric height traversing was computed using equation (2.13)

$$Cr = \frac{1}{R} \int_0^s k\ (S - x)\ dx = \frac{I}{R} \qquad (6.4)$$

in which *I* is given by equation (4.1). For a special case, when

$$s = s_1 = s_2 = \ \ldots\ = s_n,$$

this can be written as

$$I = k_1 \frac{s}{2} S + k_2 s (S - s) + k_3 s (S - 2 s) + \ldots\ldots$$

$$\ldots\ldots + \frac{1}{2} k_n s^2 \qquad (6.5)$$

where

$$k_i = \frac{502.7\ p}{T^2} \left[0.0342 + (dt/dz)_i \right] , \qquad (6.6)$$

$$dt/dz = (-1/3)\ b\ z^{-4/3} \qquad (6.7)$$

and S is the sight length divided into n equal subsections of s (S = n s).

6.1.3 Results of simulations

Figures 6.2 to 6.5 show the results of four simulations. The starting heights of the profiles were chosen arbitrarily. As can be seen, the geodetic levelling refraction effect is highly correlated with the profile of the levelling route, but, fluctuates within the limits of special order of Canadian accuracy specifications. On the other hand, the refraction errors in trigonometric height traversing are not correlated with the profile of the route. They are highly dependent on the clearance and the length of the line of sight as it would be expected. To show this dependency, one can keep the maximum length of sight unchanged while changing the clearance. In all four lines the error of refraction will be reduced by increasing the clearance, where the number of observations will be increased as well. Conversely in most of the cases, keeping the clearance unchanged while increasing the sight length, will result in a higher refraction error, and decreasing the sight length will help to decrease the refraction effect.

Many more simulation results were obtained for different cases of the sight lengths and the ray clearances. By inspection of these cases and those presented in this thesis, it is substantiated that if the lines of sight in the leap-frog method are less than 150 m with the ray clearance greater than 1 m, the refraction effect is within the limits of the Canadian specifications for the first order levelling. The Canadian specification for first order and for one-way levelling is given by Chrzanowski [1984] in terms of standard deviation as $\sigma \leq 2.0$ mm$\sqrt{K}$, where K is in kilometres. The line of sight should be less than 250 m for the clearance of 1 m in the case of reciprocal method. It should also be mentioned that the height of 2 m for the instrument is assumed for all the results shown in here. The height of instrument, according to the author's experience is usually more than 2.2 m in motorized trigonometric height traversing. A considerable improvement is noticed in the results of simulations whenever a height of larger than 2.2 m for the instrument is assumed.

6.2 Simulation of the Refraction Error Using other Values of Temperature Gradient Measurements

According to the measured temperatures (at height 0.5 m and 2.5 m above the ground), the weather condition during the levelling in Vancouver Island was quite mild. To investigate the changes of weather, one can look at the changes of sensible heat flux, *H* along the route of the above levelling lines (#1 to #4). The *H* can be estimated from the temperature gradient profile in the middle region under unstable conditions, using equation (3.32) and neglecting the adiabatic lapse rate Γ = 0.0098 (see equation (3.23));

$$\frac{dt}{dz} = -0.0274 \; H^{2/3} \; z^{-4/3} \qquad (6.8)$$

Equating the right hand sides of equations (6.7) and (6.8), *H* can be written in terms of b (see section 3.1.5)

$$H = \left[\frac{b}{0.0822} \right]^{3/2} \qquad (6.9)$$

in which, b is given in terms of Δt according to equation (3.4)

$$b = \Delta t \,/\, (2.5^{c} - 0.5^{c}) \qquad (6.10)$$

where $c = -1/3$ and Δt is the temperature difference between lower (at 0.5 m height) and higher (at 2.5 m height) sensors.

Figure 6.6 shows the variations of sensible heat flux along the line #2 . The negative values may be slightly different from those depicted in this figure, since the negative values reflect the stable condition and they have to be computed with the help of the corresponding equation (3.33) or (3.34). Table 6.1 shows the averaged coefficient b and its corresponding *H* values along the four levelling lines. Table 6.2 and 6.3 show other examples of these values in other parts of Canada (Fredericton, N.B.) and in the United States. For example in Fredericton, according to meteorological obsevations carried out, one can expect higher *H* and b values during the summer than those from Vancouver Island.

TABLE 6.1

Average Δt, b and *H* along the levelling routes

Line	Δt [°C]	b	*H* [$W\ m^{-2}$]
#1	-0.39	0.75	28
#2	-0.28	0.53	17
#3	-0.37	0.71	25
#4	-0.36	0.69	24
MEAN	-0.35	0.67	23.5

TABLE 6.2

Average Δt, b and *H* in Fredericton, *N.B.*

Date 1985	Ground Cover	Δt **	b	*H* *	Time	Remarks
Jul-19	gravel	-0.6	1.15	52	10:25-19:59	partially cloudy
Jul-19	grass	-0.3	0.57	18	10:45-19:35	partially cloudy
Jul-19	asphalt	-0.7	1.34	66	10:10-20:32	partially cloudy
Jul-23	gravel	-0.7	1.34	66	10:10-18:20	mostly sunny
Jul-23	grass	-0.6	1.15	52	09:30-18:40	mostly sunny
Jul-23	asphalt	-0.7	1.34	66	09:50-19:00	mostly sunny
Jul-24	gravel	-0.8	1.53	80	07:00-17:20	mostly sunny
Jul-24	grass	-0.7	1.34	66	07:20-18:48	mostly sunny
Jul-24	asphalt	-0.7	1.34	66	07:45-19:05	mostly sunny
Jul-29	gravel	-0.7	1.34	66	12:10-17:10	partially cloudy
Jul-29	grass	-0.9	1.72	95	11:30-16:30	partially cloudy
Jul-29	asphalt	-0.8	1.53	80	11:50-16:50	partially cloudy
Aug-06	asphalt	-0.7	1.34	66	11:00-20:15	mostly sunny
Aug-10	highway	-1.0	1.91	112	07:28-15:23	mostly sunny
Aug-	highway	-0.7	1.34	66	13:32-15:04	mostly sunny
Aug-14	highway	-0.9	1.72	95	11:13-16:25	mostly sunny
Aug-15	highway	-0.1	0.19	4	07:28-12:34	mostly cloudy
Aug-15	highway	-0.8	1.53	80	13:06-15:36	partially cloudy
MEAN		-0.7	1.32	66		

** Δt is in °C

* *H* is in W / m^2

Applying the value b = 1.25 (see Table 6.2) in the simulations along the Vancouver Island profile, one obtains a set of results which can represent the refraction error in the summer conditions of the Fredericton area.

Figures 6.7 and 6.8 show the simulation of refraction error on the same profiles as in Figures 6.3 and 6.5 . In these cases, the geodetic levelling needs to be corrected

TABLE 6.3

Average Δt, b and *H* along levelling routes in United States (after Holdahl [1982])

Date	Place	Num. of obs.	Δt	b	*H*
December 1977	Gorman, CA	714	-0.75	1.43	73
Aug.-Sept. 1979	Gaithersburg, MD	838	-0.56	1.07	47
April 1980	Tucson, AZ	844	-1.03	1.97	117
May-June 1981	Palmdale, CA	1644	-1.29	2.47	165

for refraction. They also show that the dependency on the value of b (or the magnitude of sensible heat flux, *H*) in trigonometric height traversing is lower than for geodetic levelling.

Refraction errors in both reciprocal and leap-frog trigonometric height traversing were simulated along all 4 lines. In most cases the accumulation of refraction errors in the reciprocal method is considerably lower than in the leap-frog method. Looking at these simulations, one can see that from refraction point of view, the reciprocal method is more reliable than the leap-frog approach.

6.3 Simulation on the Test Lines at UNB

The refraction error in reciprocal trigonometric height traversing was further investigated by simulation of this error on the South-Gym and Head-Hall test lines (see section 5.2 for description of these test lines). The measured temperature differences were used to compute the refraction effect for both the leap-frog UNB-method which was actually carried out, and an assumed reciprocal trigonometric height traversing on the same profile. The line of sight in the reciprocal method was selected to be longer than for the leap-frog. At the same time, it is tried to keep the reciprocal set-up on the extreme part of the line where the higher refraction effect is expected. For instance, in the case of the Head-Hall test line, the reciprocal method simulation was taking place for two points on the profile which are closer to the center by 50 metres from each side than the points used in the leap-frog measurements. The same is true for the other three lines in the South-Gym area.

Figures 6.9 to 6.12 show the results of these simulations. The starting heights of profiles were chosen arbitrarily. In all four cases, the reciprocal method is affected by the refraction error by about half the amount of the leap-frog.

It was shown in Chapter 5 that in the leap-frog method, the computed value was larger in magnitude than the actual refraction effect. If the same is true for the reciprocal method as well, then the magnitude of the actual refraction effect in reciprocal mode for these test lines may fall mostly within a range of the accuracy specification which is at least one order higher than the one for the leap-frog method. It should be noted that for the reciprocal method, the line of sight is considerably longer than in the leap-frog method. When the line of sight for the reciprocal method is twice as long as for the leap-frog, the magnitudes of refraction in both methods are about the same.

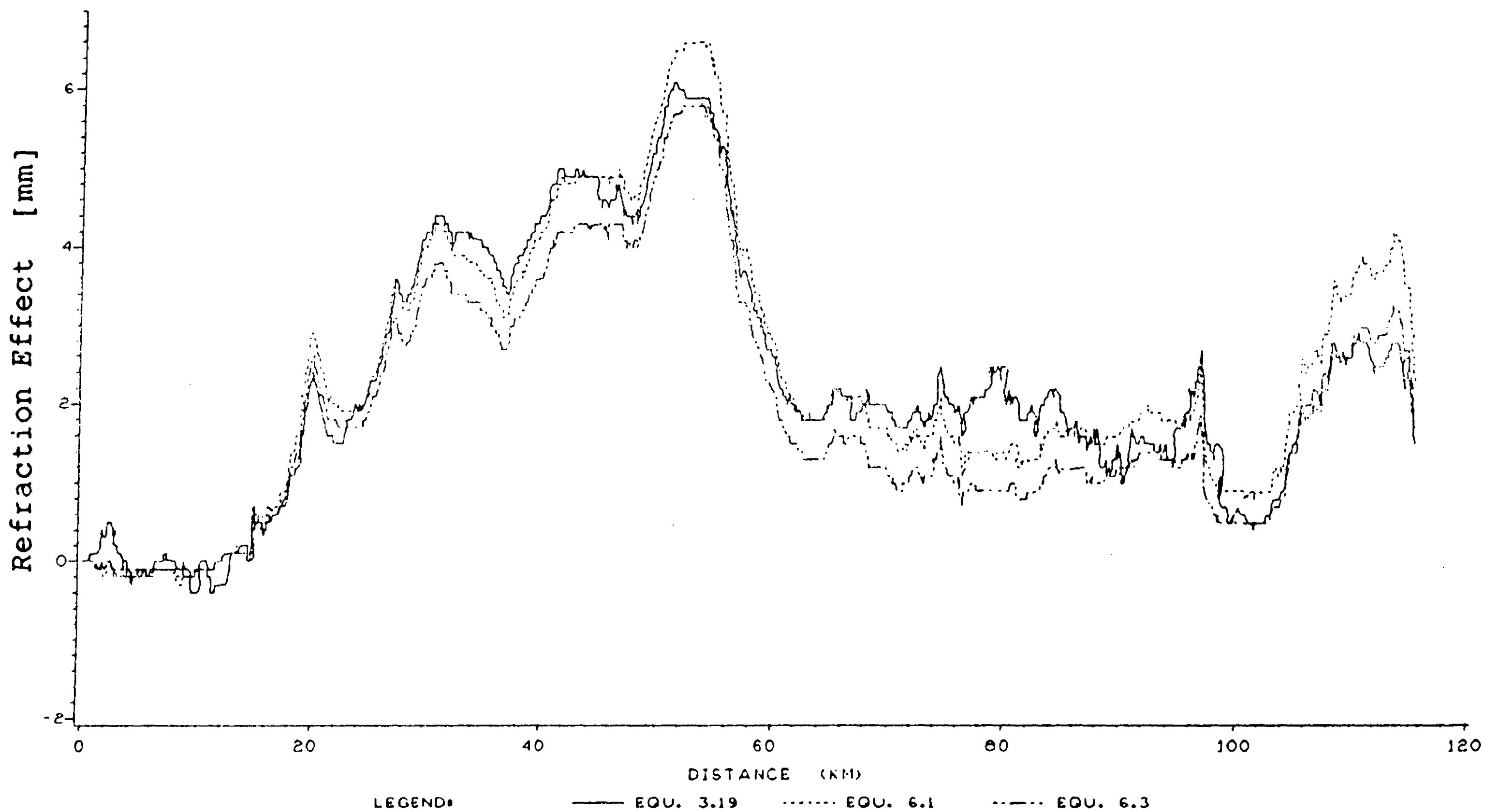

Figure 6.1: Accumulation of refraction error in geodetic levelling using equations (3.19), (6.1) and (6.3) along the line #3.

Model: $t = a + b\ z^c$ where: $c=-1/3$ and b=variable

SYMBOL	LEVELLING METHOD	MAX. SIGHT DIST. (m)	MINIMUM CLEARANCE (m)	INSTRUMENT HEIGHT (m)	NUMBER OF SET-UPS	ACCU. REFR. ERROR (mm)	REMARKS
◇	GEODETIC	40	0.5	1.5	1839	-0.1	MEASURED
○	LEAP-FROG	250	1.0	2.0	238	-1.4	SIMULATED
⌖	RECIPROCAL	250	1.0	2.0	454	1.8	SIMULATED

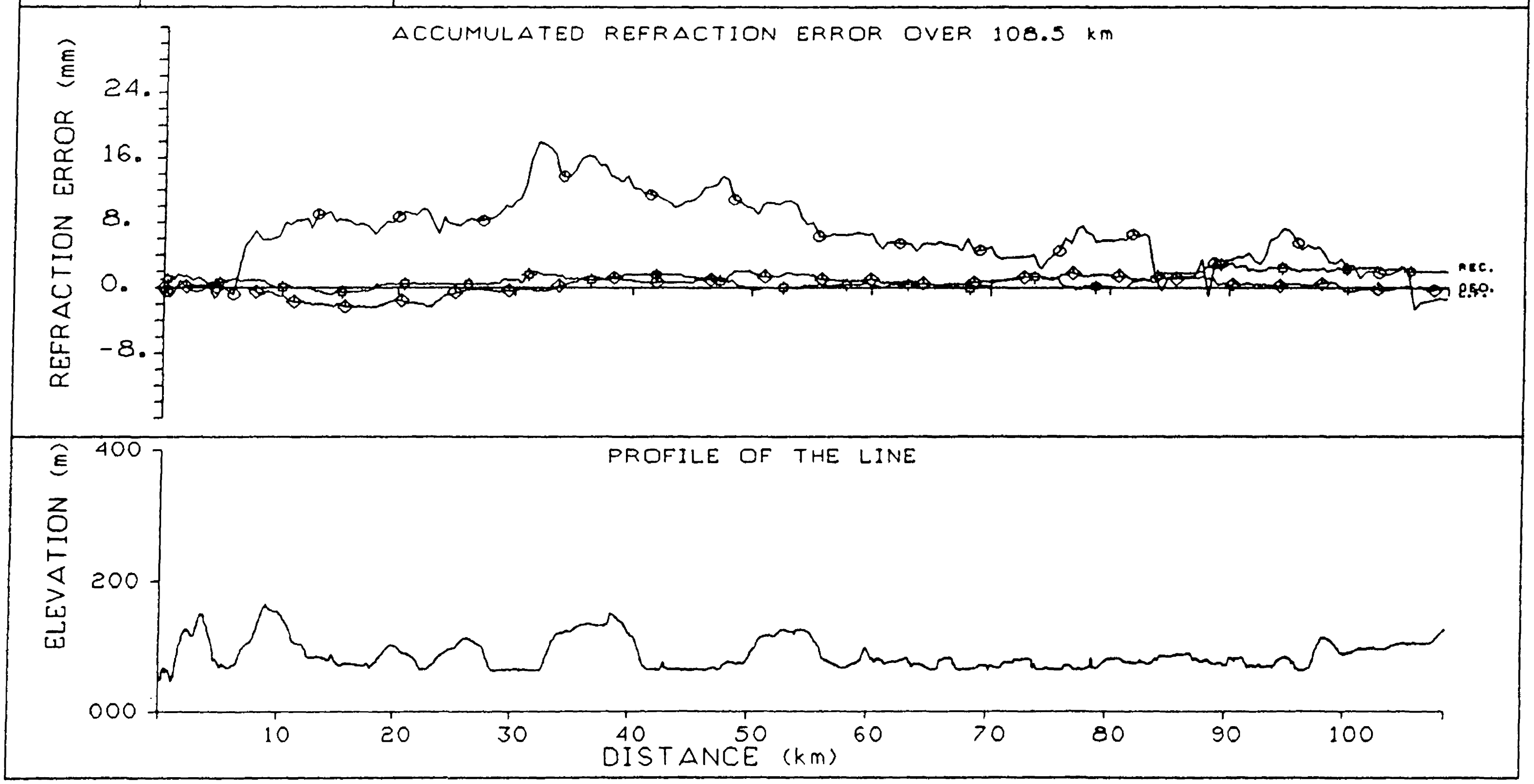

Figure 6.2: Accumulation of refraction error in geodetic levelling and trigonometric height traversing along line #1 (*UNB* leap-frog and reciprocal methods) using measured temperature gradient.

Model: $\iota = a + b\ z^{c}$ where: $c=-1/3$ and b=variable

SYMBOL	LEVELLING METHOD	MAX. SIGHT DIST. (m)	MINIMUM CLEARANCE (m)	INSTRUMENT HEIGHT (m)	NUMBER OF SET-UPS	ACCU. REFR. ERROR (mm)	REMARKS
◇	GEODETIC	40	0.5	1.5	1826	-3.9	MEASURED
○	LEAP-FROG	250	1.0	2.0	244	12.1	SIMULATED
⊕	RECIPROCAL	250	1.0	2.0	477	-10.4	SIMULATED

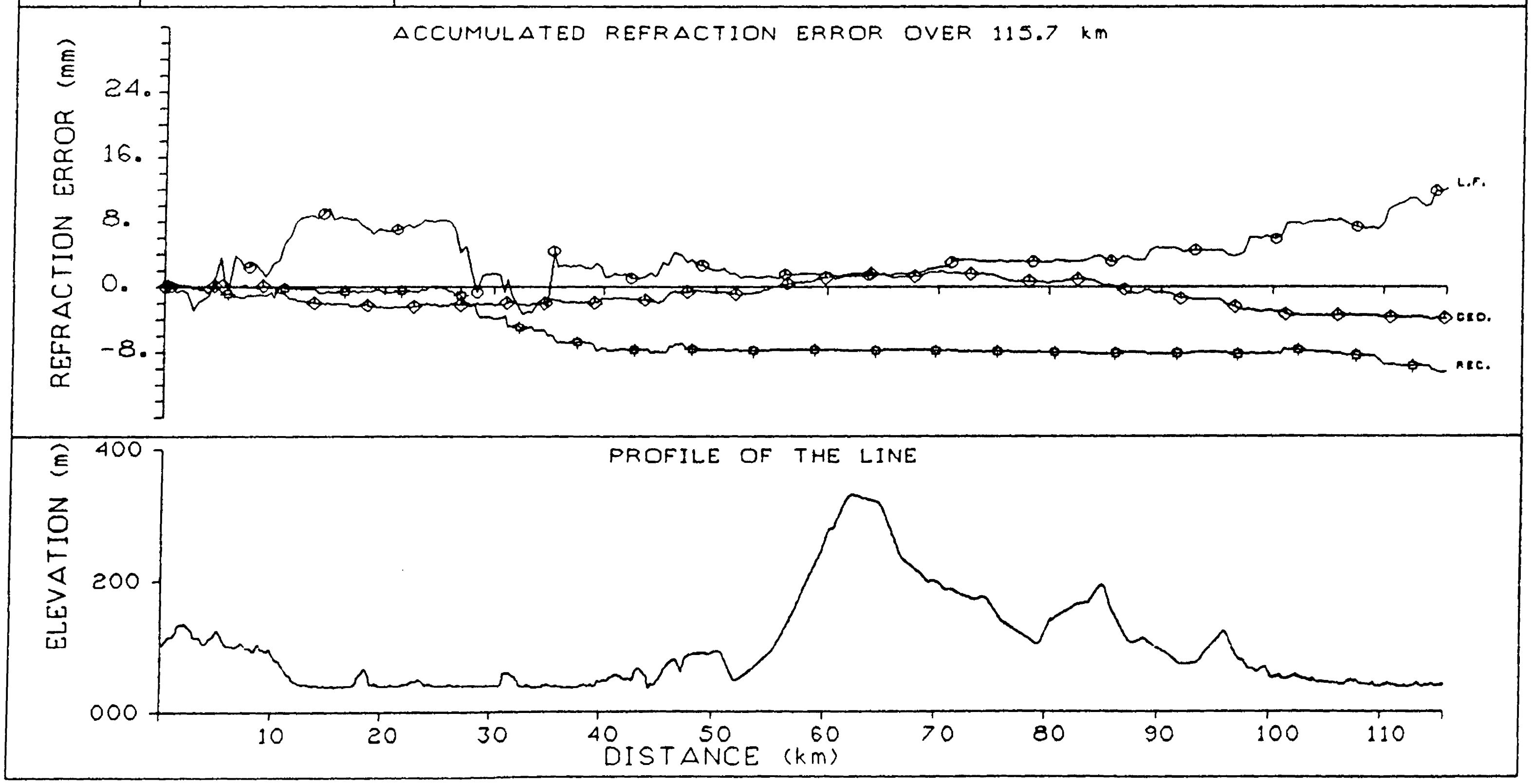

Figure 6.3: Accumulation of refraction error in geodetic levelling and trigonometric height traversing along line #2 (*UNB* leap-frog and reciprocal methods) using measured temperature gradient.

Model: $\iota = a + b\ z^{c}$ where: $c=-1/3$ and b=variable

SYMBOL	LEVELLING METHOD	MAX. SIGHT DIST. (m)	MINIMUM CLEARANCE (m)	INSTRUMENT HEIGHT (m)	NUMBER OF SET-UPS	ACCU. REFR. ERROR (mm)	REMARKS
◇	GEODETIC	40	0.5	1.5	1840	1.8	MEASURED
○	LEAP-FROG	150	1.0	2.0	392	1.2	SIMULATED
⌖	RECIPROCAL	150	1.0	2.0	778	-1.3	SIMULATED

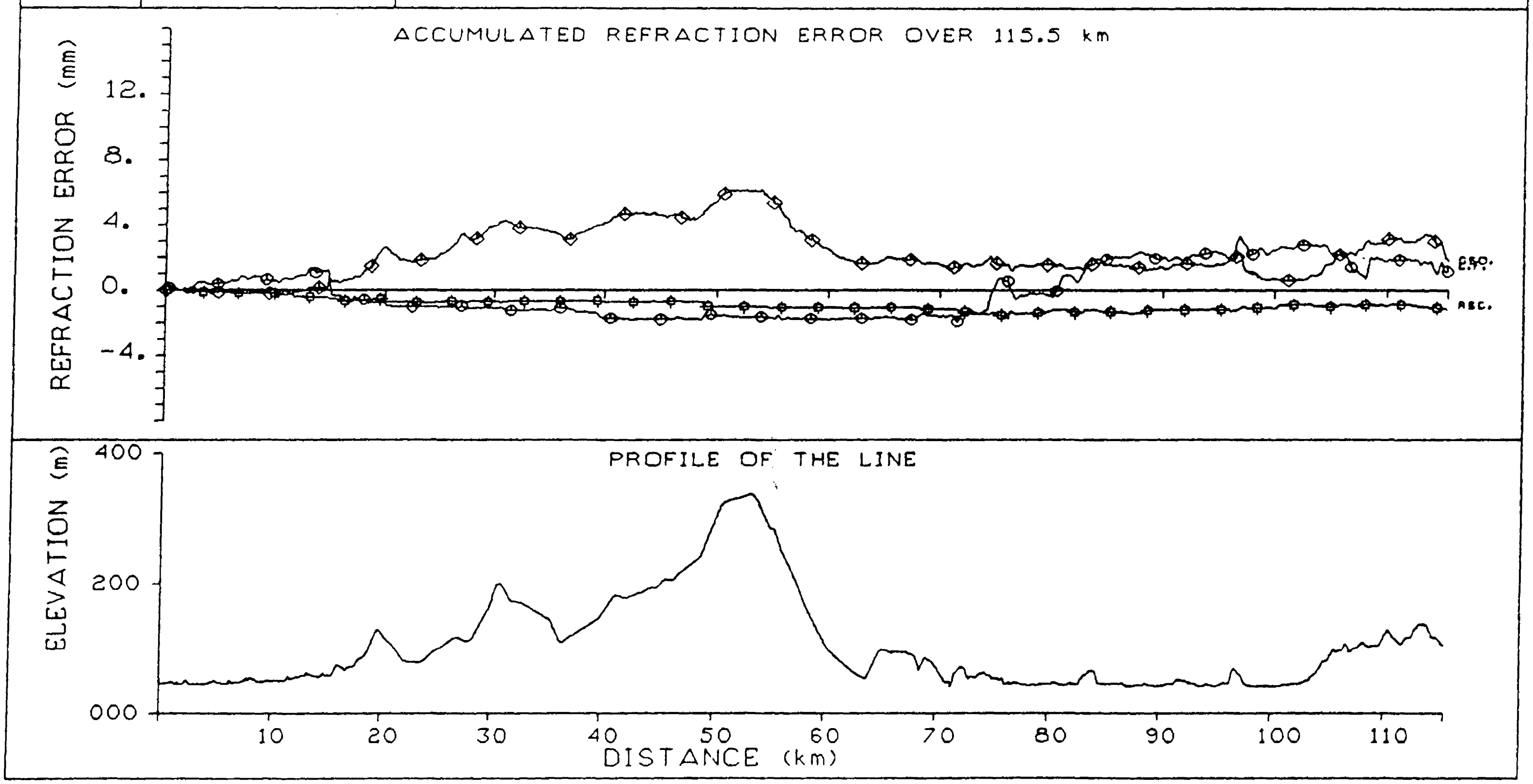

Figure 6.4: Accumulation of refraction error in geodetic levelling and trigonometric height traversing along line #3 (*UNB* leap-frog and reciprocal methods) using measured temperature gradient.

Model: $l = a + b\ z^c$ where: $c=-1/3$ and b=variable

SYMBOL	LEVELLING METHOD	MAX. SIGHT DIST. (m)	MINIMUM CLEARANCE (m)	INSTRUMENT HEIGHT (m)	NUMBER OF SET-UPS	ACCU. REFR. ERROR (mm)	REMARKS
◇	GEODETIC	40	0.5	1.5	1839	0.6	MEASURED
○	LEAP-FROG	150	1.0	2.0	378	4.1	SIMULATED
⌖	RECIPROCAL	150	1.0	2.0	743	-1.2	SIMULATED

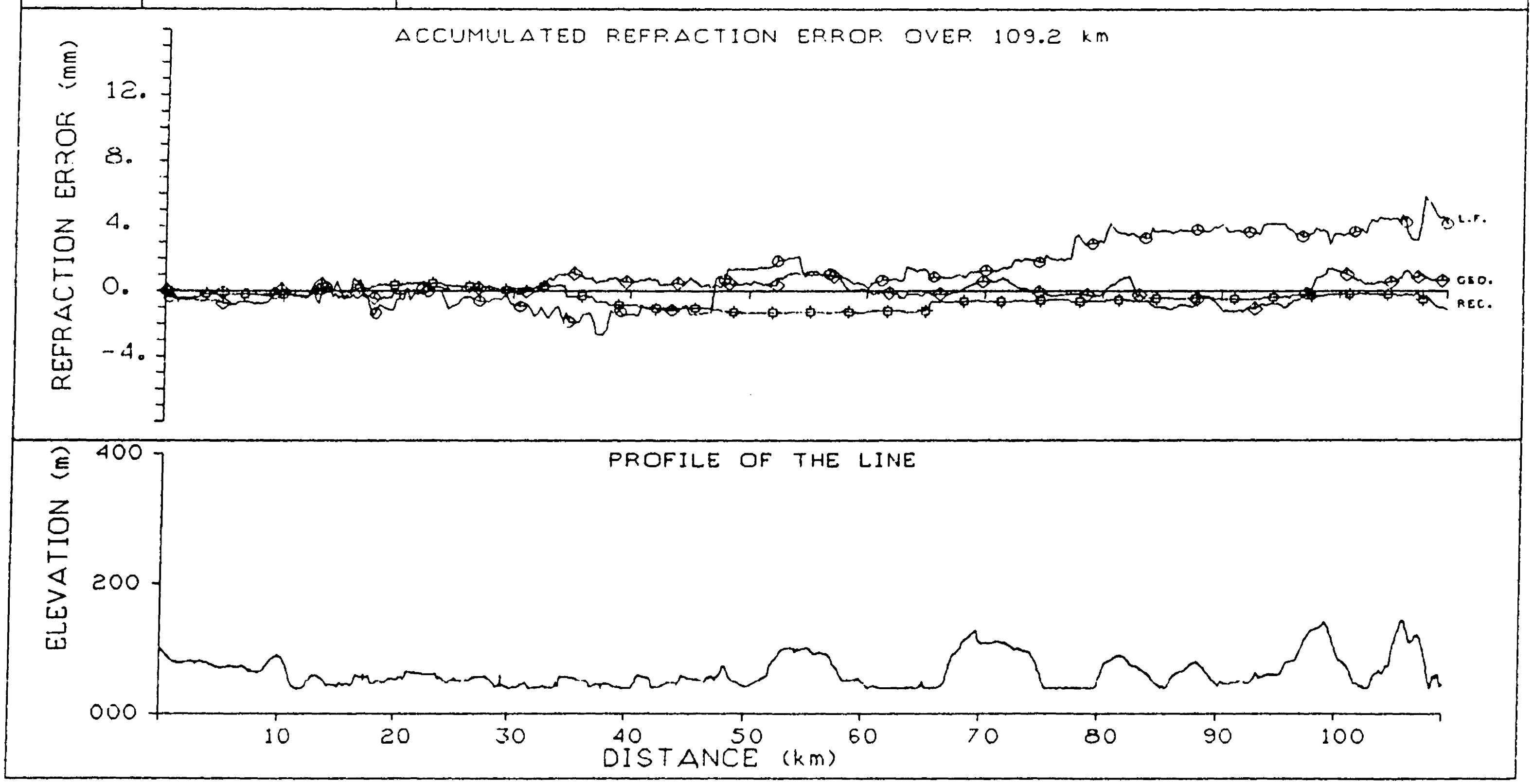

Figure 6.5: Accumulation of refraction error in geodetic levelling and trigonometric height traversing along line #4 (*UNB* leap-frog and reciprocal methods) using measured temperature gradient.

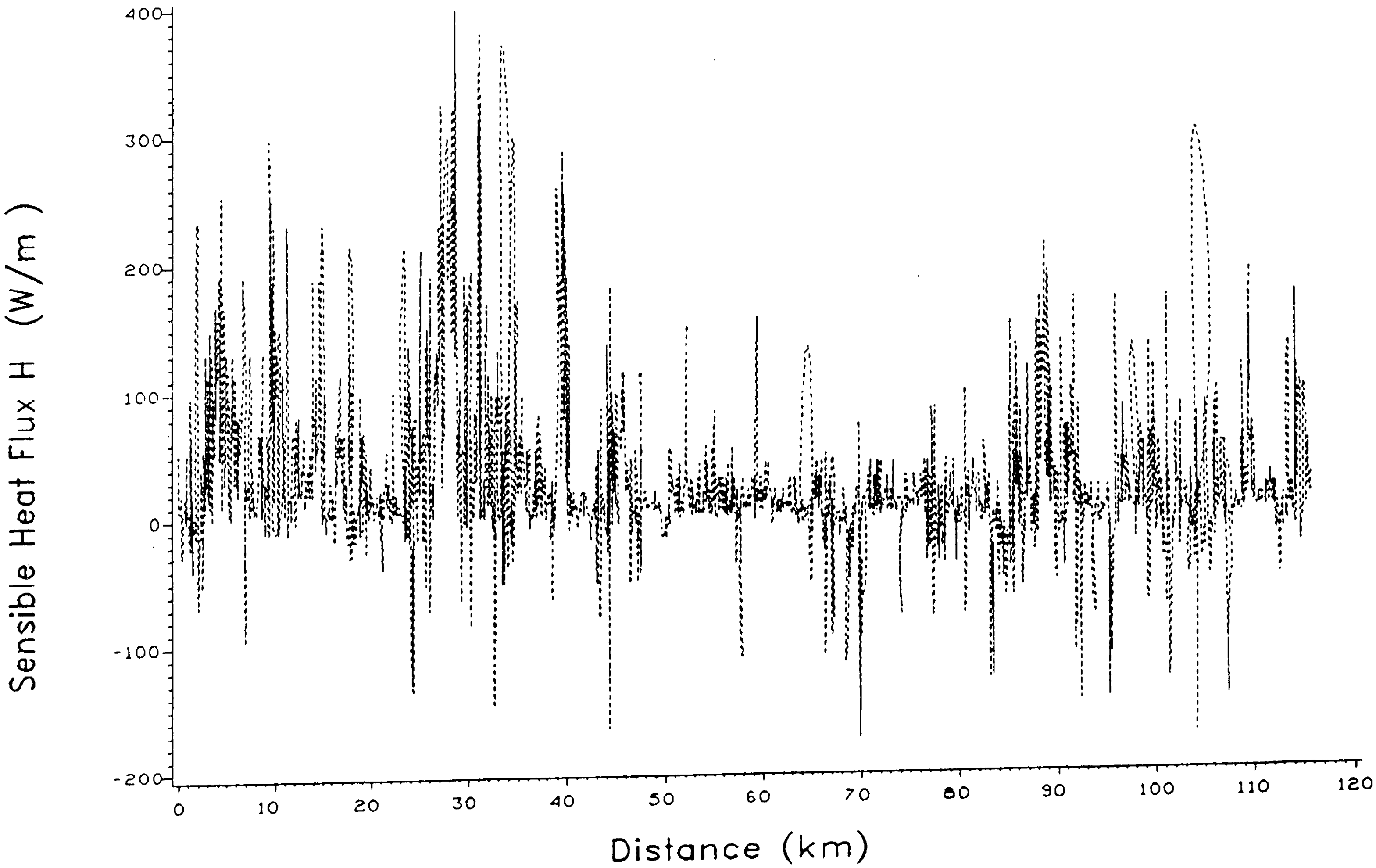

Figure 6.6: Variations of turbulent heat flux along the levelling line #2

Model $t = a + b\ z^{c}$ where: c=-1/3 and b=1.25

SYMBOL	LEVELLING METHOD	MAX. SIGHT DIST. (m)	MINIMUM CLEARANCE (m)	INSTRUMENT HEIGHT (m)	NUMBER OF SET-UPS	ACCU. REFR. ERROR (mm)	REMARKS
◇	GEODETIC	40	0.5	1.5	1826	-3.7	MEASURED
○	LEAP-FROG	150	1.0	2.0	393	0.4	SIMULATED
⊕	RECIPROCAL	150	1.0	2.0	780	-1.4	SIMULATED

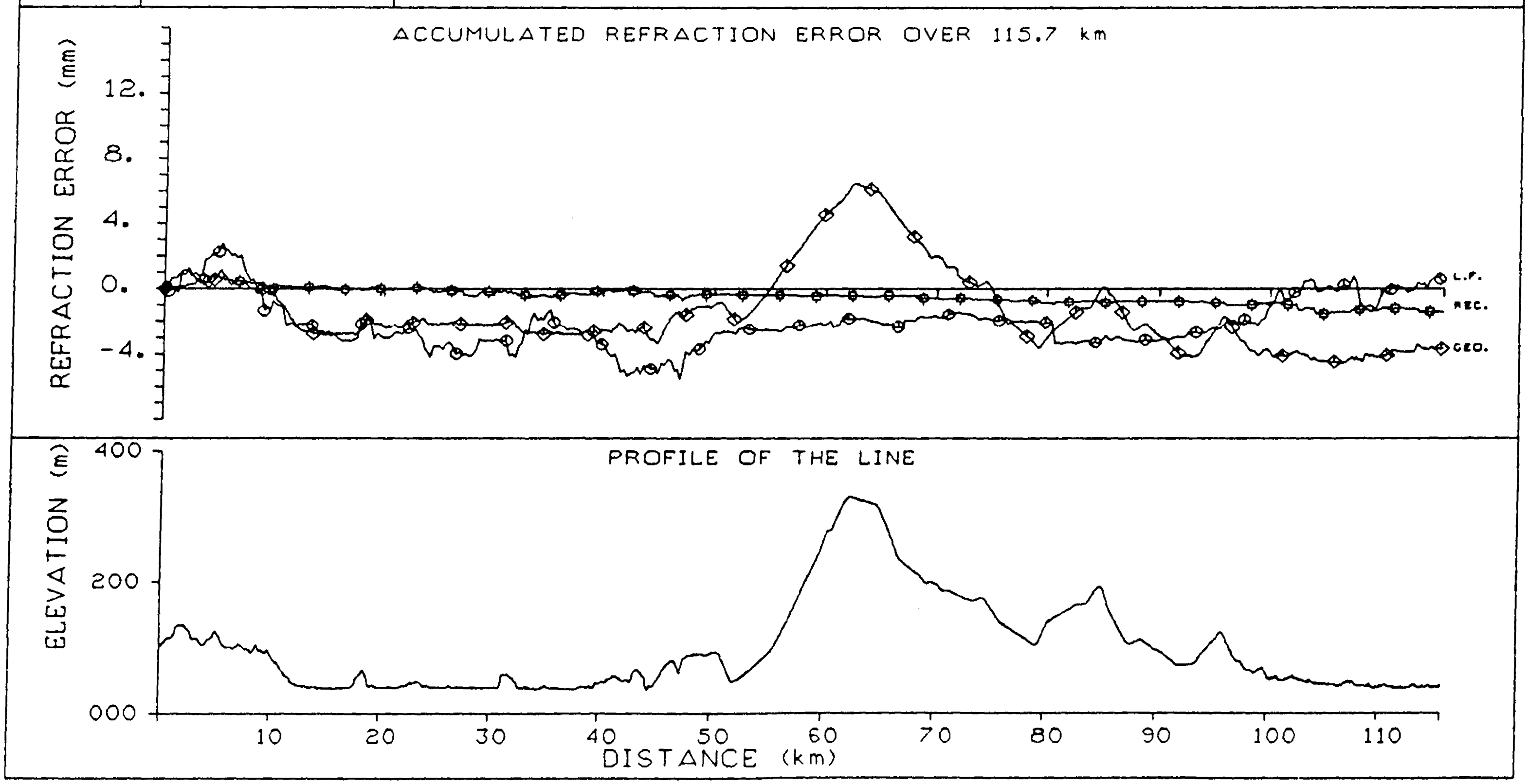

Figure 6.7: Accumulation of refraction error in geodetic levelling and trigonometric height traversing (line #2) using a simulated temperature gradient.

Model $\iota = a + b\ z^{c}$ where: $c=-1/3$ and $b=1.25$

SYMBOL	LEVELLING METHOD	MAX. SIGHT DIST. (m)	MINIMUM CLEARANCE (m)	INSTRUMENT HEIGHT (m)	NUMBER OF SET-UPS	ACCU. REFR. ERROR (mm)	REMARKS
◇	GEODETIC	40	0.5	1.5	1839	-3.4	MEASURED
○	LEAP-FROG	250	1.0	2.0	241	4.8	SIMULATED
⌖	RECIPROCAL	250	1.0	2.0	459	-3.8	SIMULATED

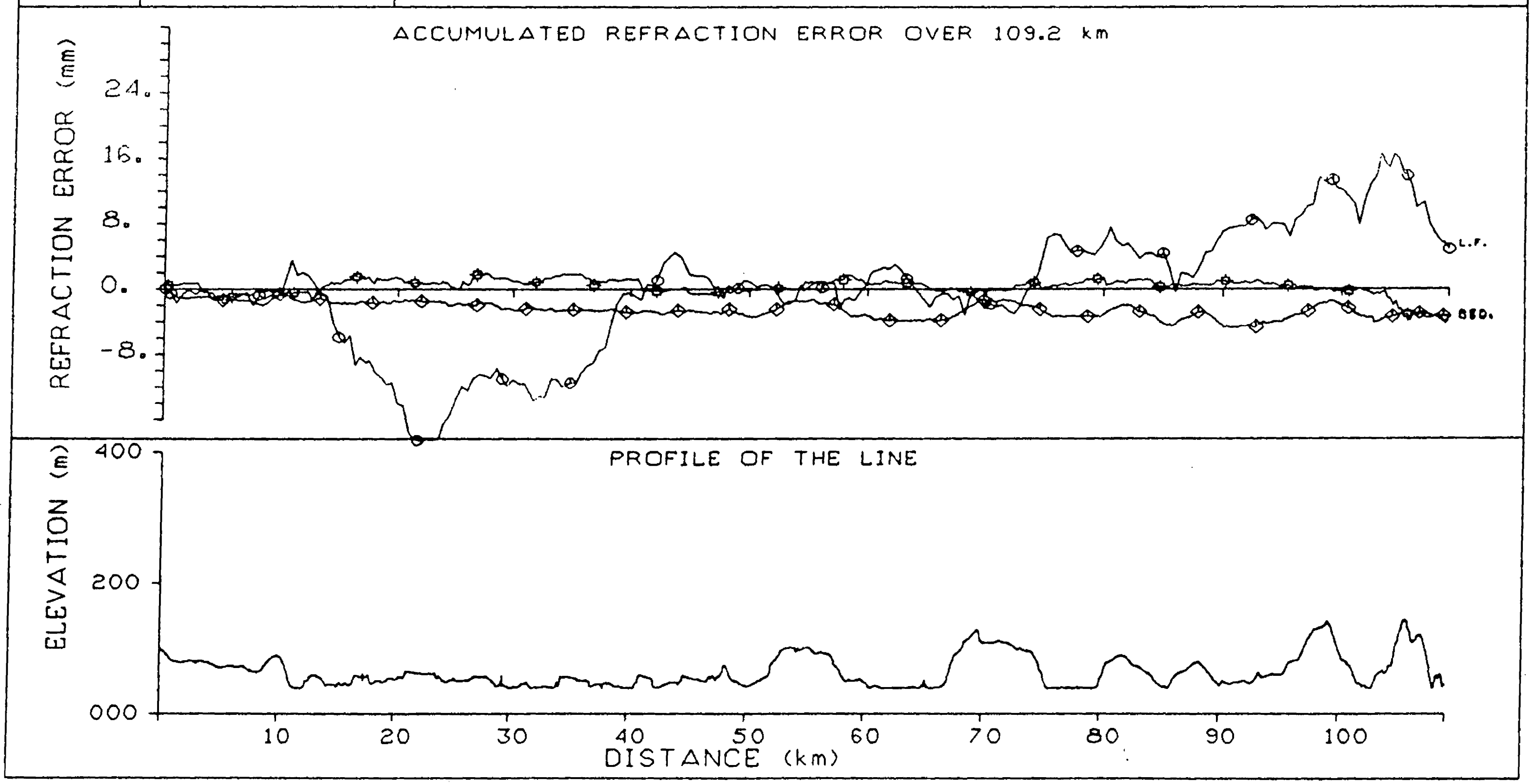

Figure 6.8: Accumulation of refraction error in geodetic levelling and trigonometric height traversing (line #4) using a simulated temperature gradient.

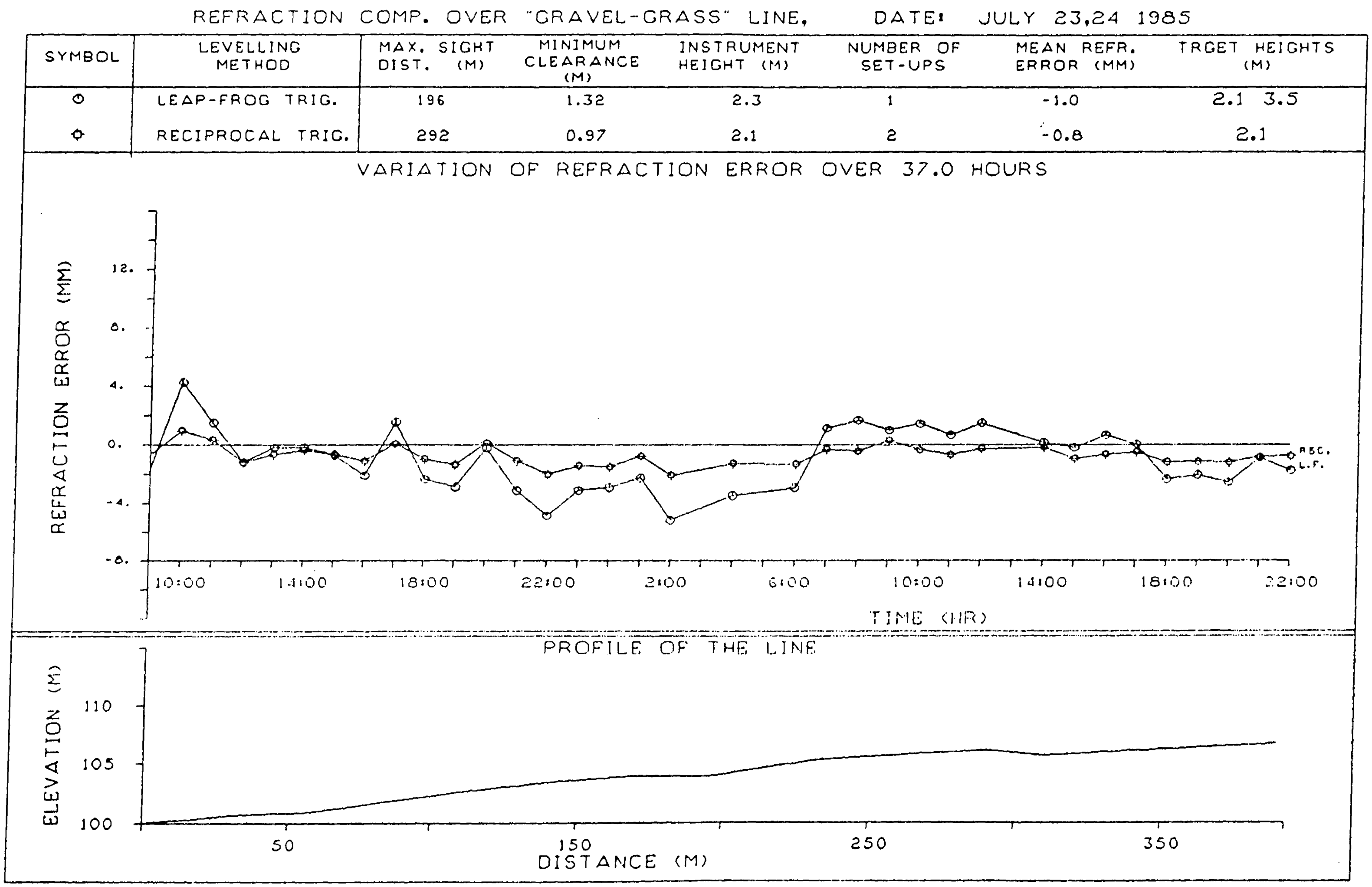

Figure 6.9: Refraction correction for line *BM1-BM2* at the South-Gym area.

REFRACTION COMP. OVER "GRASS-ASPHALT" LINE DATE: JULY 23,24 1985

SYMBOL	LEVELLING METHOD	MAX. SIGHT DIST. (M)	MINIMUM CLEARANCE (M)	INSTRUMENT HEIGHT (M)	NUMBER OF SET-UPS	MEAN REFR. ERROR (MM)	TRGET HEIGHTS (M)
⊘	LEAP-FROG TRIG.	196	1.33	2.3	1	0.7	2.1 3.5
◇	RECIPROCAL TRIG.	292	2.22	2.1	2	-0.2	2.1

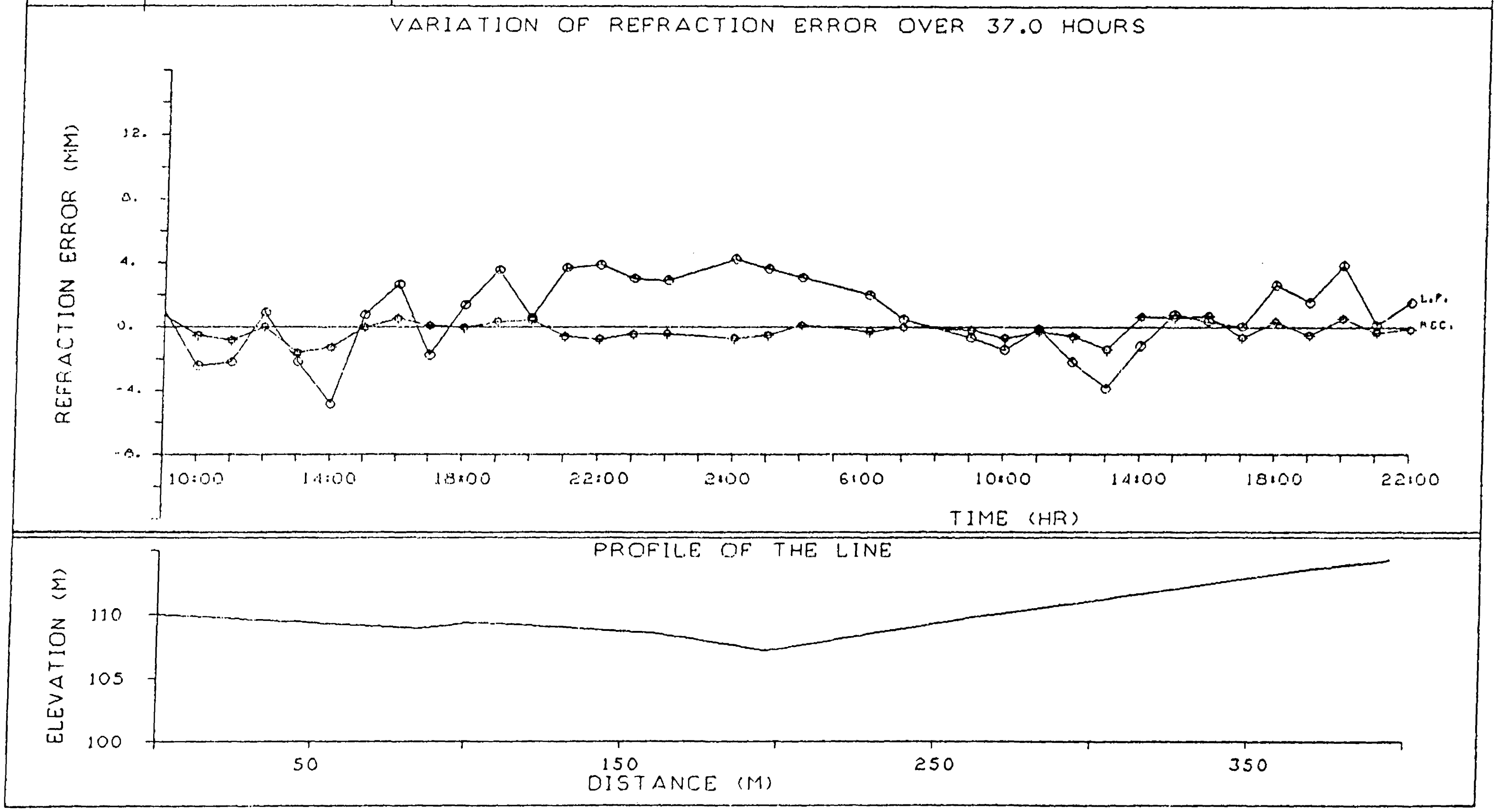

Figure 6.10: Refraction correction for line *BM2-BM3* at the South-Gym area.

"ASPHALT-GRAVEL" DATE: JULY 23,24 1985

SYMBOL	LEVELLING METHOD	MAX. SIGHT DIST. (M)	MINIMUM CLEARANCE (M)	INSTRUMENT HEIGHT (M)	NUMBER OF SET-UPS	MEAN REFR. ERROR (MM)	TRGET HEIGHTS (M)
○	LEAP-FROG TRIG.	196	1.70	2.3	1	0.1	2.1 3.5
◇	RECIPROCAL TRIG.	292	2.03	2.1	2	-0.1	2.1

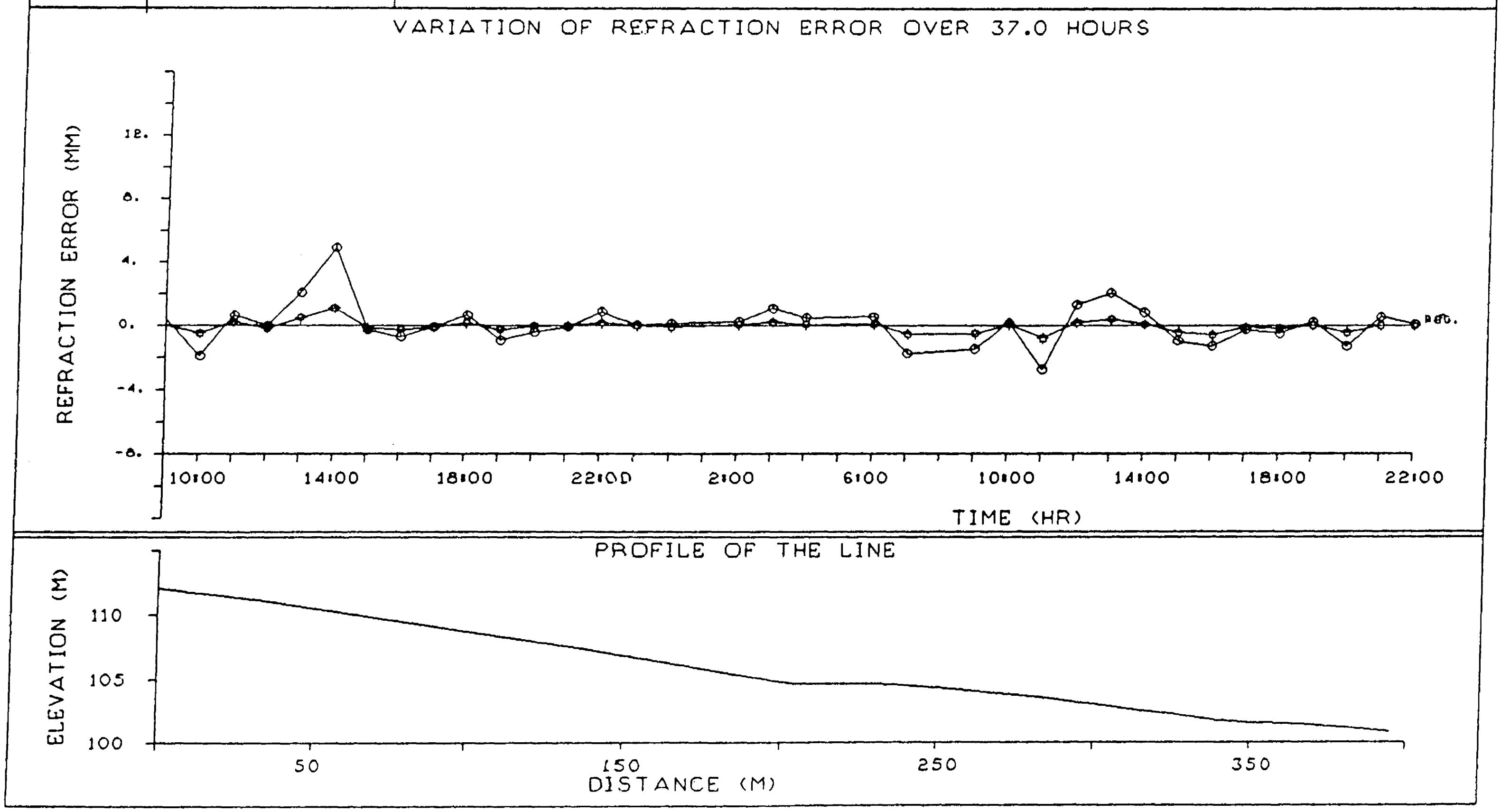

Figure 6.11: Refraction correction for line *BM3-BM1* (*UNB* leap-frog and reciprocal methods) at the South-Gym area.

OVER "ASPHALT" U.N.B. TEST LINE AUG 06/1985

SYMBOL	LEVELLING METHOD	MAX. SIGHT DIST. (M)	MINIMUM CLEARANCE (M)	INSTRUMENT HEIGHT (M)	NUMBER OF SET-UPS	MEAN REFR. ERROR (MM)	TRGET HEIGHTS (M)
⊖	LEAP-FROG TRIG.	225	0.92	2.3	1	2.7	2.1 3.5
⊕	RECIPROCAL TRIG.	350	0.71	2.1	2	-1.2	2.1

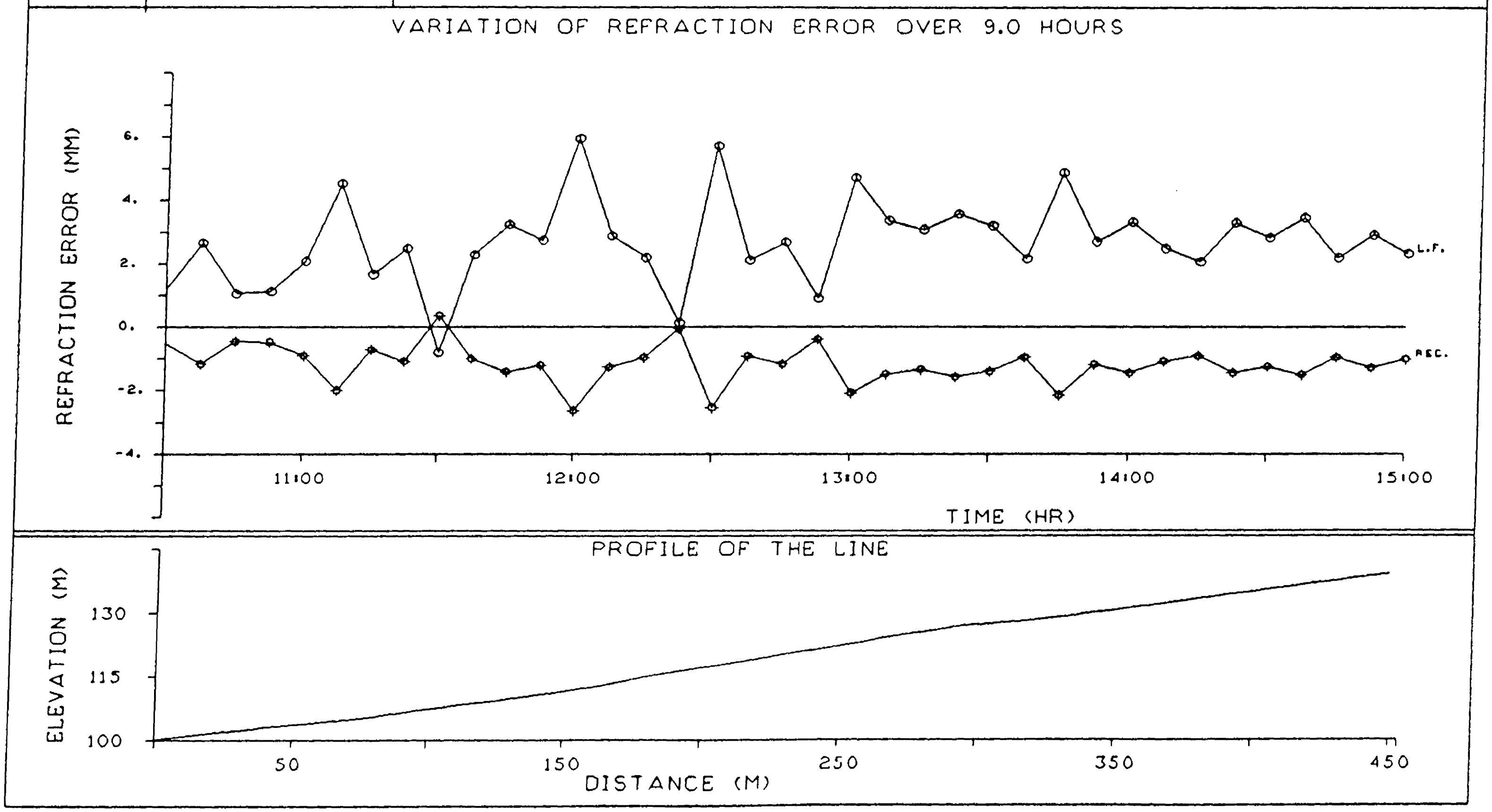

Figure 6.12: Refraction correction for the Head-Hall test line (*UNB* leap-frog and reciprocal methods).

Chapter 7

CONCLUSIONS AND RECOMMENDATIONS

7.1 Conclusions

Research studies carried out in the development of the *UNB* trigonometric method has provided some insight into the influence of refraction on height difference determination using optical techniques. Several test surveys were conducted to investigate and to understand the refraction effect. These test surveys involved long term observations of changes of the refraction angle over different types of surface coverage.

Besides these test surveys, numerous simulations of the refraction effect were completed to study the accumulation of refraction errors in trigonometric height traversing. These simulations were done along a line of geodetic levelling of special order. During the levelling operations, temperatures were measured at two different heights above the ground. The actual profile of the route is generated by utilizing the results of the geodetic levelling. Then, the accumulation of refraction error in the trigonometric method on this profile is computed by using the measured temperatures and simulated set-ups of trigonometric height traversing.

Based on these investigations the following conclusions can be drawn:

1. Through a series of computations of refraction correction and statistical testing using seven different models of the temperature profile, it was found that Kukkamäki's function is not the best model of distribution of temperature in the atmosphere close to the ground (up to a first few metres above the ground). Three new models have been proposed by the author in this thesis, which give better precision of fit and are easier to utilize than Kukkamäki's model, whenever the temperature is available at more than two points above the ground.

2. Refraction can be the major source of error in the trigonometric height traversing. In the leap-frog method with sight lengths of 200 m, under unfavourable conditions in which the fore-sight line extends over different types of ground surface than the back-sight line, the total error in height difference may reach a value of up to 4 mm. According to the pre-analysis made by Chrzanowski [1984] and because of the cyclic nature of this error which is highly correlated with the cyclic changes of the temperature gradient in prolonged observations, one can easly conclude that the major part of this error is due to the refraction effect.

The same has occurred along the Head-Hall test line where the maximum error in the leap-frog method was found to be 3.9 mm with sight lengths of about 225 m. In this case the ray clearance along the forward line of sight was very different from the backward line.

3. There is a high correlation in trigonometric height traversing between the refraction correction computed using the meteorological method and the error of traversing estimated from discrepancies with precise geodetic levelling. In spite of high correlation between the two, the computed corrections cannot be trusted in practice because they are not accurate enough and may cause too large corrections. However, the correlations show that the computed refraction in simulated trigonometric height traversing over a known profile with known temperature gradient along the traverse line is valid, and that useful information can be extracted from such simulations.

4. Unlike in geodetic levelling, the formulation for the refraction correction in trigonometric height traversing does not take into account the height difference when using the meteorological approach. Thus one can expect that refraction in the trigonometric method should not be correlated to the height difference. In fact, when the high correlation between refraction correction and the

estimated corresponding error (mentioned in point 3 overleaf) is realized, it can be understood intuitively that the refraction error in trigonometric height traversing is independent of the height gradient.

It should be mentioned here that different authors have investigated the refraction error in geodetic levelling and have verified its dependency on height differences, both theoretically and practically.

5. It has been substantiated from simulations that the refraction error in trigonometric height traversing, unlike in geodetic levelling, behaves randomly. The simulation with exaggerated sensible heat flux supported this finding.

6. As it was already shown through a series of simulations by Greening [1985], the reciprocal method is less susceptible to refraction errors than the leap-frog method. This has been verified in this thesis using an actual terrain profile and using real weather conditions as well as exaggerated conditions in which a much larger sensible heat flux was assumed.

7. Regarding the length of the line of sight and the clearance above the ground, the simulations have shown that if the lines of sight in the leap-frog method are less than 150 m with the ray clearance greater than 1 m, the refraction effect is within the limits of the

Canadian specifications for the first order levelling. The line of sight should be less than 250 m long for the clearance of 1 m in the case of reciprocal method.

8. Among four different approaches of determination of the refraction correction, discussed in Chapter 2, the meteorological method is the only one which has been developed and applied in practice.

The reflection method works the same as the reciprocal method, and precise estimation of refraction using this method is possible only, when the refracted path is a circular one.

The other two, the dispersion and the varaince of angle-of-arrival methods are promising and may show a better performance in the near future.

7.2 Recommendations

Based on the author's experience gained during his involvement in development of the *UNB* method (from 1981 to 1985), the following recommendations can be made regarding the refraction error in trigonometric height traversing:

1. For long lines of sight, i.e. longer than 250 m, the refraction correction in reciprocal height traversing may be obtained using the method in which the amplitude of the fluctuations of the target image are measured from both ends of the reciprocal set-up (section 4.1.4). More research is needed to verify the viability of the method.

2. Computation of the refraction effect based on the meteorological approach is neither accurate enough nor practical for long lines of sight in trigonometric height traversing, since the profile of the line must be known in addition to the temperature gradient (measured or modelled). A more appropriate solution is to limit the sight length to 150 m for the leap-frog and 250 m for the reciprocal methods and keep the clearance at more than 1 m; at the same time one should avoid unfavourable conditions as examined in Chapter 5.

3. For precise measurements of height differences when the long lines of sight are not avoidable, the observation should be limited to the time period when the neutral condition described in Chaper 5 can be expected. The temperature gradient should also be measured during the actual observations. If the reciprocal method is being used in this case, the total of refraction angle can be utilized also to confirm the near neutral condition time.

REFERENCES

Angus-Leppan, P.V. (1971). "Meteorological physics applied to the calculation of refraction corrections." Proc. Confer. Commonwealth Sur. Officiers, Cambridge, Paper No. B5, 9 p.

Angus-Leppan, P.V. (1979a). "Use of meteorological measurements for computing refractional effects." Refractional Influences in Astrometry and Geodesy, Edited by E. Tengstrom and G. Teleki, pp. 165-178

Angus-Leppan, P.V. (1979b). "Refraction in levelling - its variation with ground slope and meteorological conditions." Australian Journal of Geodesy, Photogrammetry and Surveying, No 31, pp. 27-41.

Angus-Leppan, P.V. (1980). "Refraction in levelling - extension to stable and neutral atmospheric conditions." Proceedings of Second International Symposium on Problems Related to the Redefinition of North American Vertical Geodetic Networks Ottawa, Canada, May 26-30, pp. 677-690.

Angus-Leppan, P.V. (1983). "Preliminary study for a new levelling system." Australian Journal of Geodesy, Photogrammetry and Surveying, No 39, pp. 69-81.

Angus-Leppan, P.V. (1984). "Refraction in geodetic levelling." Geodetic Refraction, Edited by F.K. Brunner, Springer-Verlag, pp. 163-180.

Angus-Leppan, P.V. (1985). "Refraction by reflection: test results." Proceedings of Third International Symposium on the North American Vertical Datum, Rockville, Maryland, pp. 275-285.

Angus-Leppan, P.V. and Webb, E.K. (1971). "Turbulent heat transfer and atmospheric refraction." General Assembly IUGG Travaux. IAG Sec. I, 15 p.

Banger, G. (1982). "Magnitude of refraction in levelling and its parameters." Australian Journal of Geodesy, Photogrammetry and Surveying, No. 37, pp. 29-62.

Bomford, G. (1971). Geodesy. 3rd ed., Clarendon Press, Oxford, England.

Brunner, F.K. (1975a). "Trigonometric levelling with measured slope distancess." Proceedings of the 18th Australian Survey Congress. Perth, pp. 79-94.

Brunner, F.K. (1975b). "Coefficients of refraction on a mountain slope" UNISURV G22, University of New South Wales, Sydney, Australia, pp. 81-96.

Brunner, F.K. (1979a)."Vertical refraction angle derived from the variance of the angle-of-arrival fluctuations." Refractional Influences in Astrometry and Geodesy, Edited by E. Tengstrom and G. Teleki, pp. 227-238.

Brunner, F.K. (1979b). "Atmospheric turbulence: the limiting factor to geodetic precision." Australian Journal of Geodesy, Photogrammetry and Surveying, No. 31, pp. 51-64.

Brunner, F.K. (1980). "Systematic and random atmospheric refraction effects in geodetic levelling." Proceedings of Second International Symposium on Problems Related to the Redefinition of North American Vertical Geodetic Ottawa, Canada, May 26-30, pp. 691-701.

Brunner, F.K. (1982). "The effects of atmospheric turbulence on telescopic observations." Bulletin Geodesique, No 56, pp. 341-355.

Brunner, F.K. (1984). "Modelling of atmospheric effects on terrestrial geodetic measurements." Geodetic Refraction, Edited by F.K. Brunner, Springer-Verlag, pp. 143-162.

Brunner, F.K. and P.V. Angus-Leppan (1976). "On the significance of meteorological parameters for terrestrial refraction." UNISURV G25, University of New South Wales, Sydney, Australia, pp. 95-108

Chrzanowski, A. (1983). "Economization of vertical control surveys in hilly areas by using modified trigonometric levelling." Technical Papers, 43rd American Congress of Surveying and Mapping Spring Convention, pp. 635-644.

Chrzanowski, A. (1984). "Feasibility study on the implementation of the motorized trigonometric height traversing for precise levelling." Final report prepared for the Geodetic Survey Division, Department of Energy, Mines and Resources, Contract No. OST83-00387, Ottawa, Canada.

Chrzanowski, A. (1985). "Implementation of trigonometric height traversing in geodetic levelling of high precision." Reported for the Geodetic Survey Division, Department of Energy, Mines and Resources, Contract No. OST84-00226, Ottawa, Canada.

Draper, N. and H. Smith (1981). Applied Regression Analysis. Second Edition, John Wiley & Sons, Inc., New York.

Fraser, C.S. (1977). "The empirical determination of sensible heat flux for refraction corrections." UNISURV G27, University of New South Wales, Sydney, Australia, pp. 42-51.

Garfinkel, B. (1979). "On the theory of terrestrial refraction." Second Quarterly Report, Contract No 78-40065, Yale University Observatory, New Haven, Conn., U.S.A.

Greening, W.J.T. (1985). Evaluation of Precision Trigonometric Levelling Methods. M.Sc.E. thesis, Department of Surveying Engineering, University of New Brunswick, Fredericton, N.B., Canada.

Hamilton, W.C. (1964). Statistics in Physical Science. Ronald Press Co., New York.

Heer, R. (1983). "Application of different refraction models on measuring results of the levelling test loop Koblenz." 38 Contributions to the Workshop on Precise Levelling, Hannover, Fed. Rep. of Germany, pp. 251-281.

Heer, R. and W. Niemeier (1985). "Theretical models, practical experiments and the numerical evaluation of refraction effects in geodetic levelling" Proceedings of the Third International Symposium on the North American Vertical Datum, Rockville, Maryland, pp. 321-342.

Heroux, P., W. Gale and F. Faucher (1985). "Field test report on the systematic effect of refraction in precise levelling" Proceedings of the Third International Symposium on the North American Vertical Datum, Rockville, Maryland, pp. 311-320.

Holdahl, S.R.(1979). "Removal of refraction errors in geodetic levelling." Refractional Influences in Astrometry and Geodesy, Edited by E. Tengstrom and G. Teleki, pp. 305-319.

Holdahl, S.R. (1981). "A model of temperature stratification for correction of levelling refraction." Bulletin Geodesique No 55, pp. 231-244.

Holdahl, S.R. (1982). "The correction for levelling refraction and its impact on definition of the North American Vertical Datum" National Geodetic Survey, Preprint for Presentation to the 1982 Annual Convention of the American Congress of Surveying and Mapping, Denver, Colorado, March 15-19.

Hotine, M. (1969). Mathematical Geodesy. ESSA Monograph 2, U.S. Department of Commerce, Government Printing Office, Washington, D.C., U.S.A.

Hytönen, E. (1967). "Measuring of the refraction in the second levelling of Finland." Puplication of the Finnish Geodetic Institute, No 63, Helsinki, 18 p.

Kasser, M. (1985). "Recent advances in high precision trigonometric motorized levelling in I.G.N. France." Proceedings of the Third International Symposium on the North American Vertical Datum, Rockville, Maryland, pp. 57-64

Kornacki, W. J. (1986). Computerization of Motorized Trigonometric Height Traversing of High Precision. M.Sc.E. thesis, Department of Surveying Engineering, University of New Brunswick, Fredericton, N.B., Canada.

Kukkamäki, T.J. (1938). "Über die nivellitische Refraktion." Publication of the Finnish Geodetic Institute, No. 25, Helsinki, Finland.

Kukkamäki, T.J. (1939a). "Formeln und Tabellen zur Berechnung der nivellitischen Refraktion." Publication of the Finnish Geodetic Institute, No. 27, Helsinki, Finland.

Kukkamäki, T.J. (1939b). "Verbesserung der horizontalen Winkelmessungen wegen der Seitenrefraktion." Publication of the Finnish Geodetic Institute, No. 28, Helsinki, Finland.

Kukkamäki, T.J. (1950). "Über das Flimmern und Schweben des Zielbildes." Geofisica Pura e Applicata, Milano, Bd. XVIII.

Kukkamäki, T.J. (1961). "Lateral refraction on the sideward slope." Annales Academia Scientiarum Fennica, Series A, III Geologica - Geographica, 61, Helsinki, Finland, pp. 143-153.

Kukkamäki, T.J. (1979). "Levelling refraction research, its present state and future possibilities." Refractional Influences in Astrometry and Geodesy, Edited by E. Tengstrom and G. Teleki, pp. 293-297.

Lawrence, R.S. and J.W. Strohbehn (1970). "A survey of clear-air propagation effects relevant to optical communications." Proceedings of Institute of Electrical and Electronics Engineers, IEEE, Vol. 58, No. 10, pp. 1523-1545.

Munn, R.E. (1966). Descriptive Micrometeorology. Advances in Geophysics, Academic Press, New York, U.S.A.

Obukhov, A.M. (1946). "Turbulence in atmosphere with non-uniform temperature." Boundary-Layer Meteorology 2, pp. 7-29, English Translation (1971).

Priestly, C.H.B.(1959). Turbulent Transfer in the Lower Atmosphere. University of Chicago Press, U.S.A.

Remmer, O. (1980). "Refraction in levelling." Geodetisk Institut, Meddelelse No. 54, Copenhagen, Danmark.

Rueger, J.M. and Brunner, F.K. (1981). "Practical results of EDM-height traversing." The Australian Surveyor, 30, pp. 363-372.

Rueger, J.M. and Brunner, F.K. (1982). "EDM-height traversing versus geodetic leveling." The Canadian Surveyor, 36(1), pp. 69-88.

Shaw, R.H. and P.J. Smietana (1982). "Research in the field of boundary layer micrometeorology as it impinges on the unequal refraction error on geodetic leveling." Final Report, U.S. Geological Survey Contract.

Surveys and Mapping Branch (1978). Specifications and Recommendations for Control Surveys and Survey Markers. Energy, Mines and Resources, Ottawa, Canada.

Vaníček, P., R.O. Castle and E.I. Balazs (1980). "Geodetic levelling and its applications." Review of Geophysics and Space Physics, 18(2), pp. 505-524.

Webb, E.K. (1964). "Day time temperature fluctuations in the lower atmosphere." Appl. Optics 3, pp. 1329-1336.

Webb, E.K. (1969). "The temperature structure of the lower atmosphere." Proceedings of Conference on Refraction Effects in Geodesy, Conference on Electronic Distance Measurement, University of New South Wales, Sydney, pp. 1-9.

Webb, E.K. (1984). "Temperature and humidity structure in the lower atmosphere." Geodetic Refraction, Edited by F.K. Brunner, Springer-Verlag, pp. 85-141.

Whalen, C.T. (1981). Results of Levelling Refraction Tests by the National Geodetic Survey. National Oceanic and Atmospheric Administration, Technical Report NOS 92 NGS 22, Rockville, Maryland, U.S.A.

Whalen, C.T. (1985). "Trigonometric motorized levelling at the National Geodetic Survey." Proceedings of the Third International Symposium on the North American Vertical Datum, Rockville, Maryland, pp. 65-80

Williams, D.C. (1981). "Performance tests of a two colour instrument for measuring angular refraction." FIG XVI. International Congress, Montreux, Switzerland, Paper 514.2.

Williams D.C. and H. Kahmen (1984), "Two wavelength angular refraction measurement." Geodetic Refraction, Edited by F.K. Brunner, Springer-Verlag, pp. 7-31.

Yellow Spring Instrument (1985). "Catalogue of temperature, humidity, oxygen and pressure instruments and sensors." Industrial Division, Yellow Spring Instrument Co., Inc. Ohio, U.S.A.